Effect of landuse and landcover change and climate change on the hydrological response and water quality of Big Creek Lake Watershed South Alabama USA

by

Eshita Akter Eva

A thesis submitted to the Graduate Faculty of

Auburn University

in partial fulfillment of the requirements for the Degree of

Master of Science

Auburn, Alabama
August 07, 2021

LULC, SWAT, SUFI-2, Representative concentration pathways, Evapotranspiration, Percolation

Approved By

Dr. Luke Marzen, Chair, Professor of Geosciences

Dr. Chandana Mitra, Associate Professor of Geosciences

Dr. Jasmeet Lamba, Assistant Professor of Biosystems Engineering

Abstract

Land use and climate are the two key factors affecting the hydrological processes of a watershed. This research aimed to evaluate the impact of changing land use and land cover (LULC) and climate change on hydrological responses and water quality by applying the Soil and Water Assessment Tool (SWAT) to Big Creek Lake watershed located in Mobile County, South Alabama. Digital elevation model (DEM), LULC data, weather data, soil data, observed streamflow, nitrogen, and phosphors data were input files used to calibrate and validate the SWAT model. Downscaled and bias-corrected daily projected climate data were used under moderate (Representative Concentrative Pathways4.5) and extreme (Representative Concentrative Pathways8.5) scenarios. These data were used as inputs of a calibrated SWAT model of the watershed in order to determine the effects of climate change and LULC on streamflow and total nitrogen and phosphorus in the watershed from 2020 to 2050. The SWAT model was calibrated and validated using the SUFI-2 algorithm in the SWAT Calibration Uncertainties Program (SWAT-CUP) software. LULC changes and climate changes were investigated to quantify the effects of the major hydrological components such as actual evapotranspiration, percolation, lateral flow, surface runoff, groundwater and water yield. About 11,045 acres of agricultural land and 3,350 acres of urban area has been increased and 11,482 acres of forest area has been decreased between 1991 and 2020. This changing scenario of LULC has increased not only the stream flow but also the total nitrogen and phosphorus. The average annual total precipitation would increase about 4874 mm (RCP4.5) and 5357 (RCP8.5) mm in future thirty years compare to the last three decades (1991-2020). Moreover, the temperature will also increase at about 1.8^0C and 1.7^0C for RCP4.5 and RCP8.5 scenario respectively. This increasing precipitation and temperature lead to the increasing stream flow and total nitrogen and phosphorus of the watershed. But, the impact of climate variability on the streamflow and nitrogen and phosphorus would be more profound in RCP8.5 than RCP4.5. The results obtained in this study are able to provide guidance to water resource management and plan to policy makers and water managers in the Mobile County.

Keywords: LULC, DEM, SWAT, SUFI-2, RCP

Acknowledgement

First of all, I want to thank Almighty for the intelligence, the strength, tranquility of my mind and good health that He bestowed upon me to finish this study. I am grateful to my major professor, Dr. Luke Marzen for giving me this opportunity to work under his supervision for my master's studies. I can't thank him enough for his continuous support, knowledgeable discussions, guidance and valuable time to enlighten me for the entire course of the study.

I appreciate my committee members Dr. Chandana Mitra and Dr. Jasmeet Lamba for their valuable knowledge and guidance they provided when I needed. I would like to express my gratitude towards them for their help.

Last but not the least, I would like to thanks my parents and my brother for their continuous support and loving me unconditionally.

List of contents

List of Tables

List of Figures

CHAPTER 01

INTRODUCTION

1.1 Background

The population of the Mobile County has increased by about 30,228 from the last 30 years (US Census Bureau) (http://eire.census.gov/popest/data/cities/tables/). Census results for Mobile County in 2020 count population numbers at 412,512 people, an increase of 7.3% from the 1991 population rate. A temporal analysis study from 1974 to 2008 was conducted by Ellis et al in 2008 on the changing LULC of the Big Creek Lake watershed. They concluded that forest area decreased significantly, and the urban area increased in a great percentage. Besides that, Mobile Area Water and Sewer Systems (MAWSS) in 2004 also stated the residential area is increasing day by day. In 2017, it was claimed by MAWSS and the Alabama Department of Transportation (ALDOT) that the construction of a new eight-mile stretches of Highway 98 to reduce traffic congestion is supposed to increase erosion and transport of sediment runoff and thus degrade the water quality of the watershed.

According to the U.S. Environmental Protection Agency (USEPA), nonpoint source (NPS) pollution continues to be the largest source of pollution within the USA (USEPA 2012a) causing harmful effects to fisheries, wildlife, drinking water, and other natural resources. USEPA reported that 44% of water quality was deteriorated in the United States in the 21st century (Miller, 1992). In Alabama, agriculture and forestry are known to cause NPS pollution problems (USEPA, 2006). Particularly in agricultural watersheds, NPS pollution has become a major environmental concern (USEPA,2007).

Watershed models are effective tools and techniques to simulate the streamflow and transport of pollutants under different management practices. These models are capable of simulating and

evaluating processes potential evapotranspiration, percolation, infiltration, surface runoff, baseflow, sediment transportation, and nutrient transport on a location-specific basis (Novotny, 2003). The output from these models includes water inflow and outflow, pollutant loading, and other information that can be used to manage watersheds and reduce NPS pollution. Both structural and nonstructural Best Management Practices (BMPs) are used to reduce NPS pollution (Novotony, 2003). According to Neitsch et al. (2011), the SWAT model is one of the most widely used models to assess streamflow and NPS pollution problems.

1.2 Goal and Objectives

This research focused on two main components of the watershed including the changes in hydrological response and the water quality parameters due to the changes in climatological conditions and LULC over time. Specific objectives of this study are:

1) How increasing urban area and agricultural area over time alter the hydrological response and deteriorate water quality.
2) To quantify the change of water balance components and the rate of nitrogen and phosphorus level in the watershed due to climate change

1.3 Organization of the Thesis

This study focuses on the above-mentioned two objectives. Each objective is explained in an individual chapter and each chapter is written as a separate manuscript.

Impacts of increasing urban area and expansion of the agricultural area over time (1991-2020) on streamflow as well as water quality are addressed in chapter 2.

The focus of chapter 3 is to quantify the changes in streamflow and the level of nitrogen and phosphorus in the watershed due to climate change over time (1991-2020) and to project stream

flow and amount of nitrogen and phosphorus from 2021 to 2050 under two different Representation Concentration Pathways (RCP).

Chapter 4 are the conclusions that contains the summary and suggestions for future work.

References cited-

Ellis, J., Spruce, J., Swann, R. and Smoot, J., 2008, Land-use and land-cover change from 1974-2008 around Mobile Bay, AL. NASA Stennis Space Center (SSC) and Gulf of Mexico Alliance (GOMA).

Mobile Area Water and Sewer System, 2004, Drinking water quality 2004 report: Mobile, Alabama, Mobile Area Water and Sewer System, 6 p.

Miller, G.T. 1992, Living in the Environment: An Introduction to Environmental Science, 7th ed., Wadsworth Publishing Company: Belmont, CA, USA.

Neitsch, S. L., J. G. Arnold, J. R. Kiniry, R. Srinivasan, and J. R. Williams. 2011. Soil and Water Assessment Tool theoretical documentation. College Station, Tex.: Texas Water Resources Institute.

Novotny, V. 2003. Water Quality: Diffuse Pollution and Watershed Management. New York: John Wiley and Sons.

U.S. Census Bureau. 2002, Table 10. Alabama incorporated place population estimates, sorted within county—April 1, 2000, to July 1, 2002; accessed on 23rd December, 2020, at http://eire.census.gov/popest/data/cities/tables/.

USEPA. 2006. What is Nonpoint Source (NPS) Pollution? Questions and Answers. Washington D.C. Available at: www.epa.gov/owow/nps/qa.html. Accessed 11 December 2020.

USEPA 2007. Nonpoint source pollution: The nation's largest water quality problem. EPA841-F 96-004A. Washington, D.C.: USEPA. Available at: http://www.epa.gov/owow/nps/facts/point1.htm. Accessed 11 December 2020.

US Environmental Protection Agency, 2012a, “DRAFT FINAL EPA Quality Standard for Environmental Data Collection, Production and Use by EPA Organizations.

CHAPTER 2

Impact of LULC on Hydrological Response and Nitrogen and Phosphorus of Big Creek Lake Watershed, South Alabama

2.1 Introduction

According to Zhang et al., 2017; Gao et al., 2016 and Jarsjö et al., 2012, in these recent decades, hydrological responses to the changing environment have become a research interest area. Among all the factors affecting the hydrological processes, land use change and climate change are given much importance to study (Li et al.,2009; Liu et al., 2014; Pan et al., 2017 and Yin et al., 2017). Changing Land Use and Land Cover (LULC) influence runoff-rainfall processes by affecting the surface components such as evapotranspiration, infiltration, and percolation. Various types of land use have different reflectivity (albedo), roughness, leaf areas, soil depth, which impacts the land-surface interactions by affecting temperature, humidity, wind speed and precipitation (Wei and Zhang, 2010; Pitman, 2003 and Sy et al., 2017). Changes in LULC will have impact on these interactions resulting in differences in surface moisture, heat, and momentum fluxes (Sertel et al., 2010 and Lee and Berbery, 2012). According to Marland (2003), local, regional, and global climate and hydrological processes depend on the spatial distribution, size, extent and location of land cover changes. Though many investigations have focused on the hydrological response due to changes in land use (Welde and Gebremariam, 2017; Wang et al., 2017; Lin et al., 2015 and Nie et al., 2011), the relationship between changing land use and the hydrological response deserve more investigation. Thus, an analysis of hydrologic events is important to recognize changes in LULC for the prevention of hydrological problems and for managing water quality.

According to the U.S. Environmental Protection Agency (USEPA), nonpoint source (NPS) pollution continues to be the largest source of pollution within the USA (EPA 2012a). USEPA reported that 44% of water quality was deteriorated in the United States in the 21st century. NPS pollution is a broadly elaborative category that includes many diffuse sources of aquatic contaminants carried by rainfall or snowmelt runoff (EPA 2012b), or any source of water pollution which is not meeting the legal definition of a point source within the Clean Water Act. Many sources exist for NPS pollutants, but nutrients are the most common NPS pollutants, though, pollution from pesticides, pathogens, salts, oil, grease, toxic chemicals, and heavy metals are also widespread (EPA 2012c). According to National Water Quality Assessment, agriculture is the leading contributor to water quality impairments, particularly within rivers and lakes. The inventory also reported that urban area runoff is a significant contributor to the pollutants found in estuaries (EPA 2012a). These findings also agree with the result of Dowd, Press, and Huertos (2008) which identified agricultural activities and highly impervious urban areas as major sources of NPS pollutants. NPS pollution resulting from urban areas is exacerbated by the extensive expanses of impervious surfaces that hamper the absorption of water (Esen and Uslu, 2008).

One such water body that is susceptible to pollution due to development is Big Creek Lake in Mobile County, AL. A great deal of controversy exists surrounding the lake, primarily regarding a three-year court battle between Mobile Area Water and Sewer System (MAWSS) and the Alabama Department of Transportation (ALDOT) over a new eight-mile stretch of Highway 98 which was constructed to reduce traffic congestion. In 2017, it was claimed by MAWSS and ALDOT that this construction project would increase erosion and transport of sediment runoff and it would increase pollution of the watershed and degrade water quality. This controversy led

to public awareness regarding the significance of responsible land use management within the watershed.

The use of hydrological models is essential because of the effective planning of water resources and protection under changing environmental conditions and models can simulate flow regimes under different scenarios. Therefore, various hydrological models have been developed to provide a link between change scenarios and water yields, through the simulations of the hydrological process within the watersheds. Some of the models include Agricultural Non-Point Source (AGNPS) (Young et al., 1989 and Bhuyan et al., 2003), Hydrological Simulation Program-FORTRAN (HSPF) (Bicknell et a., 1996), MIKE SHE (DHI, 1993), Soil and Water Assessment Tool (SWAT) (Arnold et al., 1998) and Agricultural Policy/Environmental Extender (APEX) (Williams, Izaurralde and Steglich, 2008). Many of these hydrological models are applied for runoff, sediment yield, and soil loss prediction. Among all these models, the SWAT model is the most widely used and it has been applied in different areas to analyze numerous problems of hydrology and water quality, including the potential changes to the streamflow under different climate scenarios. Simulation of runoff from a catchment can be carried out with the help of mathematical equations. Almost 4000 peer-reviewed articles related to the SWAT model have been published and among these almost 1000 articles are related to the hydrological responses to climate changes (Gassman et al., 2010). SWAT has achieved worldwide recognition because it is utilized to evaluate water and sediment yield and water quality parameters under present conditions, management practices, and future climate conditions with spatial and temporal resolutions that depend on the data availability. Woldesenbet et al. (2017), Kamali et al. (2017), Zhang et al. (2016), Lima et al. (2014), and Coe et al. (2009) have used conceptual and semi-distributed hydrological modeling to assess the impact of LULC on hydrological responses.

The utilization of different hydrological models is significant because it helps to adapt measures for water resource management, and to provide the basis for decision-making or choices related to sustainable development alternatives and conservation practices brought about by evaluating the changes in hydrological components due to changing LULC (Refsgaard and Abbott, 1996, Abbaspour et al., 2015 and Loucks et al. 2005). The significance of the study is the result could be used by the water resources planners and managers as the study is highlighting the changes of stream flow and water quality in terms of LULC change and future climate change scenarios.

2.2 Materials and Methods

2.2.1 Study Area

The area of Big Creek Lake or J.B. Converse Lake is 3,600 acres which is a tributary-storage reservoir in Mobile County located in southwest Alabama. Although the lake itself is only 3,600 acres, the watershed draining into it covers approximately 65,920 acres or 103 square miles (MAWSS 2011; Journey and Gill 2001). Big Creek Lake, a central reservoir, is fed by several tributaries including Big Creek, Jackson Branch, Juniper Creek, Collins Creek, Long Branch, Boggy Branch, Crooked Creek, and Hamilton Creek. Though Big Creek Lake watershed encompasses large areas in Mobile County, no large municipalities exist within the watershed but there are several smaller towns including Wilmer and Semmes which are located within the watershed boundaries. Figure 2.1 shows the location of the watershed and the location of the weather and water quality data stations. Big Creek Lake watershed lies within the Southern Hills District of the East Gulf Coastal Plain section of the Coastal Plain Physiographic Province in close proximity to the Gulf Coast. The Gulf of Mexico influences the subtropical climate of the watershed. Relative to the rest of the United States, the area encompassing the watershed is ranked second in terms of annual rainfall only to the Pacific Northwest (Baldwin, 1973). The soil

type of the watershed is mainly ultisols, consisting of well-developed profile characteristics that reflect the influence of the active factors of soil formation. These soils are well-drained and acidic. Ultisols make up 100% of the total watershed and it includes Troup-Heidel-Bama Association, Troup-Benndale-Smithton association, and Shubuta-Troup-Benndale association.

2.2.2 Data Required

A Digital Elevation Model (DEM) and associated topography, LULC, and soils, of the study watershed, are all the spatial inputs that are required to run the Soil Water Assessment Tool (SWAT) model (Monteith, 1965, Willams, 1969 and Arnold et al., 2012). Other inputs required for the model to run are long-term weather data, soil properties data, and discharge data. Moreover, several mathematical equations are also used in different analyses. Figure 2.2, 2.3 and 2.4 are representing the LULC, slope and soil data of the present study area respectively.

The DEM datasets were downloaded from the USGS National Map (https://viewer.nationalmap.gov/basic/). The spatial resolution is 10 meters which is a 1 arc-second (10m * 10m) pixel resolution. For LULC data, Landsat images obtained from the USGS data hub (https://earthexplorer.usgs.gov/) and multi-seasonal images chose from 1990 to 2020 with minimum cloud cover to have the lowest atmospheric effects. The details of the images represent in Table 2.1. Each LULC product was primarily based upon the classification of Landsat data. Classification was performed using the unsupervised approach. Initially, a given Landsat image was subjected to unsupervised classification using Iterative Self-Organizing Data Analysis Techniques (ISODATA) clustering with 20 total clusters, convergence set to 0.995 (on the scale of 0 to 1), 100 iterations, and cluster means initialization along the principal axis. The resulting classification was then reclassified into the water, forest, urban, agriculture, and rangeland. Then, the accuracy assessment was performed to evaluate the classification is done

properly or not. Table 2.2 is representing the accuracy assessment value for each LULC product. Random sampling method was chosen for the accuracy assessment and this method was associated with the points that are randomly distributed within the study area. By comparing the referenced points and observed points, accuracy matrices were generated. A matrix change detection method was applied to show from and to LULC changes within these years. The LULC change detection products was generated using standard GIS overlay analysis techniques. The change detection approach involved a comparison of two dates of LULC classifications.

For the soil data, SSURGO (Soil Survey Geographic Database) were used. The soil data and information on related soil properties were obtained from https://websoilsurvey.sc.egov.usda.gov/App/WebSoilSurvey.aspx. According to Natural Resource Conservation Service (NRCS), SSURGO is the most detailed level of county soil data. Climatic data including daily rainfall, maximum and minimum temperatures, and average wind speed at one weather station in the study were obtained from the NOAA (National Oceanic and Atmospheric Administrations) website from the period between 1990 and 2020. The link is given here https://www.ncdc.noaa.gov/cdo-web/datasets. In cases where any of the meteorological data are not included or missed in the model, the SWAT utilizes a built-in weather generator model (WXGEN) to stochastically generate daily weather values based on historical monthly averages of parameters such as temperature, precipitation, relative humidity, wind, and solar radiation. The missing values are recorded as -99. Discharge data obtained from the USGS National Water Information System: Web Interface. The data are available at this link https://waterdata.usgs.gov/nwis/rt. The data are available on daily, monthly, and annual basis. Water quality data are also available in the USGS National Water Information System Web

Interface. Water quality data are not available daily or even monthly but rather its reporting is random.

The hydrological components and processes and the amount of nutrients within a watershed have significant impact on management practices and operations. Therefore, it is important to incorporate management practices information in the SWAT model to have the sufficient and reasonable outputs. Butler and Srivastava (2007) developed Best Management Practices (BMPs) database for Alabama state. Previously this management database had been used by many studies conducted within Alabama (Mirhosseini et al., 2016; Srivastava et al., 2010). For cropland areas, Peanut - Cotton rotation was used and Bermuda grass for rangeland. The management information for the peanut-cotton rotation is included in Table 2.3. Bermuda grass was planted in the beginning of March and then harvested in July every year (Ahring et al., 1974; Shaver et al., 2006) for the period of 30 years (analyzed time).

2.2.3 SWAT Model Description

The SWAT (Soil Water Assessment Tool) is a physically based hydrologic model and requires physically based data (Jacobs and Srinivasan, 2005). SWAT is a continuous-time, spatially distributed model designed to simulate water, sediment, nutrient, and pesticide transport at a catchment scale on a daily time step under different management practices (Jain and Sharma, 2014). The SWAT model has been developing for almost 30 years now and it has been modified and adapted numerously for better performance (Simić, 2009). The SWAT model is used to estimate relevant hydrologic components such as evapotranspiration, surface runoff, and peak rate of runoff, groundwater flow, and sediment yield for each Hydrological Response Units (HRUs). The SWAT is embedded in a GIS interface called Arc-SWAT- an Arc GIS extension

that is a graphical user interface for the SWAT 2012 which evolved from AVSWAT, an ArcView extension developed for an earlier version of the SWAT.

The SWAT model is a continuous process-based, computationally efficient, and is also capable of continuous simulation over a long time. Weather, hydrology, soil temperature and properties, plant growth, nutrients, pesticides, bacteria and pathogens, and land management are the major components used to run the SWAT model. In the SWAT model, a watershed is divided into multiple sub-basins or sub-watersheds and then each sub-basin is further subdivided into an HRU. HRUs are located in the subbasin and comprised of unique land use, soil, and slope characteristics. The HRUs are used to describe spatial heterogeneity in terms of land cover, soil type, and slope class within a watershed.

Surface runoff occurs whenever the rate of water application to the ground surface exceeds the rate of infiltration. SWAT provides two methods for estimating surface runoff and these are the Modified SCS curve number procedure (SCS, 1972) and Green & Ampt infiltration method (1911). In this study, the SCS curve number method was used to estimate surface runoff.

The peak runoff rate is estimated by the use of a modification of the Rational Method. Water is routed through the channel network by using a variable storage routing method or the Muskingum routing method. In this study, Muskingum routing methods were used for surface runoff.

The model estimates the evaporation from soils and transpiration from plants. Potential evapotranspiration can be estimated by the three methods in SWAT: Priestley–Taylor (Priestley and Taylor, 1972), Penman-Monteith (Monteith, 1965), and ET–Hargreaves (Hargreaves, 1985). In this study, the Penman-Monteith method was used to estimate potential evapotranspiration

because this method includes precipitation, minimum and maximum temperature, wind speed, relative humidity, and solar radiation to measure evapotranspiration. The other two do not include all these parameters.

SWAT simulates plant growth through a simplified version of the Environmental Policy Integrated Climate model (EPIC), developed by Williams (1995), which considers the heat units (or growing Degree-Days) for each species considered.

SWAT simulates soil erosion and sediment transport throughout the drainage channels of the watershed. SWAT calculates the surface erosion for each HRU using the inbuilt Modified Universal Soil Loss Equation (MUSLE). According to Williams (1975), The MUSLE is the modified version of USLE which replaced the rainfall intensity with the runoff intensity to eliminate the need for delivery ratio, to improve sediment yield prediction, and allow the equation to be applied to individual storm events (Neitsch et al., 2002). MUSLE estimates sediment yield from surface runoff volume, peak runoff rate, area of the HRUs, soil erodibility, support practice, topography, cover and management, and coarse fragment USLE factors.

The SWAT considers two physical processes: sedimentation (deposition) and transportation, simultaneously. Briefly, the SWAT partitions soil N into five different N pools. Two of the pools are inorganic (ammonium-N [NH4-N] and nitrate-N [NO3-N]) and three pools are organic (active, stable, and fresh). Transformation of nitrogen (N) in different pools is modeled using mineralization, decomposition, immobilization, nitrification, denitrification, and ammonium volatilization processes (Chaubey et al., 2006). By using the supply and demand approach, plant use of nitrogen is estimated (Santhi et al., 2006). Unlike N, soil phosphorous (P) in SWAT is divided into six pools (three minerals and three organics). Crop residue and biomass contribute to the fresh organic phosphorus pool, and humus substances contribute to the active and stable

organic pool. Soil inorganic pool includes active, solution, and stable pools (Chaubey et al., 2006). The portion of phosphorus from solution inorganic phosphorus is taken up by plants and is in rapid equilibrium with the active pool. The active phosphorus pool is in rapid equilibrium with the solution pool and slow equilibrium with the stable pool. A stable inorganic pool is relatively unavailable for plant uptake (Neitsch et al., 2002). Like nitrogen, plant use of phosphorus is estimated using the supply and demand approach (Santhi et al., 2006).

A full explanation about SWAT model theories and structure is given in the SWAT theoretical documentation (http://swatmodel.tamu.edu/) (Neitsch et al., 2011).

2.2.4 SWAT Model set up

The SWAT model requires input parameters including DEM and associated topography, weather data, LULC data, and soil data. Besides, water infrastructure and other land management practices can also be incorporated. The first step of model set-up was the delineation of the watershed and the sub watershed reaches and the outlet. As SWAT is a physically derived model, it derived topography, contours, and slope from the DEM and it was used to divide the basin into subbasins.

Once the source DEM was added, the model then used contours and slope which were calculated during delineation, to determine flow direction and flow accumulation. When flow direction and flow accumulation were extracted, the model generated a stream network in which each reach drained a sub-basin, all of which drained into a major reach. Each reach had an outlet. Then the user had to select an outlet that corresponds to the outlet at which discharge measurements for calibration were being collected. This outlet then determined the lower boundary for the

watershed basin, which then delineated based on the location of that outlet and the stream network.

To define HRU, the model required the LULC, soil, and slope. Once the LULC, soil, and slope are defined, HRUs were created with a unique combination of those three classes. The LULC and soil data were imported to the model for determining the HRUs for each sub-basin. A Land use lookup table was used to specify the land use category and also the Soil SSURGO data were used to identify the soil types, linked to the SWAT databases to reclassify the land use and soil map. The slope was reclassified into five classes by using multiple slope option. The threshold percentage method was applied to eliminate minor land use, soil type, and slope and a 5% threshold for minimal amounts of LULC, 10% threshold for both soil and slope were used. The HRUs were generated, and the corresponding report was also generated by the model which was specifying the area of different HRUs in various subbasins.

The final step before the simulation was the creation of input tables, including the weather data. The weather data included maximum and minimum temperature, precipitation, and wind speed. For relative humidity and solar radiation, the US Weather generator was used. The files were successfully rewritten and stored in the personal geodatabases of the model. After this step, the model ran to simulate the surface runoff.

2.2.5 Uncertainty and Sensitivity Analysis

Sensitivity analysis is the identification of the sensitive parameters that have an important influence on the performance of the model so that adjustments will be precise. This operation was carried out by SWAT-CUP which is developed by the Swiss Federal Institute of Water Science and Technology (EAWAG), and it is specialized in SWAT calibration, validation, and

uncertainty analysis. The SWAT-CUP is a standalone program that links to SWAT's output text files, which integrates five different optimization algorithms: Sequential Uncertainty Fitting (SUFI-2) (Abbaspour et al., 2007), Generalized Likelihood Uncertainty Estimation (GLUE) (Beven and Binley, 1992), Parameter Solution (ParaSol) (Van Griensven and Meixner, 2006), Markov chain Monte Carlo (MCMC) (Kuczera and Parent, 1998; Marshall et al., 2004; Vrugt et al., 2003), and Particle Swarm Optimization (PSO) (Zhang et al., 2015). Among all of these algorithms, SUFI-2 is the capacity to account for all the sources of uncertainty on the parameter ranges such as uncertainty in driving variables (e.g., rainfall), conceptual model, parameters, and measured data (Abbaspour et al., 2007) and for this reason, the SUFI-2 was used in this study to analyze the sensitivity of the model.

2.2.6 SWAT Model Calibration and Validation

The calibration of the hydrological model is done to optimize its predictive capacity by comparing its simulated values with the observed or actual values of the study area. Validation is the process of demonstrating the capability of making a sufficiently accurate simulation, which may vary based on the aim of a project (Refsgaard, 1997). I used the five years of warm up periods that is from 1986 to 1990. The calibration and validation period were equal for stream flow, nitrogen and phosphorus. Predicted and observed values of streamflow and nutrient loadings at the watershed outlet were compared to determine whether the objective function satisfactorily involves running a model using the parameters during the calibration and comparing the results from the different periods of calibration to determine whether the model meets confidence limits. The model validation was done with the same SWAT parameter values calibrated without any further alterations. For calibration and validation, the period was determined by the length of the observed data record. If the observed data period is sufficiently

long that is representing the different climatic conditions, then it can be possible to split the data equally for the calibration and validation. However, if the length of the data record is not sufficiently long, then the length of the data may be different in such a way that the calibration period is sufficiently long. The SWAT input parameters are physically based, and calibration parameters are allowed to vary within a realistic uncertainty range (Gassman et al.,2005).

2.2.7 Model Evaluation

The performance of the model was evaluated by using qualitative graphical comparisons and quantitative statistical techniques. Qualitative methods were involved plotting observed and simulated streamflow, total phosphorus, and nitrogen loading at a monthly time-step. In quantitative methods, the performance of the model in the simulation was evaluated by Nash-Sutcliffe Efficiency (NSE), Percent of Bias (PBIAS), and the Coefficient of Correlation (R^2) as proposed by Moriasi et al. (2007) which are most commonly used.

$$NSE = 1 - \frac{\sum_{i=1}^{n}(Oi-Pi)^2}{\sum_{i=1}^{n}(Oi-\overline{O})^2} \quad (1)$$

$$PBIAS = \frac{\sum_{i=1}^{n}(Oi-Pi)*100}{\sum_{i=1}^{n} Oi} \quad (2)$$

$$R^2 = \frac{\sum_{i=1}^{n}(Oi-\overline{O})(Pi-\overline{P})}{\sqrt{\sum_{i=1}^{n}(Oi-\overline{O})^2}\sqrt{\sum_{i=1}^{n}(Pi-\overline{P})^2}} \quad (3)$$

where Oi is the ith observation for the constituent being evaluated; Pi is the ith simulated value for the constituent being evaluated; $\overline{O}$ is the mean of observed data for the constituent being evaluated; $\overline{P}$ is the mean of simulated data for the constituent being evaluated and n is the total number of observations.

2.3 Results

2.3.1 Land Use and Land Cover (LULC) Change

The LULC time series analysis between 1990-2020 had been done to present the comparative analysis. Figure 2.5 and Table 2.8 had been shown the percentage of land use and transformation of land use over the period. Water had a decreasing trend continuously from 1990 to 2020 and 371 acres were transformed into other LULC over this period. Forest was one of the main land uses of the watershed and forest was lost in a large percentage. From 1990-2000, almost 60% of the watershed area was forest land. But, after one decade (2010) forest area reduced by about 10%. 11,482.80 acres of forest area had been transformed into other LULC over a 30 year period (Table 2.8). On the other hand, urban areas increased (3,350 acres) in the past three decades, showing an increment of 1293 acres from 1990 to 2000, 632 acres from 2000 to 2010 and 1,423 acres from 2010 to 2020. Agricultural land increased (11,045 acres) and rangeland decreased (2,542 acres) in the last three decades. From 1990 to 2000, agricultural land had increased but from 2000 to 2010 agricultural land again decreased and in the last decade, it had increased by about 10,510 acres. The LULC time series analysis between 1990 and 2020 indicates an expansion of the agricultural land and an increase of urban area with a reduction in forest land and rangeland (Table 2.8).

Table 2.9 represents the amount of the transformation of one type of LULC to another type. Forest had been changed into rangeland and urban areas by approximately 8,086 and 3,905 acres respectively in the last three decades. Agricultural land transformed into rangeland (852 acres) and urban area (674 acres) mostly from 1990 to 2020. Meanwhile, during the same period, rangeland changed into the agricultural area (5,380 acres) and urban area (2,080 acres).

2.3.2 Sensitivity Analysis

Table 2.4 represents the fifteen parameters used to calibrate and validate the stream flow. Based on sensitivity analysis, fifteen parameters were used such as curve number (CN), biological mixing efficiency (BIOMIX), Manning's "n" value for overland flow (OV_N), peak rate adjustment factor (PRF), exponent parameter for calculating sediment re-entrained in channel sediment routing (SPEXP), USPE equation (USLE_P), plant and soil evaporation factor (ESCO and EPCO) and groundwater (ALPHA_BF, GW_DELAY, GW_REVAP, and RCHRG_DP). SOL_LABP, SOL_ORGP, LAT_ORGN, and SOL_ORGN were used to calibrate the nitrogen and phosphorus flow in the watershed.

These parameters had a significant impact on the stream flow. Table 2.5 is showing the list of the parameters that is the ranking of the parameters based on the t-stat and p-value. The highest value of t-stat and lowest value of p-values, the highest influence of that parameter, and vice versa. Based on the values, ESCO, ULSE_P, and BIOMIX are the most effective parameters, and SOL_AWC, OV_N, RCHRG_DP have less impact on the calibration and validation of the model.

2.3.3 SWAT Model Calibration and Validation

The graphs showing the observed and simulated monthly stream flow, total nitrogen and phosphorus period are shown in Figure 2.7 A, B and C respectively. The differences in average monthly observed simulated and values of stream flow were less than 1% (Table 2.7). The R^2, NSE and PBIAS values for streamflow for the calibration and validation periods are listed in Table 2.6. Based on the classified value stated by Moriasi et al. (2015), the SWAT model showed a very good level in the NSE for calibration (0.77) and validation (0.73). Adjustment between the observed, calibrated, and validated stream flow reached a good level for an R^2 of .81

for both calibration and validation. A good classification was obtained for PBIAS, with values of -10.7% and −15.4% for calibration and validation respectively.

The observed and simulated total nitrogen and phosphorus at a monthly time-step from January 1991 to September 2004 are shown in Figures 2.7 B and C. According to the classification by Moriasi et al. (2007), the SWAT model calibrated and validated the nitrogen and phosphorus satisfactorily in the determination coefficient (Table 2.5).

2.3.4 The relationship among Flow, Nitrogen, Phosphorus, and LULC

The relationship between stream flow and LULC, nitrogen, and LULC and phosphorus and LULC is shown by the Figure 2.8 (A), (B), and (C) respectively. The effect of the stream flow, nitrogen, and phosphorus was estimated for the 30-year study period (1990-2020) by running for the LU_1990, LU_2000, LU_2010, and LU_2020 scenarios. The greatest differences in the total stream flow between LU_1990 and LU_2000 and between LU_2010 and LU_2020, with a decrease of around 12 m^3/s and 21 m^3/s respectively. These differences from 1990 to 2000 were characterized by increasing urban area and agricultural land by 1,293 and 894 acres respectively and increasing stream flow from 2010 to 2020 were influenced by increasing agricultural land and urban area by 10,510 acres and 1,423 acres respectively. Moreover, comparing LU_1990 and LU_2020, total monthly stream flow increased about 38 m^3/s and it can be explained by changing LULC that is increasing agricultural land by 11045 acres and urban area by 3,350 acres. Also, the same behavior was noticed in the stream flow between LU_2000 and LU_2010, by increasing stream flow by about 5 m^3/s. This behavior can be described by decreasing agricultural land and increasing rangeland by about 7278 acres (Table 2.8 and figure 2.5).

Both nitrogen and phosphorus had an increasing trend over the last three decades. From 1990 to 2020, 1,136,919 kg nitrogen and 2010 to 2020,768893 kg nitrogen increased and this can be explained by increasing agricultural land by about 11045 and 10510 acres respectively. Though from 1990 to 2020, 324467 kg of phosphorus had increased and most of the phosphorus (around 253975 kg) increased in the last decades (2010-2020) (Table 2.8 and Figure 2.7 B and C).

2.3.5 Impacts on the Hydrological Components of the Changing LULC

The seasonal averages from 1990 to 2020 of evapotranspiration (ET), percolation (PERC), surface runoff (SURQ), lateral flow (LAT_Q), groundwater flow (GW_Q), and water yield (WYLD) for LU_1990 and LU_2020 is represented by figure 2.9. On one hand, ET had an increasing trend in all seasons but specifically, it was noticed in the spring and summer seasons because the highest precipitation occurs in those two seasons and temperature is also high. On the other hand, The PERC values represented the growing trend in all seasons and this trend can be described by the changing LULC over the period. LAT_Q increased over time and particularly a sharp increasing trend in the fall and winter season. However, SURQ and GW_Q had a decreasing trend and both had a positive relationship with the total stream flow. The depletion of GW can be caused by the increasing agricultural area because agriculture needs groundwater recharge and plants uptake groundwater also urban areas (impermeable surface) prevents to water to absorb by the surface. SURQ and GW_Q decreased mostly in the spring and summer seasons.

For scenarios LU_1990 and LU_2020, the impact of changing LULC (Figure 2.6) from 1990 to 2020 on the hydrological components over the average monthly values and their relative changes are depicted in figure 2.10 and table 2.10. A general increasing trend can be observed in monthly ET. A significant increase is noticed in May, June, and July at about 4.43 mm, 8.93 mm, and

6.56 mm respectively. The annual average of increasing ET value is 1.77 mm (Table 2.10) and it can be associated with the increase of agricultural land by 11,045 acres between 1990 and 2020. PERC had a decreasing trend over the three decades on a monthly scale with -5.38 mm. Both SURQ and LAT_Q had a growing trend in the relative changes on a monthly scale for the period between LU_1990 and LU_2020. LAT_Q ranges from 0.17 mm in July to 0.60 mm in January. Monthly variations for SURQ range from -0.59 mm in July to 2.91 mm in April, with an annual average increase of 1.51 mm (Table 2.10, Figure 2.10 A and B). GW_Q had shown a decrease for all the months of the year with relative changes ranging from -2.18 mm in February to -11.10 mm during august with an annual average decrease of -5.12 mm. Both PERC and GW_Q had decreasing trends all over the month and it can be related in such a way that reducing PERC can cause the decreasing water availability from the bottom layer of the soil to the shallow aquifer thus creating a negative impact on the GW_Q. Moreover, the WYLD also had shown a negative trend all over the month in a year ranging from -0.4 mm in March to -10.58 mm during July (Table 2.10). A -3.56 mm decrease in the relative annual average WYLD between 1990 and 2020 can be the result of the decreasing trend of WYLD because reducing GW_Q accelerates the negative trend of the WYLD.

2.4 Discussion

2.4.1 Hydrological Modeling

SWAT modeling is one of the most widely used and recognized models in terms of simulating water balance components within a watershed (Tuppad et al., 2011 and Thai et al., 2017). However, the software has some limitations associated with a large number of input parameters. According to Nyeko (2014) and Saxton and Rawls (2006), some parameters must be obtained or estimated from global databases, equations, or other software. However, the SWAT has been

tried with continuous development in its geospatial structure to represent the physical characteristics of the landscape as realistically as possible (Bosch et al., 2010, Bonuma et al., 2014 Rathjens et al., 2015 and Sun et al., 2015). In this study, the different scenarios of LULC data were obtained from the USGS earth explorer data hub and the LULC were derived from the unsupervised classification using ERDAS imagine software. The weather data were available for only one station, however, by choosing the right parameters and performing good calibration, these weather data can be used with satisfactory results, as it was used in the present study. The simulation of nitrogen and phosphorus were difficult due to the availability of observed data. The error statistics for calibrations and validations obtaining by SWAT-CUP range from 'satisfactory to good' categories according to Moriasi et al. (2005). The use of the same period for one calibration and validation allowed for better results of the different water balance components on monthly, seasonal and annual scales under different LULC scenarios.

2.4.2 Water Balance Components Under Different Land-Use Scenarios

The study shows that changing LULC that occurred from 1990 to 2020 in the Big Creek Lake watershed were characterized by a substantial increase in agricultural land and expansion of the urban area. These results complement the study of the comparison of temporal images of LULC for the watershed that was done by Ellis et al. (2008) and another study conducted by MAWSS (2011). Both studies stated urban area expansion and the percentage of high residential areas and low residential areas is 2.3% and 10.1% respectively. A Previous work conducted by Auburn University relied on Landsat Thematic Mapper satellite images for 1984,1992, and 1995 to identify changes in land use in the Big Creek Lake watershed over time (Reutebuch and others, 1997). The most dramatic change was noticed as net regrowth of forest cover from 1984 to 1992, and that was followed by a net loss of forest in 1995. However, minimal change was observed in

agricultural lands. The significant impact of changing LULC directly have impacts the behavior of the hydrological cycle components. According to Moran-Tejeda et al. (2014), ET is the key element to understand the impact of changing LULC on water production. The increase of 1.77 mm per year of ET between LU_1990 and LU_2020 could be caused by the increase in agricultural land. This result agrees with the statement by Neitsch et al. (2005) that the SWAT model estimates the ET based on the water intercepted by the plant canopy, the maximum plant transpiration rate, and the maximum soil evaporation rate. Esen and Uslu (2008) compared various cropland and found dry croplands to produce the highest runoff. He (2003) simulated a watershed model which showed that expansion of urban areas is likely to increase in surface runoff as well as peak flow. Another study by Corbett et al. (1997), stated the runoff from the urban area is much higher than the forested one in the South Carolina coast.

PERC had decreased by -5.38 % from LU_1990 to LU_2020. On the other hand, LAT_Q and SURQ had been increased and this increasing LAT_Q and SURQ accelerated the total stream flow by about 38 m3/s over the last three decades. According to Cristina et al. (2015), they have reported that a reduction of forested areas reduces increases surface runoff (SURQ) and stream flow, particularly during the rainy season. When forestland is converted into agricultural land, soil compaction reduces infiltration due to cattle ranching, decreasing organic matter and hence increase overland flow in agricultural land compared to forest land (Biggs et al., 2006 and Moraes et al. 2006). Another factor is a large fraction of precipitation becomes surface runoff (SURQ) because of reduced infiltration. According to Lin et al. (2015) and Yan et al. (2013), deforestation and urbanization usually decrease percolation, increase SURQ, and lead to increase in runoff. According to Lampartar et al. (2016), changing LULC could have negative impacts on water balance components, such as decreased evapotranspiration (ET) and infiltration as well as

the increase in streamflow (Q) and surface runoff (SURQ). These can have a direct or indirect influence on the functions and services of the hydro systems and biodiversity conservation.

2.4.3 The Increasing Nitrogen and Phosphorus Under Changing LULC

The increasing LAT_Q and SURQ complement the increase of total nitrogen and phosphorus in the watershed by 1,136,919 kg and 32,4467 kg respectively over the past thirty years. Lateral flow and surface runoff contribute to the stream flow and these two types of flow also carry the pollutants from the agricultural land. According to Journey and Gill (2001), the percentage of agricultural lands is highest in the Crooked Creek subbasin, accounting for over 41% of the subbasin. Much of the land in the subbasin is designated as row crops. Hamilton Creek has also the highest percentage of agricultural land (36.1 %).

Potential sources of nutrients in the Big Creek Lake watershed are from nonpoint contributions associated with fertilizer applications on agricultural and residential land, livestock wastes, residential runoff, failing septic systems, contaminated groundwater. No known point sources are located in the Big Creek Lake watershed. According to Journey and Gill (2001), the total annual nutrient loads to Big Creek Lake for the 1991 water year were 118,000 kg for total nitrogen and 5,245 kg for total phosphorus. As population growth continues, the conversion of forested areas to agriculture and urban areas, loadings of nutrients are expected to increase because most of the land use is converted to urban areas. Basnyat et al. (2000) showed that forests act as nitrite linkage and thus reduce pollution rates and woodlands have low hydrological activities due to high surface storage in leaves.

A study conducted by Gill et al. (2005) and prepared in cooperation with MAWSS and concluded that total nitrogen (except for Long Branch), total Kjeldahl nitrogen (except for

Hamilton Creek), total organic nitrogen (except Boggy Branch), ammonia (except Long Branch), total inorganic nitrogen, and total phosphorus (except for Long and Boggy Branches) exhibited a significant, positive relation with streamflow, which indicates the dominant source of nutrient input to the watershed is from nonpoint sources. The more residential and agricultural subbasins of Crooked Creek and Hamilton Creek, however, yielded over twice the total phosphorus per hectare of land use. Crooked and Hamilton Creek subbasins also had higher total inorganic nitrogen yields. These results complement the present study, that with time, the stream flow increases with the total nitrogen and phosphorus. This increasing nature has a completely positive relation with increasing agricultural land and urban areas.

A significant, positive relation between streamflow and nutrient concentration indicates that nonpoint sources are the dominant source of input. Different land-use practices contribute different levels of nutrients by nonpoint sources. According to study done by Jones and Allain (2001) on the Big Creek Lake watershed, they ranked agricultural land as the highest for run-off risk. A study by Reckhow and others (1980) summarized that nutrient export coefficients for total nitrogen and phosphorus are the smallest for forested land and greatest for agricultural and urban land-use categories. The range in nutrient yields is due to differences in climate, soils, and land-management practices for each category.

2.5 Conclusion

The SWAT model is very significant and useful because it can predict the future hydrological responses**.** This model has the power of stimulating the stream flow, water quality, and the components of the water balance such as ET, PERC, SURQ, LAT_Q, GW_Q, and WYLD.

The total stream flow has been growing by 38 m^3/s, and total nitrogen and phosphorus have been increased by about 113,619 kg and 32,4467 kg respectively over the last three decades. The ET, LAT_Q, SURQ has been increased by 1.77%, 0.35%, and 1.51% respectively but on the other hand, PERC, GW_Q, and WYLD have been decreased by -5.38%, -5.12%, and -3.56% respectively between LU_1990 and LU_2020. These changes have been caused by the decreasing forest and increasing agricultural and urban areas. The results can be used by the decision-makers and public policy changers because this study is quantifying the impact of the changing LULC on the water balance components and water quality and can be used for future projections in terms of LULC changes. If this rate of LULC change is going on, it can have a serious affect on the environment and the people living in Mobile county. Future projection of LULC could be modeled using remote sensing technology and land use models, and simulated future LULC that could be used to assess the impacts of changing LULC on the hydrological components. The changing LULC should be considered by policy makers and planners associated with watershed management for sustainable and effective management of water resources.

References cited-

Abbaspour, K. C., Yang, J., Maximov, I., Siber, R., Bogner, K., Mieleitner, J., Zobrist, J. and Srinivasa, R. 2007, Modelling hydrology and water quality in the pre-alpine/alpine Thur watershed using SWAT. *Journal of Hydrology*, 333(2/4), 413-430. https://doi.org/10.1016/j.jhydrol.2006.09.014.

Abbaspour, K.C.; Rouholahnejad, E.; Vaghefi, S.; Srinivasan, R.; Yang, H.; Kløve, B. 2015, A continental-scale hydrology and water quality model for Europe: Calibration and uncertainty of a high-resolution large-scale SWAT model. *Journal of Hydrology*, 524, 733–752. [CrossRef]

Ahring, R. M., Huffine, W. W., & Taliaferro, M. 1974, Stand establishment of Bermudagrass from Seed. *Agronomy Journal*, 67.

Allen, J. I., P. Somerfield, and F. Gilbert. 2007, Quantifying uncertainty in high-resolution coupled hydrodynamic-ecosystem models. *Journal of Marine System*, 64 (1–4), 3–14. https://doi.org/10.1016/j.jmarsys.2006.02.010.

Allen, M.R., Ingram,W.J. 2002, Constraints on future changes in climate and the hydrologic cycle. *Nature*, 419, 224. [CrossRef]

Arnold, J.G., Allen, P.M., Bernhardt, G. A.1993, Comprehensive surface-groundwater flow model. *Journal of Hydrology*,142, 47–69. [CrossRef]

Arnold, J.G., Kiniry, J.R., Srinivasan, R., Williams, J.R., Haney, E.B. 2012, Soil and water assessment tool input/output documentation. TR-439, Texas Water Resources Institute, College Station, 1-650.

Arnold, J.G.; Raghavan, S.; Ranjan, S.M.; Jimmy, R.W. 1998, Large area hydrologic modeling and assessment part I: Model development. *JAWRA Journal of the American Water Resource Association*, 34, 91–101.

Basnyat, P., Teeter, L.D., Lockaby, B.G., and Flynn, K.N. 2000, The use of remote sensing and GIS in watershed level analyses of non-point source pollution problems. *Forest Ecology and Management*, 128, 65-73.

Beven, K., Binley, A. 1992, The future of distributed models: model calibration and uncertainty prediction. *Hydrological Processes*, 6(3), 279-298.

Bhuyan, S.J., Koelliker, J.K., Marzen L.J., and Harrington J.A 2003, An integrated approach for

water quality assessment of a Kansas watershed, *Environmental Modelling & Software*, 18, 473-484,

Bicknell, B.R., Imhoff, J.C., Kittle, J.L., Jr., Donigian, A.S., Jr., Johanson, R.C. 1996, Hydrological Simulation Program-FORTRAN. User's Manual for Release 11; US EPA: Athens, Greece.

Biggs, T.W., Dunne, T., Muraoka, T. 2006, Transport of water, solutes and nutrients from a pasture hillslope, southwestern Brazilian Amazon. *Hydrological Process*, 20, 2527–2547. [CrossRef]

Bonumá, N.B., Rossi, C.G., Arnold, J.G., Reichert, J.M., Minella, J.P., Allen, P.M., Volk, M. 2014, Simulating Landscape Sediment Transport Capacity by Using a Modified SWAT Model. *Journal of Environmental Quality*, 43, 55–66. [CrossRef]

Bosch, D.D., Arnold, J.G., Volk, M., Allen, P.M. 2010, Simulation of a Low-Gradient Coastal Plain Watershed Using the SWAT Landscape Model. Transaction of the Society of Agricultural and Biological Engineers (ASABE), 53, 1445–1456. [CrossRef]

Butler G.B., & Srivastava, P. 2007, An Alabama BMP database for evaluating water quality impacts of alternative management practices. American Society of Agricultural and Biological Engineers, 23(6), 727–736.

Chaubey, I., Migliaccio, K. W., Srinivasan, R., H, G. C., & Arnold, J. G. 2006, Phosphorus Modeling in Soil and Water Assessment Tool (SWAT) Model, 163–188.

Coe, M.T., Costa, M.H., Soares-Filho, B.S. 2009, The influence of historical and potential future deforestation on the stream flow of the Amazon River—Land surface processes and atmospheric feedbacks. *Journal of Hydrology*, 369, 165–174. [CrossRef]

Corbett, C.W., Wahl, M., Porter, D.E., Edwards, D., and Moise, C. 1997, Nonpoint source runoff modeling a comparison of a forested watershed and an urban watershed on the South Carolina Coast. *Journal of Experimental Marine Biology and Ecology*, 213, 133-149.

Cristina, L., Dias, P., Macedo, M.N., Heil, M., Coe, M.T., Neill, C. 2015, Effects of land cover change on evapotranspiration and streamflow of small catchments in the Upper Xingu River Basin, Central Brazil. *Journal of Hydrology*, 4, 108–122. [CrossRef]

Crossmann, J., Futter, M.N., Oni, S.K., Whitehead, P.G., Jin, L., Butterfield, D., Baulch, H.M.,

Dillon, P.J. 2013, Impacts of climate change on hydrology and water quality: Future proofing management strategies in the Lake Simcoe watershed, Canada. *Journal of Great Lakes Resources*, 39, 19–32. [CrossRef]

Danish Hydraulic Institute (DHI). 1993, MIKE SHE WM—water movement module, A short description; Danish Hydraulic Institute: Hørsholm, Denmark.

De Moraes, J.; Schuler, A.E.; Dunne, T.; Figueiredo, R.O.; Victoria, R.L. 2006, Water storage and runoff processes in plinthic soils under forest and pasture in Eastern Amazonia. *Hydrological Process*, 20, 2509–2526. [CrossRef]

Dowd, B.M., Press, D., and Huertos, M.L. 2008, Agricultural nonpoint source water pollution policy: The case of California's Central Coast. *Agriculture, Ecosystems and Environment*, 128, 151-161.

EPA. 2012a. Nonpoint Source Pollution: The Nation's Largest Water Quality Problem. [http://water.epa.gov/polwaste/nps/outreach/point1.cfm]. Last accessed 2 January 2021.

EPA. 2012b. What is Nonpoint Source Pollution? [http://water.epa.gov/polwaste/nps/whatis.cfm]. Last accessed 2 January 2021.

EPA. 2012c. Managing Nonpoint Source Pollution from Forestry. [http://water.epa.gov/polwaste/nps/outreach/point8.cfm]. Last accessed 2 January 2021.

Esen, E. and Uslu, O. 2008, Assessment of the effects of agricultural practices on non-point source pollution for a coastal watershed: A case study Nif Watershed, Turkey. *Ocean & Coastal Management*, 51, 601-611.

Gao, G., Fu, B., Wang, S., Liang,W., Jiang, X. 2016, Determining the hydrological responses to climate variability and land use/cover change in the Loess Plateau with the Budyko framework. *Science of the Total Environment*, 557, 331–342. [CrossRef]

Gassman, P.W., Reyes, M.R., Green, C.H., Arnold, J.G. 2005, SWAT peer-reviewed literature: A review. In Proceedings of the 3rd International SWAT Conference, Zurich, Switzerland, 13–15 July 2005.

Gill, A.C., McPherson, A.K., and Moreland, R.S. 2005, Water quality and simulated effects of urban land-use change in J.B. Converse Lake watershed, Mobile County, Alabama, 1990–2003: U.S. Geological Survey Scientific Investigations Report 2005–5171, 110 p.

Hargreaves, G. and Samani, Z.A. 1985, Reference crop evapotranspiration from temperature. *Applied Engineering in Agriculture*, 1, 96–99. [CrossRef]

He, C. 2003, Integration of geographic information systems and simulation model for watershed management. *Environmental Modeling & Software*, 18: 809-813.

Jacobs J.H. and Srinivasan R., 2005, Effects of curve number modification on runoff estimation using WSR-88D rainfall data in Texas watersheds, *Journal of Soil and Water Conservation*, 60 (5), pp 274-278.

Jain, M., Sharma, S.D. 2014, Hydrological modeling of Vamshadara River Basin, India using SWAT. International Conference on Emerging Trends in Computer and Image Processing (ICETCIP-2014), Pattaya, Thailand.

Jarsjö, J., Asokan, S.M., Prieto, C., Bring, A., Destouni, G. 2012, Hydrological responses to climate change conditioned by historic alterations of land-use and water-use. *Hydrological Earth System Science*, 16, 1335–1347. [CrossRef]

Journey, C.A. and Gill, A.C. 2001, Assessment of water-quality conditions in the J.B. Converse Lake Watershed, Mobile County, Alabama, 1990-98. U.S. Geological Survey Water-Resources Investigations Report 01-4225. [http://pubs.er.usgs.gov/publication/wri014225]. Last accessed 28 December 2020.

Kamali, Bahareh & Houshmand Kouchi, Delaram & Yang, Hong & Mikayilov, Fariz. 2017, Multilevel drought hazard assessment under climate change scenarios in semi-arid regions—A case study of the Karkheh River Basin in Iran. *Water*, 9, 10.3390/w9040241.

Kuczera, G., Parent, E. 1998, Monte Carlo assessment of parameter uncertainty in conceptual catchment models: The Metropolis algorithm. *Journal of Hydrology*, 211(1/4), 69-85.

Lam, Q.D., Schmalz, B., Fohrer, N. 2012, Assessing the spatial and temporal variations of water quality in lowland areas, Northern Germany. *Journal of Hydrology*, 438, 137–147. [CrossRef]

Lee, S.J. and Berbery, E.H. 2012, Land cover change effects on the climate of the La Plata Basin. *Journal of Hydrometeorology*, 13, 84–102. [CrossRef]

Li, Z., Liu, W. Z., Zhang, X.C., Zheng, F.L. 2009, Impacts of land use change and climate variability on hydrology in an agricultural catchment on the Loess Plateau of China. *Journal of Hydrology*, 377, 35–42. [CrossRef]

Lima, L.S., Coe, M.T., Soares Filho, B.S., Cuadra, S.V., Dias, L.C.P., Costa, M.H., Lima, L.S.,

Rodrigues, H.O. Feedbacks between deforestation, climate, and hydrology in the Southwestern Amazon: Implications for the provision of ecosystem services. *Landscape Ecology*, 2014, 29, 261–274. [CrossRef]

Lin, B., Chen, X., Yao, H., Chen, Y., Liu, M., Gao, L., James, A.2015, Analyses of landuse change impacts on catchment runoff using different time indicators based on SWAT model. *Ecological Indicators*, 58, 55–63. [CrossRef]

Liu, Z., Yao, Z., Huang, H., Wu, S., Liu, G.2014, Land use and climate changes and their impacts on runoff in the Yarlung Zangbo river basin, China. *Land Degradation and Development*, 25, 203–215. [CrossRef]

Loucks, D.P., Van Beek, E., Stedinger, J.R., Dijkman, J.P.M., Villars, M.T. 2005, Water resources systems planning and management and applications: An introduction to methods, models and applications. United Nations Educational (UNESCO): Bangalore, India, pp. 39–56, ISBN 92-3-103998-9.

Marland, G. 2003, The climatic impacts of land surface change and carbon management, and the implications for climate-change mitigation policy. *Climate Policy*, 3, 149–157. [CrossRef]

Marshall, L., Nott, D., Sharma, A.2004, A comparative study of Markov chain Monte Carlo methods for conceptual rainfall-runoff modeling. *Water Resources Research*, 40(2), 1-11. Mobile Area Water and Sewers Systems (MAWSS). 2011, Water System. [http://www.mawss.com/waterSystem.html]. Last accessed 31 December 2020.

Mirhosseini, G., Ph, D., Asce, S. M., Srivastava, P., & Ph, D. 2016a, Effect of irrigation and climate variability on water quality of coastal watersheds: case study in Alabama. *Journal of Irrigation and Drainage Engineering*, 142(2), 1–11.

Monteith, J. L. 1965, Evaporation and environment. Symposia of the Society for Experimental Biology, 19, 205-234.

Morán-Tejeda, E., Zabalza, J., Rahman, K.; Gago-Silva, A., López-Moreno, J.I., Vicente-Serrano, S., Beniston, M. 2014, Hydrological impacts of climate and land-use changes in a mountain watershed: Uncertainty estimation based on model comparison. *Ecohydrology,* 8, 1396–1416. [CrossRef]

Moriasi, D. N., Gitau, M.W., Pai, N. and Daggupati, P. 2015, Hydrologic and water quality

models: performance measures and evaluation criteria. Transaction of the Society of Agricultural and Biological Engineers (ASABE), 58 (6), 1763-1785. https://doi.org/ 10.13031/trans.58.10715.

Neitsch, S.L., Arnold, J.G., Kiniry, J.R., Williams, J.R. 2002, Soil and Water Assessment Tool (SWAT) User's Manual; Version 2000; Grassland Soil and Water Research Laboratory: Temple, TX, USA; Texas Water Resources Institute: Collage Station, TX, USA,pp. 1–506.

Neitsch, S.L., Arnold, J.G., Kiniry, J.R., Williams, J.R. 2011, Soil and water assessment tool theoretical documentation version 2009; Texas. Water Resources Institute: College Station, TX, USA.

Neitsch, S.L., Arnold, J.G., Kiniry, J.R., Williams, J.R. 2005, Soil and water assessment tool theoretical documentation. version. Texas A&M AgriLife Blackland Research & Extension Center: Temple, TX, USA.

Nie, W., Yuan, Y., Kepner, W., Nash, M.S., Jackson, M., Erickson, C. 2011, Assessing impacts of land use and land cover changes on hydrology for the upper San Pedro watershed. *Journal of Hydrology*, 407, 105–114. [CrossRef]

Nyeko, M. 2014, Hydrologic modelling of data scarce basin with SWAT model: capabilities and limitations. *Water Resources Management*, 29, 81–94. [CrossRef]

Pan, S., Liu, D., Wang, Z., Zhao, Q., Zou, H., Hou, Y., Liu, P., Xiong, L. 2017, Runoff responses to climate and land use/cover changes under future scenarios. *Water*, 9, 475. [CrossRef]

Pitman, A.J. 2003, The evolution and revolution in land surface schemes designed for climate models. *International Journal of Climatology*, 23, 479–510. [CrossRef]

Priestley, C., Taylor, R.1972, On the assessment of surface heat flux and evaporation using large-scale parameters. *Monthly Weather Review*, 100, 81–92. [CrossRef]

Rathjens, H., Oppelt, N., Bosch, D.D., Arnold, J.G., Volk, M. 2015, Development of a grid-based version of the SWAT landscape model. *Hydrological Process*, 914, 900–914. [CrossRef]

Refsgaard, J. C. 1997, Parameterization, calibration, and validation of distributed hydrological models. *Journal of Hydrology*, 198, 69–97.

Refsgaard, J.C. and Abbott, M.B. The role of distributed hydrological modelling in water

resources management. In Distributed Hydrological Modelling; Abbott, M.B., Refsgaard, J.C., Eds., Kluwer Academic Publishers: Dordrecht, The Netherlands, 1996; Volume 22, 336p, ISBN 0-7923-4042-6.

Reutebuch, E.M., Bayne, D.R., and Seesock, W.C.1997, Land use/land cover changes in the Big Creek watershed derived from Landsat TM data 1984-1995: Auburn, Alabama, Auburn University, 16 p.

Santhi, C., Srinivasan, R., Arnold, J. G., & Williams, J. R. 2006, A modeling approach to evaluate the impacts of water quality management plans implemented in a watershed in Texas. *Environmental Modelling & Software*, 21(8), 1141–1157.

Saxton, K.E. and Rawls, W.J. 2006, Soil water characteristic estimates by texture and organic matter for hydrologic solutions. *Soil Science Society of American Journal*, 1578, 1569–1578. [CrossRef]

Sertel, E., Robock, A., Ormeci, C. 2010, Impacts of land cover data quality on regional climate simulations. *International Journal of Climatology*, 30, 1942–1953. [CrossRef]

Shaver, B. R., Richardson, M. D., McCalla, J. H., Karcher, D. E., & Berger, P. J. 2006, Dormant seeding bermudagrass cultivars in a transition-zone environment. *Crop Science*, 46(4), 1787–1792. https://doi.org/10.2135/cropsci2006.02-0078

Simić, Z. 2009, SWAT-based runoff modeling in complex catchment areas theoretical background and numerical. *Journal of the Serbian Society for Computational Mechanics*, 3, 38-63.

Srivastava, P., Gupta, A. K., & Kalin, L. 2010, An ecologically-sustainable surface water withdrawal framework for cropland irrigation: A case study in Alabama. *Environmental Management*, 46(2), 302–313.

Sun, X., Garneau, C., Volk, M., Arnold, J.G., Srinivasan, R., Sauvage, S., Sánchez-Pérez, J.M. 2015, Improved simulation of river water and groundwater exchange in an alluvial plain using the SWAT model. *Hydrological Process*, 30, 187–202. [CrossRef]

Sy, S., Noblet-Ducoudre, N., Quesada, B., Sy, I., Dieye, A.M., Gaye, A.T., Sultan, B. 2017, Land-surface characteristics and climate in West Africa: Models' biases and impacts of historical anthropogenically-induced deforestation. *Sustainability*, 9, 1917. [CrossRef]

Thai, T.H., Thao, N.P., Dieu, B.T. 2017, Assessment and simulation of impacts of climate

change on erosion and water flow by using the soil and water assessment tool and GIS: case study in Upper Cau River basin in Vietnam. Vietnam. *Journal of Earth Science*, 39, 376–392. [CrossRef]

Tuppad, P., Douglas-Mankin, K.R., Lee, T., Srinivasan, R., Arnold, J.G. 2011, Soil and water assessment tool (SWAT) hydrologic/water quality model: extended capability and wider adoption. Transaction of the Society of Agricultural and Biological Engineers (ASABE), 54, 1677–1684. [CrossRef]

U.S. Department of Agriculture, 1994, State Soil Geographic (STATSGO) database for Alabama: U.S. Department of Agriculture, Natural Resources Conservation Service, Soil Survey Division, accessed July 31, 2020, at URL http://www.ftw.nrcs.usda.gov/ stat_data.html.

Van Griensven, A.; Meixner, T. 2006, Methods to quantify and identify the sources of uncertainty for river basin water quality models. *Water Science and Technology*, 53(1), 51-59.

Vrugt, J. A., Gupta H.V., Bouten, W. and Sorooshian, S. 2003, A shuffled complex evolution Metropolis algorithm for optimization and uncertainty assessment of hydrologic model parameters. *Water Resources Research*, 39(8), 1-14.

Wang, H., Sun, F., Xia, J., Liu,W. 2017, Impact of LUCC on streamflow based on the SWAT model over the Wei River basin on the Loess Plateau in China. *Hydrology and Earth System Sciences*, 21, 1929. [CrossRef]

Wang, X., Siegert, F., Zhou, A., Franke, J. 2013, Glacier and glacial lake changes and their relationship in the context of climate change, Central Tibetan Plateau 1972–2010. *Global Planetary Change*, 111, 246–257. [CrossRef]

Wei, X.; Zhang, M. 2010, Quantifying streamflow change caused by forest disturbance at a large spatial scale: A single watershed study. *Water Resources Research*, 46, 1–15. [CrossRef]

Welde, K.; Gebremariam, B. 2017, Effect of land use land cover dynamics on hydrological response of watershed: Case study of Tekeze Dam watershed, northern Ethiopia. *International Soil Water Conservation Resources*, 5, 1–16. [CrossRef]

Willams, J. 1969, Flood routing with variable travel time or variable storage coefficients. Transaction of the Society of Agricultural and Biological Engineers (ASABE), 12, 100-103.

Williams, J. 1975, Sediment-yield prediction with universal equation using runoff energy factor. In Present and Prospective Technology for Predicting Sediment Yield and Sources; Agriculture Research Service, US Department of Agriculture: Washington, DC, USA, pp. 244–252.

Williams, J.R., R.C. Izaurralde, and E.M. Steglich. 2008, Agricultural Policy/Environmental eXtender Model: Theoretical documentation version 0604 (Draft). BREC Report # 2008-17. Temple, TX: Texas AgriLIFE Research, Texas A&M University, Blackland Research and Extension Center.

Woldesenbet, T.A.; Elagib, N.A.; Ribbe, L.; Heinrich, J. 2017, Hydrological responses to land use/cover changes in the source region of the Upper Blue Nile Basin, Ethiopia. *Science and Total Environment*. 575, 724–741. [CrossRef] [PubMed]

Yan, B., Fang, N.F., Zhang, P.C., Shi, Z.H. 2013, Impacts of land use change on watershed streamflow and sediment yield: An assessment using hydrologic modelling and partial least squares regression. *Journal of Hydrology*, 484, 26–37. [CrossRef]

Yin, J., He, F., Xiong, Y.J., Qiu, G.Y. 2017, Effects of land use/land cover and climate changes on surface runoff in a semi-humid and semi-arid transition zone in northwest China. *Hydrology and Earth System Sciences*, 21, 183–196. [CrossRef]

Young, R., Onstad, C., Bosch, D., Anderson, W. 1989, AGNPS: A nonpoint-source pollution model for evaluating agricultural watersheds. *Journal of Soil Water Conservation*, 44, 168–1 73.

Zhang, J., Li, Q., Guo, B. and Gong, H. 2015, The comparative study of multi-site uncertainty evaluation method based on swat model. *Hydrological Processes*, 29(13), 2994-3009.

Zhang, M., Liu, N., Harper, R., Li, Q., Liu, K., Wei, X., Ning, D., Hou, Y., Liu, S. 2017, A global review on hydrological responses to forest change across multiple spatial scales: Importance of scale, climate, forest type and hydrological regime. *Journal of Hydrology*, 546, 44–59. [CrossRef]

Zhang, Y., Zhao, Y., Wang, Q., Wang, J., Li, H., Zhai, J. Zhu, Y., Li, J. 2016, Impact of land use on frequency of floods in Yongding River Basin, China. *Water*, 8, 401. [CrossRef]

Table 2.1: Description of acquired images

Sensor	Instrument	Acquired Date	Path	Row	Resolution
Landsat	TM-5	01-10-1990	021	039	30 m
Landsat	TM-5	01-06-2000	021	039	30 m
Landsat	TM-5	02-02-2010	021	039	30 m
Landsat	OLI-TIRS	02-14-2020	021	039	30 m

Table 2.2: Accuracy assessment of the classified images

	Overall Classification Accuracy (%)	Overall Kappa Coefficient
LU_1990	80	0.71
LU_2000	85	0.77
LU_2010	85	0.78
LU_2020	90	0.81

Table 2.3: Management operations for cropland of the study area

Plant Type	**Operation Date**	**Operation Type**	**Operation Attributes**	**Land use**
Bermudagrass	01-March	Planting		Rangeland
	01-July	Harvesting		
Peanut	15-May	Planting		Agricultural land
	21-October	Harvesting		
Cotton	25-March	Tillage	Generic Conservation tillage	
	15-April	Planting		
	15-April	Fertilizer application	45 kg/ha Nitrogen	

	15-April	Fertilizer application	40 kg/ha Phosphorus	
	10-June	Fertilizer application	50 kg/ha Nitrogen	
	15-September	Harvesting		

Table 2.4: Model parameters and their descriptions in surface flow, total nitrogen and phosphorus calculations

Parameter	Parameter Description	Fitted value	Minimum value	Maximum value
ADJ_PKR	Peak rate adjustment factor for sediment routing in sub watershed	2	0.5	2
ALPHA_BF	Baseflow alpha factor (days)	0.1	0	1
BIOMIX	Biological mixing efficiency	0.2	0	1
CN	Curve number	Decrease 20%	35	98
EPCO	Plant evaporation compensation factor	0.95	0	1
ESCO	Soil evaporation compensation factor	1	0	1
GW_DELAY	Groundwater delay time (days)	20	0	500
GW_REVAP	Groundwater “revap” coefficient	0.02	0.02	0.2
OV_N	Manning's "n" value for overland flow "n" value for overland flow	1	0.01	30
PRF	Peak rate adjustment factor for sediment routing in the main channel	1	0	1
RCHRG_DP	Deep aquifer percolation factor	0.05	0	1
SOL_AWC	Available water capacity of soil layer	0.7	0	1
SOL_K	Saturated hydraulic conductivity	0.2	0	2000
SPEXP	Exponent parameter for calculating sediment retrained in channel sediment routing	1.5	1	1.5
USLE_P	USLE equation support practice factor	1	0	1
SOL_LABP	Initial soluble P concentration in sol layer	0.01	0	100

SOL_ORGP	Initial organic P concentration in sol layer	0.01	0	100
LAT_ORGN	Organic N in the baseflow	0.01	0	200
SOL_ORGN	Initial organic N concentration in the soil layer	0.01	0	10

Table 2.5: Sensitive parameters ranking based on t-Stat and p-Value

Parameter Name	t-Stat	p-Value
r__ESCO.bsn	-0.215278727	0.829640698
r__USLE_P.mgt	-0.226950855	0.820557782
r__BIOMIX.mgt	0.227096486	0.820444606
r__ALPHA_BF.gw	-0.278863619	0.780468599
r__SOL_K().sol	0.671455455	0.502250766
r__GW_REVAP.gw	-0.728852367	0.466444494
r__GW_DELAY.gw	0.846668373	0.39759842
r__SPEXP.bsn	-0.969346487	0.332856487
r__EPCO.bsn	1.115696614	0.265105646
r__CN2.mgt	-1.333777787	0.18290399
r__ADJ_PKR.bsn	-1.443612737	0.149494876
r__PRF_BSN.bsn	-1.948062549	0.051985146
r__RCHRG_DP.gw	-1.994993478	0.046603828
r__OV_N.hru	-2.862365089	0.004387183
r__SOL_AWC().sol	-38.3178933	0

Table 2.6: Statistical evaluation of the model for calibration and validation time periods

	R^2		**NSE**		**PBIAS**	
	Calibration	Validation	Calibration	Validation	Calibration	Validation
Stream Flow	0.81	0.81	0.77	0.73	-10.7	15.4
Nitrogen	0.75	0.77	0.62	0.65	9.34	-3.45
Phosphorus	0.5	0.54	0.34	0.24	-20.45	-21.76

Table 2.7: Average annual observed and simulated streamflow, total nitrogen and phosphorus

Variable	Average Annual Value
Average Observed Stream Flow	4.14 m^3/s
Average Simulated Stream Flow	4.16 m^3/s
Average Observed Nitrogen	5157.79 Kg/Ha
Average Simulated Nitrogen	6214.33 Kg/Ha
Average Observed Phosphorus	651.79 Kg/Ha
Average Simulated Phosphorus	1040.19 Kg/Ha

Table 2.8: Area of LULC (acres) for the LU_1990, LU_2000, LU_2010 and LU_2020 and their relative changes

	LULC (Acres)				Relative Change (Acres)			
	LU_1990	LU_2000	LU_2010	LU_2020	1990-2000	2000-2010	2010-2020	1990-2020
Water	3476.90	3212.34	3207.57	3105.90	264.56	4.77	101.67	371.00
Forest	39780.30	39716.30	32168.40	28297.50	64.00	7547.90	3870.90	11482.80
Urban	3321.40	4615.20	5248.02	6671.53	-1293.80	-632.82	-1423.51	-3350.13
Agriculture	2813.51	3707.91	3349.13	13859.49	-894.40	358.78	-10510.36	-11045.98
Rangeland	17409.50	15550.20	22828.60	14867.30	1859.30	-7278.40	7961.30	2542.20

Table 2.9: Area of changing LULC (acres) between 1990-2000, 2000-2010, 2010-2020 and 1990-2020

From	To	1990-2000	2000-2010	2010-2020	1990-2020
Water	**Forest**	303.88	40.88	153.57	155.54
Water	**Agriculture**	7.54	365.07	6.42	2.06
Water	**Rangeland**	18.02	1.35	11.78	10.20
Water	**Urban**	29.69	0.00	3.15	4.60
Forest	**Water**	79.99	83.56	72.12	190.25
Forest	**Agriculture**	1064.39	417.80	855.63	2681.43
Forest	**Rangeland**	2663.39	6446.73	4707.84	8086.32

Forest	**Urban**	1996.45	3607.81	1794.97	3905.79
Agriculture	**Water**	6.02	10.15	0.66	6.37
Agriculture	**Forest**	864.23	552.36	112.02	595.45
Agriculture	**Rangeland**	964.12	2325.02	538.36	852.80
Agriculture	**Urban**	606.61	348.08	313.65	674.76
Rangeland	**Water**	21.38	26.41	14.15	38.47
Rangeland	**Forest**	3782.74	1554.82	2504.36	3530.49
Rangeland	**Agriculture**	1722.49	1688.72	6700.13	5380.06
Rangeland	**Urban**	1782.42	809.48	4101.49	2080.01
Urban	**Water**	4.22	38.99	2.00	8.37
Urban	**Forest**	695.52	1337.47	2170.33	598.22
Urban	**Agriculture**	497.82	431.96	461.21	2.06
Urban	**Rangeland**	18.02	2309.30	2005.74	1091.64

Table 2.10: Monthly relative change of ET, PERC, SURQ, LAT_Q, GW_Q, and WYLD; scenario LU_1990 vs. LU_2020

Monthly Relative Change (%)						
Month	ET	PERC	LAT_Q	SURQ	GW_Q	WYLD
January	0.092967	-2.82793	0.6043	1.7946	-2.98183	-0.80053
February	0.4675	-2.44937	0.433	1.110567	-2.18667	-0.8156
March	0.8779	-4.3346	0.4109	2.379067	-3.00897	-0.4
April	0.651633	-5.6409	0.317233	2.914767	-4.01437	-0.97933
May	4.437667	-5.8051	0.2837	1.494867	-5.02763	-3.489
June	8.936233	-9.27813	0.2335	0.5405	-6.99267	-6.52203
July	6.568333	-13.1515	0.1716	-0.5965	-9.76327	-10.5898
August	-1.64097	-7.82033	0.334767	1.496967	-11.1069	-9.77337
September	0.277067	-3.1561	0.337733	2.0043	-6.19113	-4.27487
October	0.795633	-2.8852	0.256267	1.2022	-3.38637	-2.32613
November	0.011333	-4.7338	0.322533	2.170833	-3.1713	-1.02953
December	-0.15163	-2.51407	0.508767	1.7197	-3.6822	-1.72827
Annual Average	1.776972	-5.38308	0.351192	1.519322	-5.12611	-3.56071

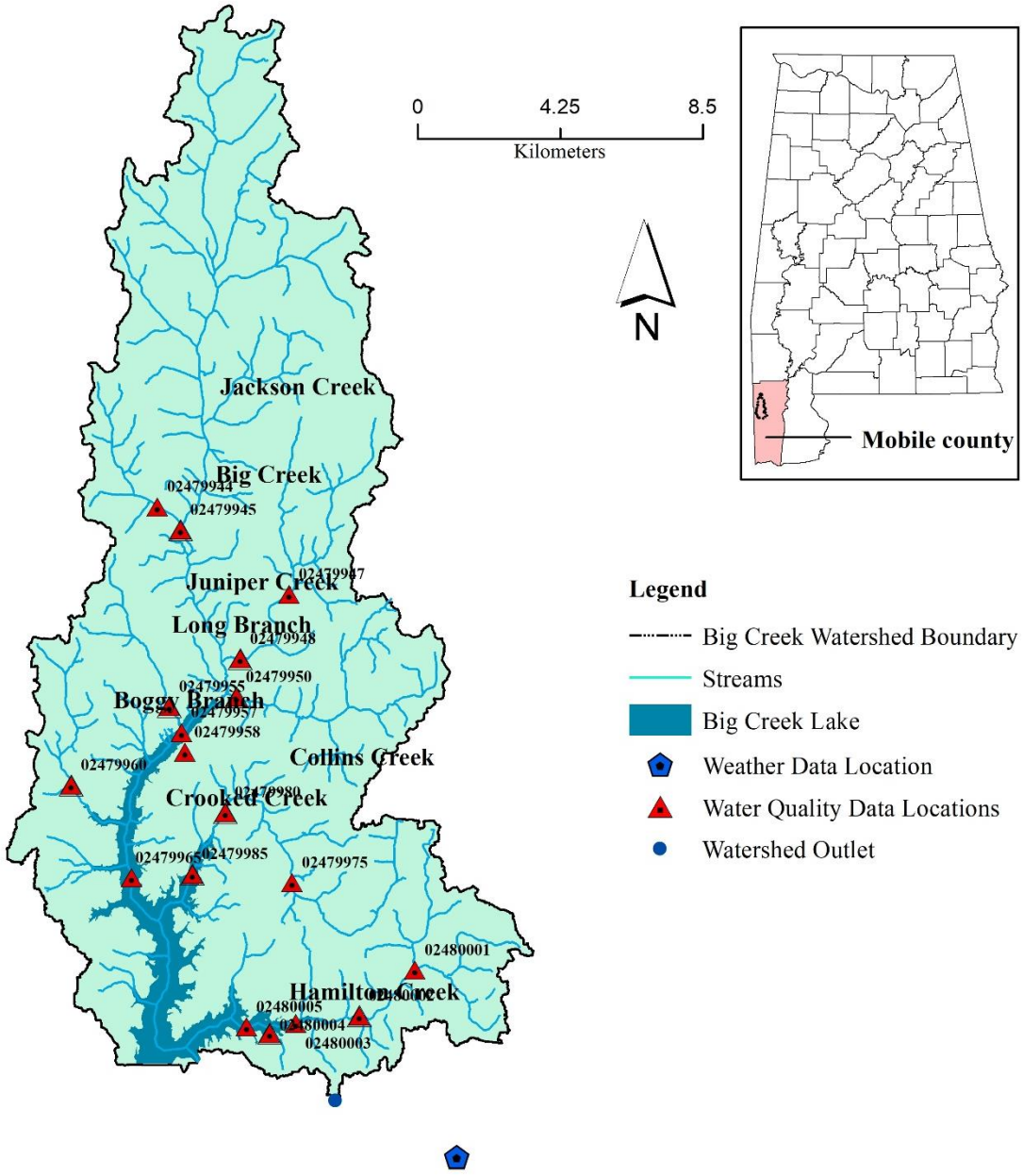

Figure 2.1: Location map of the study area

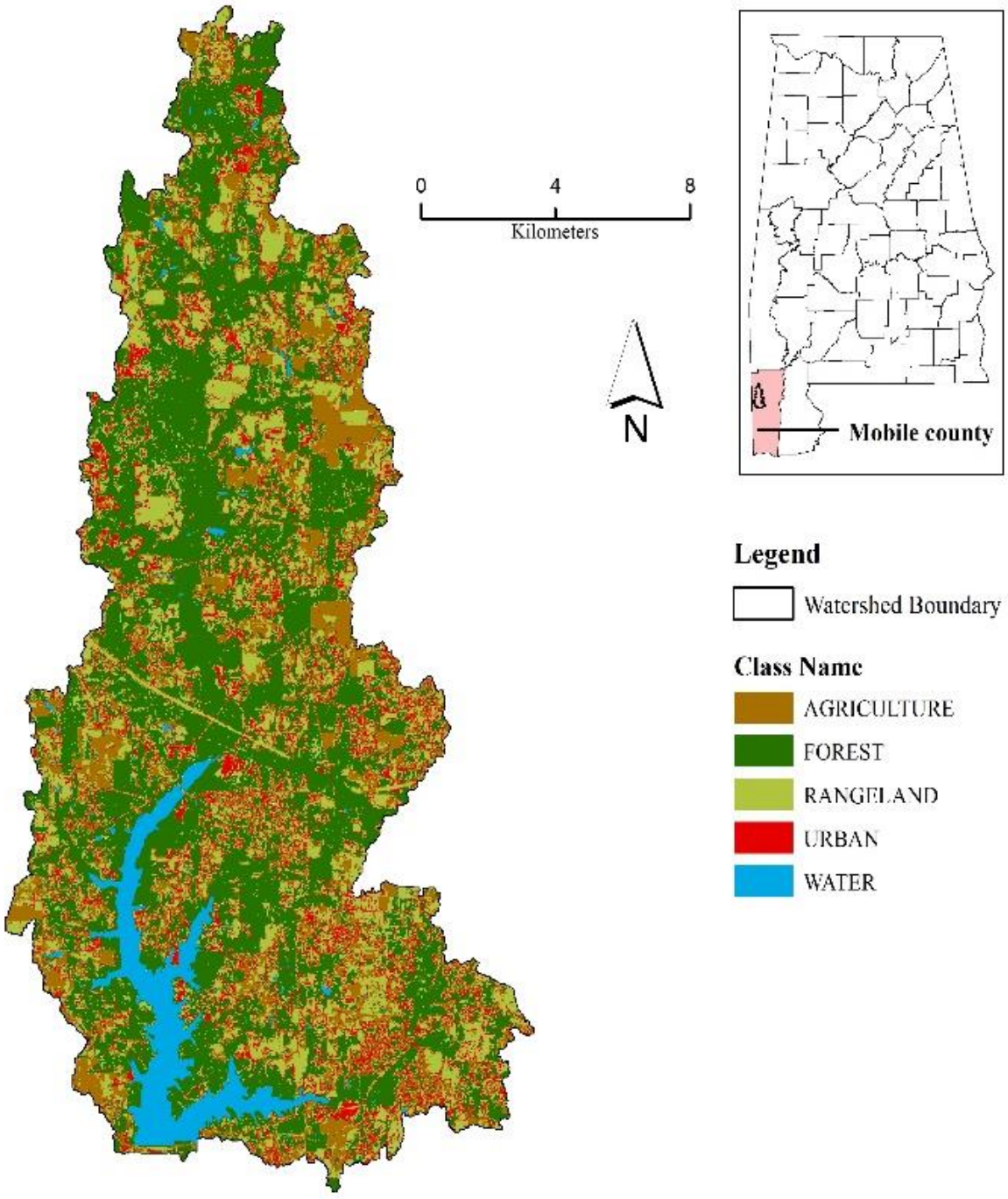

Figure 2.2: land use map of the study area

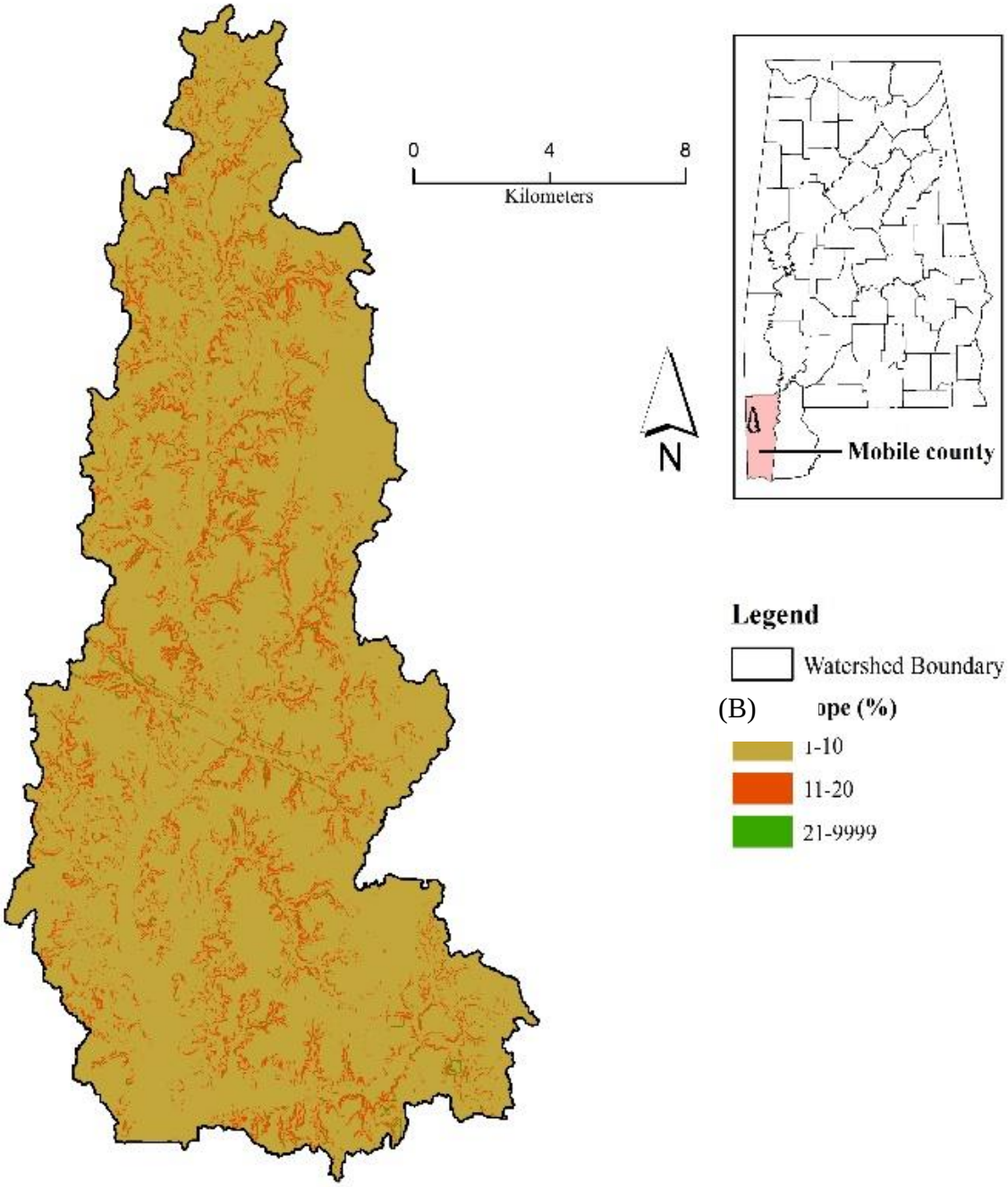

Figure 2.3: Soil class map of the study area

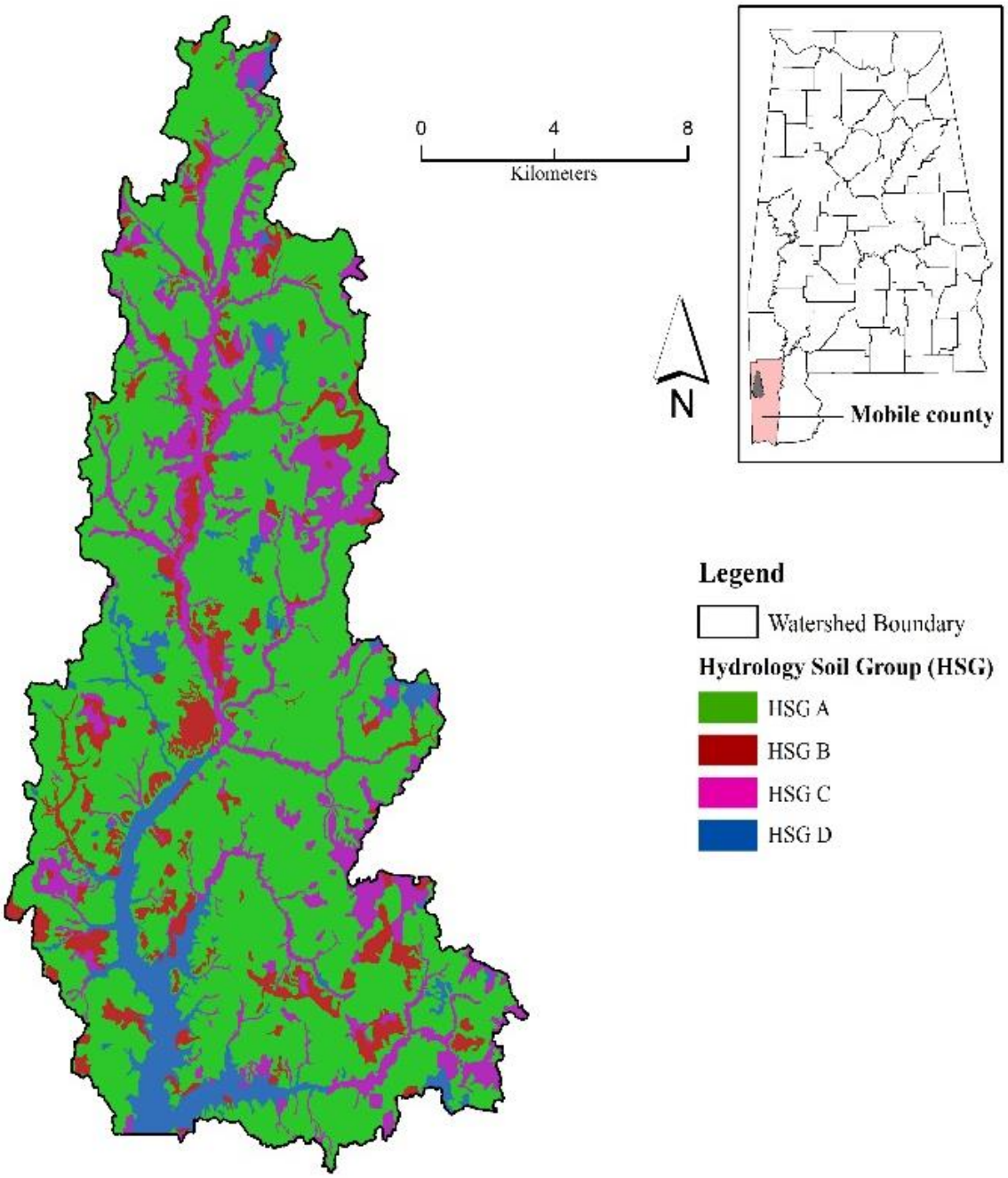

Figure 2.4: Slope class map of the study area

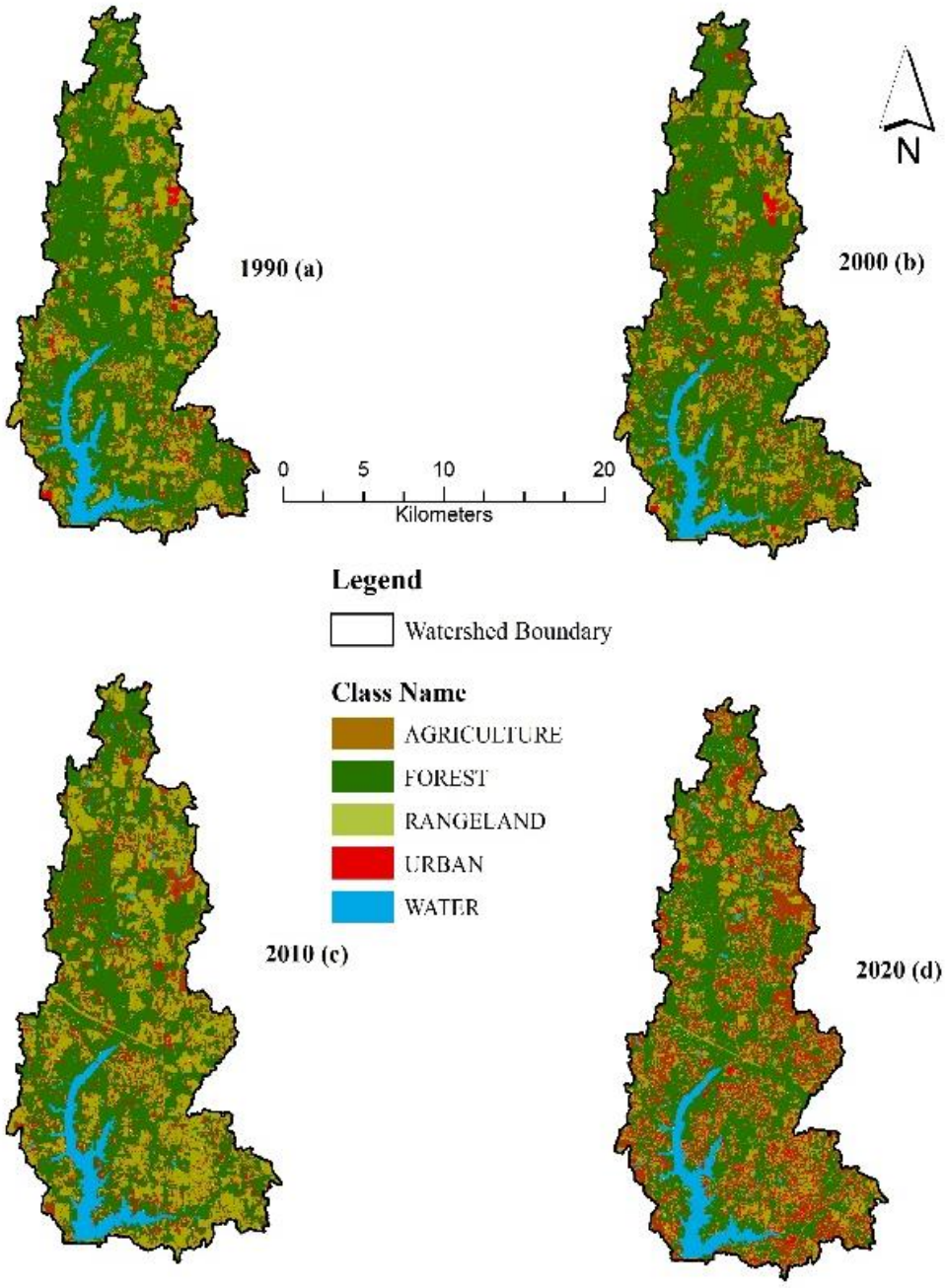

Figure 2.5: Spatial representation of the LULC of the study area for LU_1990 (a), LU_2000 (b), LU_2010 (c) and LU_2020 (d)

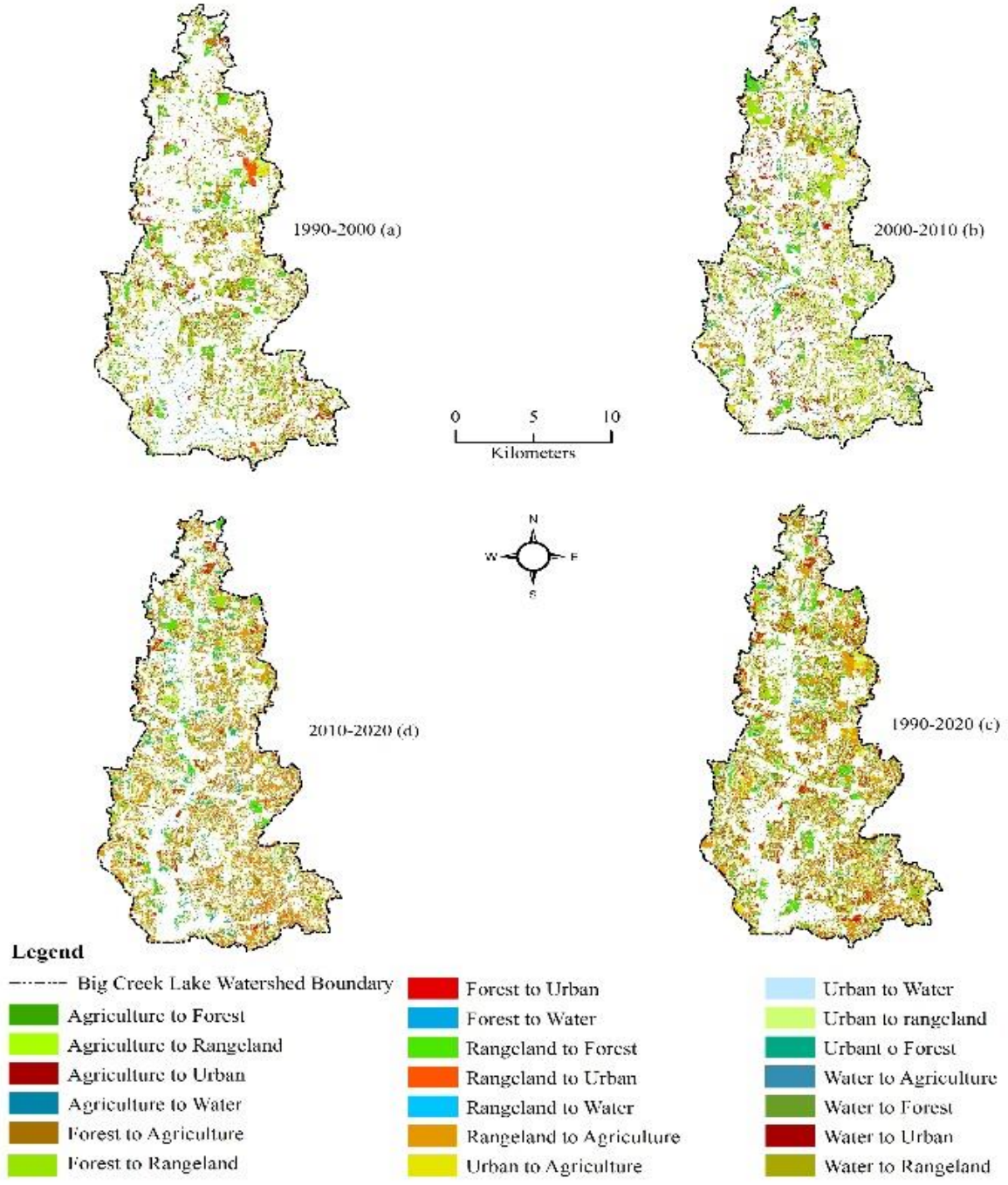

Figure 2.6: Changing LULC of the study area between 1990-2000 (a), 2000-2010 (b), 2010-2020 (c) and 1990-2020 (d)

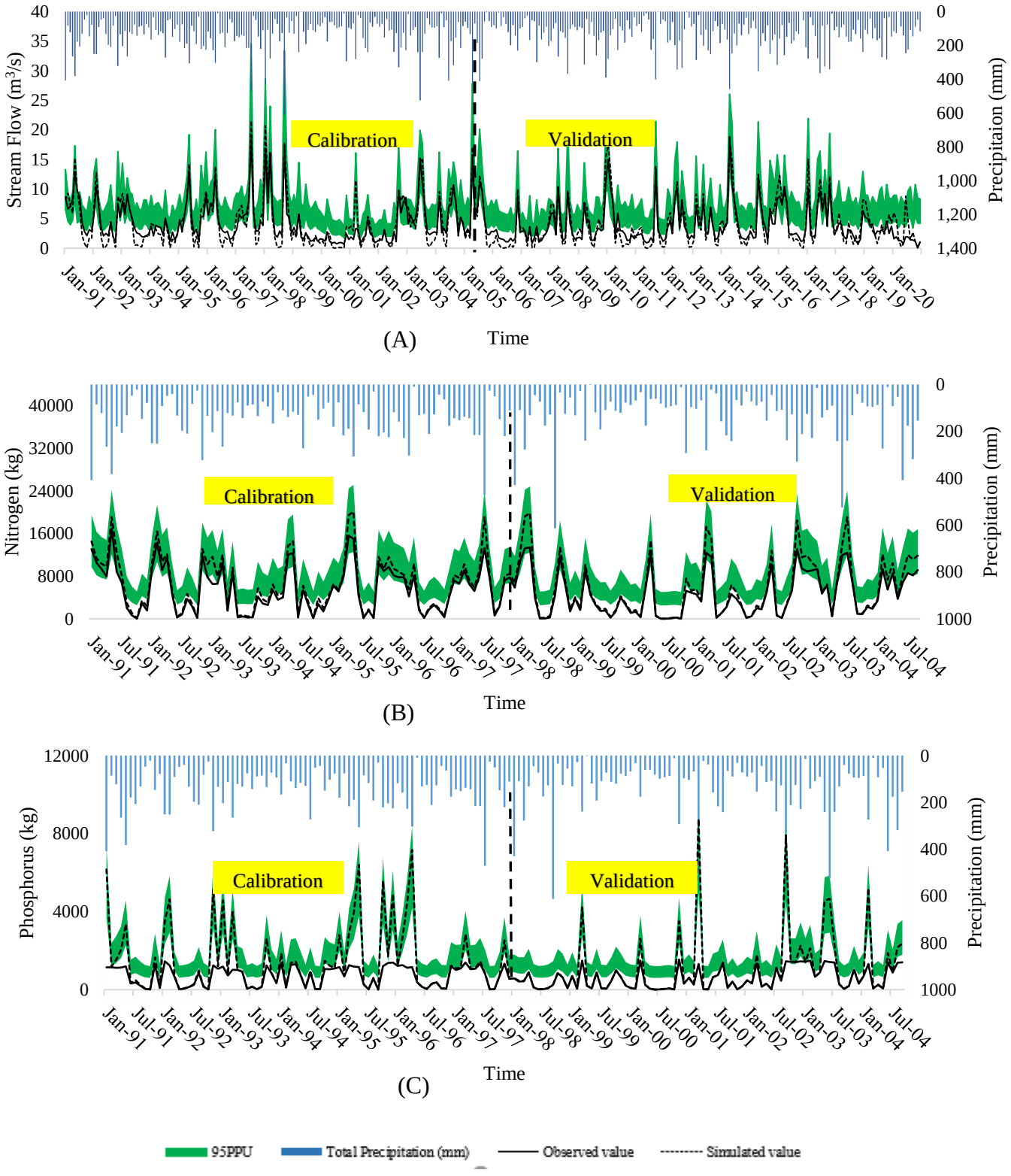

Figure 2.7: Observed vs. simulated stream flow (m^3/s) from 1991-2020 (A), total nitrogen (Kg/Ha) from 1991-2004 (B) and total phosphorus (Kg/Ha) (C) from 1991-2004

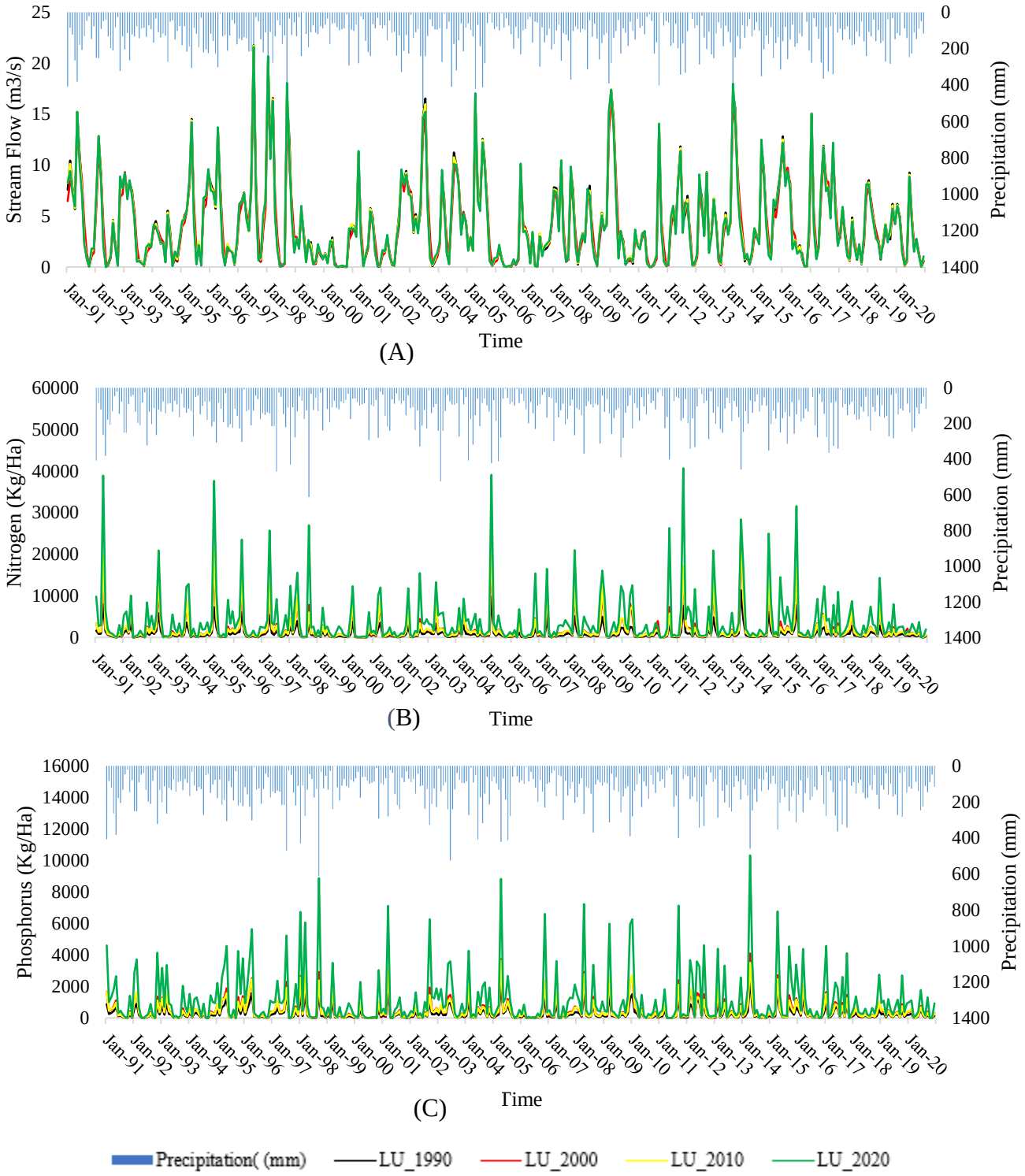

Figure 2.8: Simulated monthly flow (m^3/s) (A), total nitrogen (Kg/Ha) (B) and total phosphorus (Kg/Ha) (C) between 1991–2020 for different LULC scenarios (LU_1900, LU_2000, LU_2010 and LU_2020)

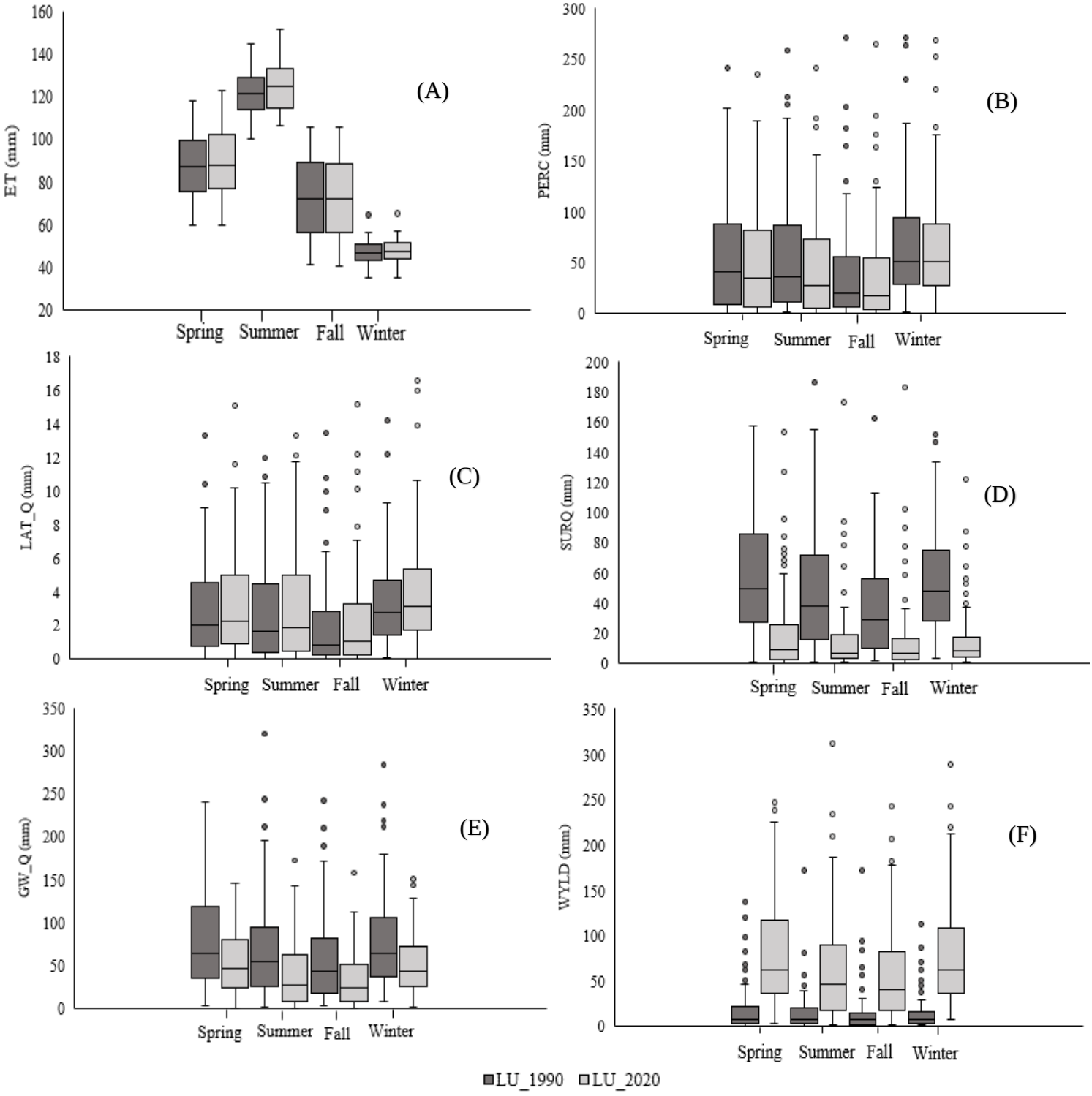

Figure 2.9: Seasonal average: spring (March, April and May), summer (June, July, August), fall (September, October and November) and winter (December, January and February) of the water balance parameters (evapotranspiration (ET) (A), percolation (PERC) (B), surface flow (SURQ) (C), lateral flow (LAT_Q) (D), groundwater (GW_Q) (E), and water yield (WYLD) (F), for the LU_1990 and LU_2020 scenarios.

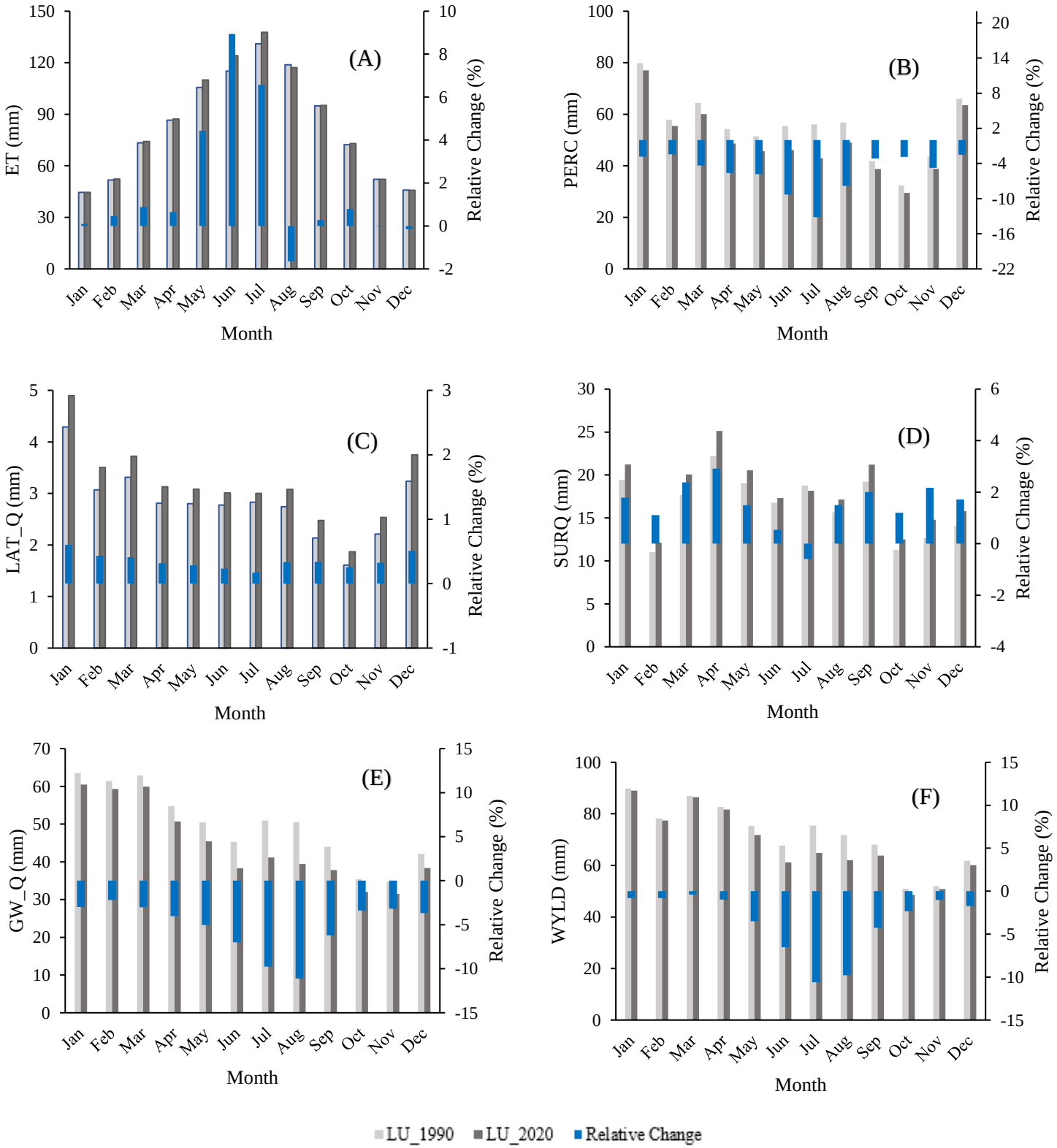

Figure 2.10: Monthly averages and relative changes of ET (A), PERC (B), SURQ (C), LAT_Q (D), GW_Q (E) and WYLD (F) for scenarios LU_1990 and LU_2020.

CHAPTER 3

Modelling Climate Change on Hydrological Response and Nitrogen and Phosphorus of Big Creek Lake Watershed, South Alabama

3.1 Introduction

The changing climate has a significant affect on river discharge, extreme events, and on the availability and quality of water (Betts et al., 2018; Krysanova and Hattermann, 2017; Li et al, 2016; Sorribas et al., 2016; Mehta et al., 2015; Yan et al., 2015; Elliott et al., 2014; Madsen et al., 2014 and Schewe et al., 2014). Climate change and its associated threats are among the utmost challenges of recent times. According to Intergovernmental Panel on Climate Change (IPCC) Fifth Assessment Report, climate change will cause substantial alterations in the quality and availability of water resources. A recent study conducted by Betts et al. (2018) showed that the spatial global trends in extreme precipitation and hydrological events including an increase of 2^0C temperature that water scarcity could reach unprecedented levels in some countries. At the same time, extreme hydrological and climatic events have added more necessity to investigate changes in hydrological processes (Burn et al., 2010; Taye et al., 2011 and Hoang et al., 2016). According to Wu et al., 2013; Allen and Ingram, 2002 and Donat et al., 2016, the hydrological cycle has changed due to climate change. Some investigations concluded that in most of the world extreme precipitation has been observed (Alexander et al., 2006; Westra et al., 2013 and Min et al., 2011) and in the 21st century, extreme precipitation will further increase projections from various climate models (Kharin et al., 2013; Sillmann et al., 2013 and Field et al., 2012) thus posing a threat to water availability and security.

Global increases of mean temperature, changes in the pattern of precipitation, and also an increased frequency and intensity of the extreme events can lead to substantial impact on the water cycle (Klove et al., 2014; Kundzewica, 2008 and Wang et al., 2013), vegetation, and

biodiversity (Linderholm, 2006; Vittoz et al., 2013; Kittel et al., 2013 and Lindner et al., 2014). Both the water quality and quantity are directly and indirectly influenced by climate change (Whitehead et a., 2009; Kundzewicz et al., 2007; Crossmann et al., 2013; Dunn et al., 2012 and Mimikou et al., 2000). According to the United States Environmental Protection Agency (2017), due to increasing temperature and evapotranspiration, water availability is decreasing and the reduced discharge will likely accelerate algal growth and reduce dilution of point source pollutants. Furthermore, climate change would have an impact on the nutrient turnover and transport processes (Denitrification, nitrification, volatilization, and leaching) in the basins because of the changing temperature and precipitation (Whitehead et al., 2006 and Macleod et al., 2012).

To maintain ecosystem services, it is essential to keep an appropriate hydrological balance within a watershed. This is related to the source of water which is different for specific kinds of watersheds (Acreman and Miller, 2007). The services and functions of the watersheds may be altered by rising temperatures and changing patterns of precipitation. Recently, the nutrient loss dynamics are expected due to global warming in watersheds by atmospheric and meteorological properties, such as precipitation patterns, atmospheric water vapor, and evaporation. In recent years, climate change and its qualitative and quantitative aspects of water have been studied (Thakali et al., 2016 and Chen et al, 2008). Integration of climate change into hydrological systems is necessary.

Generally, there are three methods of assessing the hydrological systems due to changing climate which include time series analysis, paired catchment experiments, and hydrological modeling (Li et al., 2009). Hydrological models have often been applied to study the relationship between hydrological processes and climate change (Park et al, 2014; Khoi and Suetsugi, 2014 and Tu,

2009). The use of hydrological models is essential and increasing in recent decades because these modeling outputs can be used for effective planning of quality and quantity of water resources and protection under changing environmental conditions and models can simulate flow regimes under different scenarios. Therefore, various hydrological models have been developed to have an understanding between climate change scenarios and water balance components, through the simulations of the hydrological process within the watersheds. Agricultural Non-Point Source (AGNPS) (Young et al., 1989), Hydrological Simulation Program-FORTRAN (HSPF) (Bicknell et a., 1996), MIKE SHE (DHI, 1993), Soil and Water Assessment Tool (SWAT) (Arnold et al., 1998) and Agricultural Policy/Environmental Extender (APEX) (Williams and Izaurralde, 2008) are some of the models used by various researchers. Many of these hydrological models are applied for streamflow, groundwater, base flow sediment yield, nutrients, pollution and soil loss simulation, and future predictions. Though many researchers have used various models for different purposes, the SWAT model is the most widely used and it has been applied in different areas to analyze numerous problems associated with hydrology and water quantity and quality, including the potential changes to the streamflow under different climate scenarios. Almost 4,000 peer-reviewed articles related to the SWAT model have been published and among these almost 1,000 articles are related to the hydrological responses due to climate changes (Gassman et al., 2010). The SWAT model has significant utilization because it can evaluate water and sediment yield and water quality parameters under present conditions, management practices, and future climate conditions.

3.2 Materials and Methods

3.2.1 Study Area

The Big Creek Lake is a tributary-storage reservoir in Mobile County located in southwest Alabama which has an area of 3,600 acres. Although the lake itself is only 3,600 acres, the watershed area around the lake is approximately 65,920 acres or 103 square miles Mobile Area Water and Sewer System (MAWSS) (MAWSS 2011; Journey and Gill 2001). The Big Creek, Jackson Branch, Juniper Creek, Collins Creek, Long Branch, Boggy Branch, Crooked Creek, and Hamilton Creek are several tributaries feeding by Big Creek Lake which is a central reservoir. Though Mobile County is occupied by the large area of the Big Creek Lake watershed, no large municipalities exist within the watershed. Wilmer and Semmes are two smaller towns including others that are located within the watershed boundaries. Figure 3.1 shows the location of the watershed and the location of the weather and water quality data stations used for modeling. Big Creek Lake watershed is located relatively close to the Gulf Coast and more specifically within the Southern Hills District of the East Gulf Coastal Plain section of the Coastal Plain Physiographic Province. The subtropical climate of the watershed is affected by the Gulf of Mexico's influences. Relative to the rest of the United States, the area encompassing the watershed is ranked second in terms of annual rainfall only to the Pacific Northwest. The soil type of the watershed is mainly Ultisols. Ultisols have characteristics including the well-developed profile that reflect the influence of active factors of soil formation, including well-drained and acidic. The watershed is made of 100% Ultisols and it includes Troup-Heidel-Bama Association, Troup-Benndale-Smithton association, and Shubuta-Troup-Benndale association.

3.2.2 Data Utilized

According to Monteith (1965), Willams (1969), and Arnold et al. (2012), a Digital Elevation Model (DEM) and associated topography, land use and land cover (LULC), and soil data are the spatial inputs that are required datasets to run the Soil Water Assessment Tool (SWAT) model.

Other than these datasets, long-term weather data, water quality data, Land use and Land cover (LULC), soil properties data, and discharge data are required for the model to run. Moreover, several mathematical equations are also used in different analyses. Figure 3.2, 3.3, and 3.4 represent the LULC, slope, and soil data of the analyzed study area respectively.

The USGS National Map was the provider of the DEM datasets and the datasets downloaded from the link (https://viewer.nationalmap.gov/basic/). The spatial resolution is 10 meter which is 1 arc-second (10m * 10m) pixel resolution. For LULC data, Landsat images obtained from the USGS data hub (https://earthexplorer.usgs.gov/) and the latest images (2020) of January were chosen because January has the minimum cloud cover to have the lowest atmospheric effects. Moreover, winter month has the ability to differentiate the different features such as deciduous vs. coniferous forests and lack of crops. An unsupervised approach was performed for classification. The unsupervised classification using Iterative Self-Organizing Data Analysis Techniques (ISODATA) clustering with 20 total clusters, convergence set to 0.995 (on the scale of 0 to 1), 100 iterations, and cluster means initialization along the principal axis was applied on the images. The resulting classification was then reclassified into the water, forest, urban, agriculture, and rangeland.The random sampling method was applied for the accuracy assessment. This method has no rules for choosing the points and the points are scattered within the study area. The overall accuracy value is 85% and the kappa coefficient values is 0.82.

The SSURGO (Soil Survey Geographic Database) soil data were used because according to Natural Resource Conservation Service (NRCS), the SSURGO is the most detailed level of county soil data. The soil data and other information about the properties of the soil were downloaded from https://websoilsurvey.sc.egov.usda.gov/App/WebSoilSurvey.aspx. The NOAA (National Oceanic and Atmospheric Administrations) was the provider of the climatic data

including daily rainfall, maximum and minimum temperatures, and average wind speed. The data at one weather station were only available for the study area from the period between 1990 and 2020. The datasets were downloaded from this website (https://www.ncdc.noaa.gov/cdo-web/datasets). For future climate data, two Representative Concentrated Pathways (RCP) have been used in this study. According to Moss et al. (2010), the RCPs are plausible representations of future climatic scenarios (based on various assumptions on future atmospheric concentrations of greenhouse gases and socio-economic development). The Intergovernmental Panel on Climate Change (IPCC) adopted the RCPs for its Fifth Assessment Report (AR5) in 2014 and IPCC defined the RCPs as the four greenhouse gas concentration trajectories (Taylor et al., 2014). The RCP2.6, RCP4.5, RCP6.5, and RCP8.5 are the four scenarios that consider the future climate conditions and LULC changes. The numbers associated with them indicate the predicted amount of increasing the radiative forcing to be reached by the year 2100 (Moss et al., 2010). The downscaled and bias-corrected data of moderate (RCP 4.5) and extreme (RCP 8.5) scenarios up to 2050 (available up to 2100) were used as input to calibrate the SWAT model. One advantage of the SWAT model is if any of the meteorological data are limited, it is still possible to run the model and have the reasonable values of hydrological parameters The SWAT model has a built-in weather generator model (WXGEN) and it can be utilized to stochastically generate daily weather values based on historical monthly averages of parameters such as temperature, precipitation, relative humidity, wind, and solar radiation near the study area. The SWAT model recorded the missing precipitation, temperature, and other climate data as -99. Discharge data were obtained from the USGS National Water Information System: Web Interface. The data are available in this link https://waterdata.usgs.gov/nwis/rt. In this study, the discharge data on the monthly based were used. The water quality data were also extracted from the USGS National

Water Information System Web Interface. Though the water quality data are not available on a daily or monthly basis, some random water quality data were found.

It has a significant impact to incorporate the management operations data within a watershed because the hydrological processes and the number of nutrients depend on the management practices information, and it helps to produce better results of hydrological parameters. The Best Management Practices (BMPs) database was developed by Butler and Srivastava (2007) for Alabama state. Mirhosseini et al. (2016) and Srivastava et al. (2010) used this management practices database for their research purposes within Alabama. Bermuda grass was used for rangeland and peanut-cotton crop rotation was used for cropland and the detailed information about the management practices are included in Table 3.1. Bermuda grass was normally planted in early March and then harvested at the beginning of July each year (Ahring et al., 1974; Shaver et al., 2006) for the period of the last three decades (study period).

3.2.3 SWAT Model Description

The SWAT (Soil Water Assessment Tool) is a physically based hydrologic model and requires physically based data (Jacobs and Srinivasan, 2005). The SWAT is a continuous-time, spatially distributed model designed to simulate water, sediment, nutrient, and pesticide transport at a catchment scale on a daily time step under different management practices (Jain and Sharma, 2014). The SWAT model has been developing for over 30 years and it has been modified and adapted numerous times for better performance (Simić, 2009). The relevant hydrologic components such as evapotranspiration, surface runoff, lateral flow, percolation, peak rate of runoff, groundwater flow, water yield, and sediment yield are computed by the SWAT model for each subbasin and Hydrological Response Units (HRUs) as well. Arc-SWAT is an extension of ArcGIS as the SWAT is embedded in a GIS interface. The SWAT 2012 is evolved from

AVSWAT which is an extension of ArcView developed for an earlier version of the SWAT2012.

The SWAT model can run the continuous simulation over a long time as well as it is a continuous process-based, computationally efficient hydrological model. Some major components are used to run the SWAT model including weather, hydrology, different types of soil, plant growth, nutrients, pesticides, bacteria and pathogens, land use, and management practices. While running the SWAT model, a watershed or basin is divided into multiple sub-basins or sub-watersheds and then each sub-basin or sub-watershed is further subdivided into multiple HRUs based on the DEM properties. The HRUs are composed of unique land use, soil, and slope characteristics. The HRUs are used to describe spatial heterogeneity in terms of land cover, soil type, and slope class within a watershed or basin.

The SCS (Soil Conservation Services) curve number procedure (SCS, 1972) and Green & Ampt infiltration method (1911) are the two methods to estimate the surface runoff used by the SWAT model. In this present study, the SCS curve number method was used to estimate surface runoff. The modification of the Rational Method was used to measure the peak runoff rate. There are two methods to estimate the water routing through the channel such as the variable storage routing method and the Muskingum routing method. In this study, the Muskingum routing method was used to compute the surface runoff.

To estimate the hydrological components, the model estimates the evaporation from soils and transpiration from plants. Potential evapotranspiration can be estimated by the three methods in SWAT: Priestley–Taylor (Priestley and Taylor, 1972), Penman-Monteith (Monteith, 1965), and ET–Hargreaves (Hargreaves, 1985). The Penman-Monteith includes precipitation, minimum and maximum temperature, wind speed, relative humidity, and solar radiation to measure

evapotranspiration. For this reason, this method was used to estimate potential evapotranspiration. But the Priestley–Taylor and the ET–Hargreaves methods do not include all the parameters.

Sedimentation (deposition) and transportation are two physical processes that SWAT considers in the processes simultaneously. Briefly, in the SWAT, soil Nitrogen (N) is comprised of five different Nitrogen pools. Two of the pools are inorganic (ammonium-N [NH4-N] and nitrate-N [NO3-N]) and three pools are organic (active, stable, and fresh). Mineralization, decomposition, immobilization, nitrification, denitrification, and ammonium volatilization processes are used to transform one type of nitrogen into another nitrogen pool used by the SWAT model (Chaubey et al., 2006). The estimation of nitrogen by the plant use is estimated by using the supply and demand approach (Santhi et al., 2006). Unlike N, soil phosphorous (P) in the SWAT is divided into six pools (three minerals and three organics). The fresh organic phosphorus pool and active and stable organic pool are contributed to by the crop residue, and biomass and humus substances respectively. The soil inorganic pool includes active, solution, and stable pools (Chaubey et al., 2006). The portion of phosphorus from solution inorganic phosphorus is taken up by plants and is in rapid equilibrium with the active pool. The active phosphorus pool is in rapid equilibrium with the solution pool and slow equilibrium with the stable pool. The stable inorganic pool is relatively unavailable for plant uptake (Neitsch et al., 2002). Like nitrogen, plant use of phosphorus is estimated using the supply and demand approach (Santhi et al., 2006).

3.2.4 SWAT Model set up

The first step of model set-up was the delineation of the watershed, the subwatershed, and the outlet using the 10 m DEM data. As the SWAT is a physically derived model, it derived the topography, contour, and slope from the DEM and it was used to divide the basin into subbasins.

Once the source DEM was added, the model then used contours and slope to determine flow direction and flow accumulation which were calculated during delineation. When flow direction and flow accumulation were depicted, a stream network was generated by the model in which each reach drained a sub-basin, all of which drained into a major reach. Each reach had an outlet. Then an outlet was selected that corresponds to the outlet at which discharge measurements for calibration were being collected. This outlet then determined the lower boundary for the watershed basin, which was then delineated based on the location of that outlet and the stream network.

To define the HRU, the model required LULC, soil, and slope. Once the LULC, soil, and slope were defined and incorporated in the model, the HRUs were created with a unique combination of those three classes. A LULC lookup table was created manually and used to specify the land use category and also the Soil SSURGO data were used to identify the soil types and then linked to the SWAT databases to reclassify the land use and soil map. Slope was reclassified into three classes by using multiple slope options because the topography of the study area was not verified. The threshold percentage method was applied to eliminate the minor land use, soil type, and slope, and a 5% threshold for minimal LULC, 10% threshold for both soil and slope were used. The HRUs generated and the corresponding report was also generated by the model which would be specifying the area of different HRUs in various subbasins.

The final step before running the model was the creation of input tables, including the weather data. In this study, maximum and minimum temperature, precipitation, and wind speed were incorporated in the model. As relative humidity and solar radiation were not available, the US Weather generator was used. The files were successfully rewritten and stored in the personal

geodatabases of the model. After this step, the model became capable to simulate the streamflow, water balance components, total nitrogen, and phosphorus.

3.2.5 Uncertainty and Sensitivity Analysis

Some parameters have the greatest impact on the hydrological parameters and water balance components. The model is sensitive to some parameters to provide reasonable outputs. Sensitivity analysis is done to identify the parameters by altering some parameters to the acceptable ranges to get the better performance of the model. The SWAT-CUP software was used to identify the sensitive parameters which are developed by the Swiss Federal Institute of Water Science and Technology (EAWAG). This method is useful for model calibration, validation, and uncertainty analysis by altering some parameters. The SWAT-CUP has five different optimization algorithms: Sequential Uncertainty Fitting (SUFI-2) (Abbaspour et al., 2007), Generalized Likelihood Uncertainty Estimation (GLUE) (Beven and Binley, 1992), Parameter Solution (ParaSol) (Van Griensven and Meixner, 2006), Markov chain Monte Carlo (MCMC) (Kuczera and Parent, 1998; Marshall et al., 2004; Vrugt et al., 2003), and Particle Swarm Optimization (PSO) (Zhang et al., 2015). In this study, SUFI-2 has been used because it has the ability to take all the considerations of all the sources of uncertainty on the parameter ranges such as uncertainty in driving variables (e.g., rainfall), conceptual model, parameters, and measured data (Abbaspour et al., 2007).

3.2.6 SWAT Model Calibration and Validation

The calibration of the SWAT model was based on the optimization of the parameter values by adjusting its simulated values with the observed or actual values of the analyzed area. The validation involved the process of performing accurate calibration steps and enabling the

capability of making a sufficient simulation according to the purposes of the study (Refsgaard, 1997). Comparison of the predicted and actual values was essential to achieve the satisfactory acceptable values of objective function which involves running a model and continuously comparing the results for the different periods of calibration until the model meets confidence limits. The model validation was done with the same SWAT parameter values calibrated without any further alterations because it is one of the requirements to follow to do the validation. For calibration and validation, the period will be determined by the length of the observed data record. The time frame can be equally divided for the calibration and validation if the observed data period is sufficiently long because long periods can represent the different climates. In this study, the total time length was divided equally; the first fifteen years (1991-2005) is for calibration and the last fifteen years (2006-2020) for the validation. The warmup period of 5 years from 1985-1990 was chosen to achieve a steady-state for modeling. However, if the length of the data record is not sufficiently long, one should remember to use the time length in such a way that the calibration period is way longer than the validation. According to Gassman et al. (2005), the SWAT input parameters are physically based and researchers are allowed to change calibration parameters within an acceptable range.

3.2.7 Model Evaluation

In this study, the qualitative graphical comparisons and quantitative statistical techniques both were used to evaluate the performance of the model. The plotting observed and simulated streamflow, total phosphorus, nitrogen loading at a monthly time-step, and the relationship of water balance components with these parameters were the qualitative methods used. The performance of the model was also evaluated by different statistical measures such as Nash-

Sutcliffe Efficiency (NSE), Percent of Bias (PBIAS), and the Coefficient of Correlation (R^2). According to Moriasi et al. (2007), these three statistics are most commonly used.

$$NSE = 1 - \frac{\sum_{i=1}^{n}(Oi-Pi)^2}{\sum_{i=1}^{n}(Oi-\overline{O})^2} \quad (1)$$

$$PBIAS = \frac{\sum_{i=1}^{n}(Oi-Pi)*100}{\sum_{i=1}^{n} Oi} \quad (2)$$

$$R^2 = \frac{\sum_{i=1}^{n}(Oi-\overline{O})(Pi-\overline{P})}{\sqrt{\sum_{i=1}^{n}(Oi-\overline{O})^2}\sqrt{\sum_{i=1}^{n}(Pi-\overline{P})^2}} \quad (3)$$

where Oi is the ith observation for the constituent being evaluated; Pi is the ith simulated value for the constituent being evaluated; $\overline{O}$ is the mean of observed data for the constituent being evaluated; $\overline{P}$ is the mean of simulated data for the constituent being evaluated and n is the total number of observations.

3.3 Results

3.3.1 Climate Variability

Figure 3.5 is representing the total precipitation of the last three decades and two RCPs (RCP4.5 and RCP8.5) from 2021 to 2050. The average total precipitation between 1991 and 2020 is 1708 mm. The maximum average precipitation is 2197.60 mm and occurs in 1998. However, the minimum precipitation is 1161.79 mm in 2000. The average total precipitation is showing irregular behavior between 1991 and 2020. On the other hand, the average total precipitation for RCP4.5 and RCP8.5 is 6582.43 mm and 7065.77 mm respectively which is more than the last thirty years. The difference of the maximum average total precipitation between RCP4.5 (8872.53 mm) and RCP8.5 (9564.16 mm) is 691.63 mm. The minimum average total precipitation for RCP4.5 and RCP8.5 is 3989.10 mm and 4127.35 mm. Though the values are

representing the growing trend from the past thirty years, the average total precipitation has an irregular trend for both RCP4.5 and RCP8.5.

Figure 3.6 is showing the growing trend of the average yearly temperature from 1991 to 2020 and the irregular trend of two RCPs (RCP4.5 and RCP8.5) between 2021 and 2050. The average, maximum, and minimum temperatures between 1991 and 2020 are 19.84^0C, 20.96^0C, and 18.50^0C respectively. On the other hand, the average temperature is 21.76^0C for RCP4.5 and 21.67^0C for RCP8.5 which is almost 1.8^0C and 1.7^0C more than the last thirty years. The difference between the maximum (23.58^0C) and minimum (20.23^0C) average temperature for RCP4.5 is 3.35^0C. The maximum and minimum average temperature for RCP8.5 is 23.18^0C in 2033 and 20.21^0C in 2021.

3.3.2 Sensitivity Analysis

The sensitivity analysis has been done by the SUFI-2. Some parameters were chosen to calibrate and validate the model and the parameters are shown in table 3.2. The table is showing the fifteen parameters to calibrate and validate the streamflow such as curve number (CN), biological mixing efficiency (BIOMIX), Manning's "n" value for overland flow (OV_N), peak rate adjustment factor (PRF), exponent parameter for calculating sediment re-entrained in channel sediment routing (SPEXP), USLE equation (USLE_P), soil and plant evaporation factor (ESCO and EPCO) and groundwater (ALPHA_BF, GW_DELAY, GW_REVAP, and RCHRG_DP). However, all the parameters did not have the same impact on the streamflow. However, some parameters had the greatest influence on the streamflow modeling, and a list of the parameters ranking is shown in table 3.3 based on the t-stat and p-value. The parameter which has the highest impact on the streamflow modeling has the highest value of t-stat and lowest value of p-values, and vice versa. Based on the highest t-stat and low p-value, ESCO is

the highest, ULSE_P is the second highest, and then BIOMIX is the impactful parameter. SOL_AWC, OV_N, RCHRG_DP rank as the least impactful for the calibration and validation of the model.

According to table 3.2, to calibrate and validate the total nitrogen and phosphorus in the watershed, four parameters have been used such as initial soluble Phosphorus concentration in sol layer (SOL_LABP), initial organic Phosphorus concentration in sol layer (SOL_ORGP), organic Nitrogen in the baseflow (LAT_ORGN), and initial organic Nitrogen concentration in the soil layer (SOL_ORGN). Before calibrating the total nitrogen and phosphorus, streamflow needed to be calibrated because there is a correlation between the streamflow and the amount of nitrogen and phosphorus.

3.3.3 SWAT Model Calibration and Validation

Table 3.4 is representing the value of R^2, NSE, and PBIAS values for streamflow, total nitrogen, and phosphorus for the calibration and validation periods. The R^2 value is 0.81 indicating a good level of classification for both calibration and validation of streamflow. The calibration value (0.75 for nitrogen and 0.77 for phosphorus) and the validation value (0.50 for nitrogen and 0.54 for phosphorus) are different but falling in the good criteria of classification. According to criteria set by Moriasi et al. (2007), the NSE value for evaluating the model performance in calibration and validation between .55 and 0.70 for streamflow, 0.35 to .60 for nitrogen, and 0.40 to 0.50 for phosphorus is considered “satisfactory”, a value between 0.70 and 0.85 for streamflow, 0.60 to 0.70 for nitrogen and more than 0.70 for phosphorus is considered as “good” and more than 0.85 for streamflow, more than 0.70 for nitrogen and more than 0.65 for phosphorus is attributed as “very good”. Therefore, calibration and validation of the streamflow are rated as “good”. The calibration and validation value of total nitrogen are also “good”, on the

other hand, the calibration and validation of total phosphorus do not seem “satisfactorily” (Table 3.4). Moreover, the PBIAS value for the streamflow calibration is negative, which indicates model overestimation. On the other hand, the PBIAS value for the streamflow validation is positive, indicating an underestimation. Besides, nitrogen calibration and validation scenarios are just the opposite. PBIAS values for calibration and validation are negative, therefore phosphorus is overestimated (Table 3.4 and 3.5).

Figure 3.7 A, B and C is showing the observed and simulated streamflow, total nitrogen, and phosphorus respectively. The difference between the average actual streamflow (4.14 m^3/s) and average simulated streamflow (4.16 m^3/s) is less than 1% and a bit overestimated but the percentage for total nitrogen and phosphorus are higher and overestimated.

3.3.4 Relationship between Precipitation, Temperature and Stream Flow

Figures 3.8 and 3.9 represent the relationship between precipitation with streamflow and temperature with streamflow respectively. From 1991 to 2020, precipitation was highest (5856.22 mm) in July though the maximum streamflow (5.90 m^3/s) was in January likely because lower temperature causes lower evaporation. For RCP4.5 and RCP8.5, the maximum precipitation is also in July and the highest streamflow is in February month. It is clear from the graph that streamflow will be higher in January, February and March for all the scenarios but precipitation will be higher in July, August and September.

The temperature was highest in June, July, August and September ranging from 25.6 to 27.8 ^0C, but the streamflow was high in January, February and March. Again, for RCP4.5 and RCP8.5, the temperature will be high in June, July, August and September and streamflow will be low in October, November and December. There is a negative correlation between temperature and

streamflow and it is justified because higher temperature means more evaporation and leads to less streamflow.

3.3.5 The Projected Stream Flow and the Total Nitrogen and Phosphorus Loadings

The projected streamflow for RCP4.5 and RCP8.5 scenarios is shown in figure 3.10 (by year) and 3.11 (by month). The average streamflow between 1991 and 2020 was 4.15 m^3/s, while the average streamflow from 2021 to 2050 is 4.54 m^3/s and 4.77 m^3/s for RCP4.5 and RCP8.5 respectively. The maximum streamflow is 7.41 m^3/s in 1998 over the past thirty years. The maximum streamflow is more than 8 $m^{3/}$s for both scenarios. The average streamflow is minimum in June and November and maximum in January and February between 1991 and 2020. The same scenario is noticed in RCP4.5 and RCP8.5.

Figure 3.12 (by year) and 3.13 (by seasonal) are representing the total nitrogen for RCP4.5 and RCP8.5 scenarios. The average total nitrogen is ranging from 20910 kg/ha to 100600 kg/ha and the average total nitrogen is 50290.33 kg/ha over the past three decades. Conversely, the average total nitrogen is 58920.33 kg/ha for the RCP4.5 scenario and 61282.33 kg/ha for the RCP8.5 scenario. The total nitrogen is high in April amounting to 14941.66 kg/ha and the total nitrogen is also high in April (11384.52 kg/ha) for RCP4.5 and March for RCP4.5 (15400.64 kg/ha). The strongest nitrogen loading will increase in the winter season. Overall, the simulations show that nitrogen loadings will increase in the future.

The total phosphorus is shown in figure 3.14 (by year) and 3.15 (by seasonal) for RCP4.5 and RCP8.5 scenarios. The total phosphorus value is ranging from 6193 kg/ha to 24570 kg/ha but the average value is 14032 kg/ha. The average value of total phosphorus is 15003 kg/ha which is higher than RCP4.5 (13397.3 kg/ha). The total phosphorus is higher in February and March

between 1991 and 2020 and this case is also true for RCP4.5 and RCP8.5. In general, the phosphorus loadings will increase in the future, and the rate of increase will be higher in the spring season.

3.3.6 Impact on the Water Balance Components of RCP4.5 and RCP8.5

The effect of the two climate scenarios on the changing water balance components such as evapotranspiration (ET), percolation (PERC), surface runoff (SURQ), lateral flow (LAT_Q), groundwater flow (GW_Q), and water yield (WYLD), and the relative change from the last thirty years to the future thirty years are depicted in figure 3.16. Most of the months are showing an increasing trend of monthly ET except April, July, October and December. The PERC has been growing for both RCP4.5 and RCP8.5 for the last three decades. The PERC value is supposed to increase about 135 mm and 168 mm for RCP4.5 and RCP8.5 respectively. Overall, the monthly value of PERC will increase almost every month in both scenarios. The trend is also same for the LAT_Q which is growing for the past thirty years. The increasing value for RCP4.5 is 5 mm and RCP8.5 is 9 mm. On the contrary, SURQ is showing a significantly decreasing trend. In the case of RCP4.5 and RCP8.5, 174 mm and 84 mm of SURQ will be low in the future thirty years. On contrary, GW_Q will increase at about 132 mm (RCP4.5) and 165 mm (RCP8.5) from the last thirty years. Overall, the monthly change is showing a positive trend that is increasing the GW_Q almost every month.

3.4 Discussions

3.4.1 Hydrological Modeling

According to Arnold et al. (1998), among the most commonly used continuous-time, semi-distributed, and physically-based models is the SWAT model, which can assess different

hydrological components and pollution problems for watersheds. Modeling uncertainties originate from the model structural uncertainties, input data uncertainties as it requires a large number of input datasets, and parameter uncertainties because these are associated with the global database, equations, or by using other software (Nyeko, 2014 and Saxton and Rawls, 2006). However, representation of the physical characteristics of the landscape as realistically as possible is significant to run the model and the SWAT model developer has been used to develop it continuously (Bosch et al., 2010, Bonuma et al., 2014 Rathjens et al., 2015 and Sun et al., 2015). In this study, the historic climate data were only available for one station in proximity of the study area. The two scenarios (RCP4.5 and RCP8.5) of climate data have been used. The weather information is one of the important input variables in the SWAT model including precipitation and temperature. The quantity and quality of the precipitation data have a significant effect on the accuracy of the hydrological simulation. Regular and sufficient rain gauges can help to extract the exact spatial distribution of the weather data. According to Chen et al. (2013) and Miao et al. (2015), there are fewer rain gauges in some areas but Mobile County AL has relatively homogenous precipitation. This study used weather data from one rain gauge. The actual total nitrogen and phosphorus data were not available for the whole watershed and available only for few years. The calibration and simulation of total nitrogen and phosphorus were difficult because the data were not available for a good amount and a good range of years. However, altering some parameters by SWAT-CUP provided a solution to get a satisfactory to good' clasification (Moriasi et al., 2005) of streamflow, total nitrogen, and phosphorus calibration and validation.

3.4.2 Changing Precipitation and temperature Pattern on Stream Flow

The study shows that the precipitation and temperature will increase in the next thirty years in comparison to the past thirty years. According to the RCPs and observed data the precipitation will increase at about 4874 mm and 5357 mm for RCP4.5 and RCP8.5 respectively. The study also shows the pattern of the precipitation is irregular through the years. The average streamflow will also increase, and these results complement the increase in the precipitation. The irregular yearly trend of the precipitation also goes with the irregular trend of the streamflow. The variability and changing pattern of precipitation could lead to the changes in the frequency and intensity of extreme precipitation events, which could result in the variation in streamflow and peak flow (Chen et al., 2009; Sajikumar and Remya, 2015 and Tadesse et al., 2015). The results show the precipitation is highest in the year 2047 for the RCP8.5 scenario. The streamflow is also high in 2047 with a value of more than 8 m^3/s.

The temperature from the last three decades will increase for both RCP4.5 and RCP8.5 scenarios. The highest temperature will increase about 3^0 C in the future thirty years. The overall trend of the temperature will increase but the pattern is irregular on a yearly basis. This increasing temperature could theoretically decrease the streamflow by increasing evapotranspiration but due to increasing precipitation, streamflow will be growing. The irregular trend in the average temperature goes with the resultant irregular behavior of the streamflow. The result agrees with the study done by Oki and Kanae (2006) and Stocker (2014), in general the increased temperature is the result of corresponding changes in the timing and volume of flooding and streamflow. The increase in the streamflow is the result of the average increase in the precipitation but the seasonally disproportionate precipitation of the watershed results in higher flows during the winter season.

3.4.3 Water Balance Components due to Climate Change

In addition to streamflow, other major hydrological components such as evapotranspiration, water yield, percolation are considered to provide beneficial information for sustainable water management in the future. Moreover, surface runoff, groundwater flow, and lateral flow are important to describe and understand the changes in the water yield and streamflow. The study represents the changing climate is characterized by substantial changes in the water balance components. Though the temperature will increase; the evaporation rate will decrease. Therefore, the temperature is not the major driving source for evapotranspiration. Evapotranspiration also depends on the available water and increasing precipitation also contributes to this as it complements the overland flow and reduces infiltration. Another reason is likely associated with the changing LULC. In comparison, the percolation will increase from the last thirty years and this rate of percolation will have influences on the streamflow. Moreover, the lateral flow will also have a growing trend in the next thirty years and lateral flow will impact the volume of the streamflow. Conversely, the surface runoff will decrease. Again, the groundwater flow will have an increasing trend in future years, and it will have substantial impacts on the pattern of the streamflow. The groundwater normally has a high positive correlation with increased precipitation and a high negative correlation with temperature.

3.4.4 The Increasing total Nitrogen and Phosphorus due to Climate Change

In both scenarios of climate change, the total amount of nitrogen will increase from the last three decades. However, the rate of increasing total nitrogen is more in the RCP8.5 than the RCP4.5. The total amount of phosphorus will also have a growing trend for both the RCP4.5 and RCP8.5 scenarios. Like nitrogen, the amount is also high in the RCP8.5 than the RCP4.5. Increasing nitrogen and phosphorus is primarily driven by increased streamflow and rainfall intensity. These results complement the findings of Woznicki and Nejadhashemi (2012) on Big Blue

watershed in Kansas and Nebraska state, USA as they showed increase of the total nitrogen and phosphorus yields also using SWAT outputs under future climate change. The increasing precipitation intensity affects the Dissolved Reactive Phosphorus (DRP) yields. Similar studies conducted by Gombaults et al. (2015) on Pike River watershed in southern Québec, Canada and Ahmadi et al. (2013) on Eagle Creek watershed in Indiana state, USA and their results were similar to this study that the amount of nitrogen will also increase in the winter season. This also can be explained by the variation in the future seasonal changes in precipitation. The increasing precipitation accelerates the runoff passing through the groundwater and thus the pollutants accumulated on the surface are carried into the waterbody, causing the pollution of surface water and even groundwater within the drainage area (Kaste et al., 2006). Therefore, the change in the precipitation intensity and increasing frequency will affect the non-point source pollution. Nitrogen and phosphorus are the two main elements of non-point source pollution, and both are influenced by the precipitation process. If the precipitation increases, then the effect of the runoff will intensify and the nitrogen and phosphorus loadings flowing in the waterbody will increase accordingly (Whitehead et al., 2009). The surface temperature will also increase due to the increase of the air temperature. It leads to an increase in the temperature difference and the thermocline in the upper and lower layers of water. The formation of anoxic layers at the bottom of water bodies such as lakes can develop because of the presence of the thermoclines. The nitrogen and phosphorus loadings release easily from sediments to the bottom of the water environment and can lead to an increase in nitrogen and phosphorus concentrations in surface water, which is the main reason that nitrogen and phosphorus loadings increase with the surface runoff coming into the watersheds. Moreover, the increase in the water temperature will also increase the activities of microorganisms and release the endogenous nitrogen and phosphorus in

the sediment. If the temperature and light are sufficient and the nitrogen in the water reaches a certain level, then the eutrophication will be intensified (Luo et al., 2013). The increasing precipitation and temperature accelerate the eutrophication process in a water body (Ducharne, 2008; Harvell, et al, 2002 and Walter et al., 2006).

3.5 Conclusion

In this study, the trend and variations of hydro-meteorological and climate elements (precipitation, temperature, evaporation, streamflow, groundwater flow, and percolation) have been investigated during historical and future periods. The SWAT model is employed to simulate the effects of climate change on the hydrological elements using the method of scenarios simulation. By integrating the downscaled and corrected future climatic data with the SWAT, the trends, variations of the hydrological components from 2021-2050 are predicted and compared with the climatic data from 1991-2020 used as reference data. Results indicated that, with increasing precipitation and temperature, the streamflow, percolation, lateral flow, groundwater flow will increase. As climate variability has a profound impact on the water balance components, planners and resource managers should emphasize the importance of increasing the adaptation to climate variability when planning and managing water resources.

Refences cited-

Abbaspour, K. C., Yang, J., Maximov, I., Siber, R., Bogner, K., Mieleitner, J., Zobrist, J. and Srinivasa, R. 2007, Modelling hydrology and water quality in the pre-alpine/alpine Thur watershed using SWAT. *Journal of Hydrology*, 333(2/4), 413-430. https://doi.org/10.1016/j.jhydrol.2006.09.014.

Acreman, M.C.; Miller, F. 2007, Practical approaches to hydrological assessment of wetlands lessons from the UK. In Wetlands: Monitoring, Modelling and Management; Okruszko, T., Maltby, E., Szatyłowicz, J., S´wia˛tek, D., Kotowski,W., Eds. *Taylor & Francis*, London, UK.

Ahmadi, M.; Records, R.; Arabi, M. 2013, Impact of climate change on diffuse pollutant fluxes at the watershed scale. *Hydrological Process*, 28, 1962–1972. [CrossRef]

Ahring, R. M., Huffine, W. W., & Taliaferro, M. 1974, Stand establishment of Bermudagrass from Seed. *Agronomy Journal*, 67.

Alexander, L.; Zhang, X.; Peterson, T.; Caesar, J.; Gleason, B.; Klein Tank, A.; Haylock, M.; Collins, D.; Trewin, B.; Rahimzadeh, F. 2006, Global observed changes in daily climate extremes of temperature and precipitation. *Journal of Geophysical Research Atmosphere* 111. [CrossRef]

Allen, M.R., Ingram,W.J. 2002, Constraints on future changes in climate and the hydrologic cycle. *Nature*, 419, 224. [CrossRef]

Arnold, J.G., Kiniry, J.R., Srinivasan, R., Williams, J.R., Haney, E.B. 2012, Soil and water assessment tool input/output documentation. TR-439, Texas Water Resources Institute, College Station, 1-650.

Arnold, J.G.; Raghavan, S.; Ranjan, S.M.; Jimmy, R.W. 1998, Large area hydrologic modeling and assessment part I: Model development. *JAWRA Journal of the American Water Resource Association*, 34, 91–101.

Betts, R.A.; Alfieri, L.; Bradshaw, C.; Caesar, J.; Feyen, L.; Friedlingstein, P.; Gohar, L.; Koutroulis, A.; Lewis, K.; Morfopoulos, C.; et al. 2018, Changes in climate extremes, fresh water availability and vulnerability to food insecurity projected at 1.5^0C and 2^0C global warming with a higher-resolution global climate model. *Philosophical Transactions of the Royal Society*. 376, 20160452. [CrossRef]

Beven, K., Binley, A. 1992, The future of distributed models: model calibration and uncertainty prediction. *Hydrological Processes*, 6(3), 279-298.

Bicknell, B.R., Imhoff, J.C., Kittle, J.L., Jr., Donigian, A.S., Jr., Johanson, R.C. 1996, Hydrological Simulation Program-FORTRAN. User's Manual for Release 11; US EPA: Athens, Greece.

Bonumá, N.B., Rossi, C.G., Arnold, J.G., Reichert, J.M., Minella, J.P., Allen, P.M., Volk, M. 2014, Simulating Landscape Sediment Transport Capacity by Using a Modified SWAT Model. *Journal of Environmental Quality*, 43, 55–66. [CrossRef]

Bosch, N.S.; Evans, M.A.; Scavia, D.; Allan, J.D. 2014, Interacting effects of climate change and agricultural BMPs on nutrient runoff entering Lake Erie. *Journal of Great Lakes Research*. 40, 581–589. [CrossRef]

Burn, D.H.; Sharif, M.; Zhang, K. 2010, Detection of trends in hydrological extremes for Canadian watersheds. *Hydrological Process*. 24, 1781–1790. [CrossRef]

Butler G.B., & Srivastava, P. 2007, An Alabama BMP database for evaluating water quality impacts of alternative management practices. American Society of Agricultural and Biological Engineers, 23(6), 727–736.

Chaubey, I., Migliaccio, K. W., Srinivasan, R., H, G. C., & Arnold, J. G. 2006, Phosphorus modeling in Soil and Water Assessment Tool (SWAT) Model, 163–188.

Chen, C.; Ahmad, S.; Kalra, A. 2018, Hydrologic responses to climate change using downscaled GCM data on a watershed scale. *Journal of water Climate Change.* [CrossRef]

Chen, Y.; Xu, Y.; Yin, Y. 2009, Impacts of land use change scenarios on storm-runoff generation in Xitiaoxi basin, China. *Quaternary International*. 208, 121–128. [CrossRef]

Chen, Z.; Chen, Y.; Li, B. 2013, Quantifying the effects of climate variability and human activities on runoff for Kaidu River Basin in arid region of northwest China. *Theory of Applied Climatology*. 111, 537–545. [CrossRef]

Crossmann, J., Futter, M.N., Oni, S.K., Whitehead, P.G., Jin, L., Butterfield, D., Baulch, H.M., Dillon, P.J. 2013, Impacts of climate change on hydrology and water quality: Future proofing management strategies in the Lake Simcoe watershed, Canada. *Journal of Great Lakes Resources*, 39, 19–32. [CrossRef]

Danish Hydraulic Institute (DHI). 1993, MIKE SHE WM—water movement module, A short

description; Danish Hydraulic Institute: Hørsholm, Denmark.

Donat, M.G.; Lowry, A.L.; Alexander, L.V.; O'Gorman, P.A.; Maher, N. 2016, More extreme precipitation in the world's dry and wet regions. *Nature Climate Change.* 6, 508. [CrossRef]

Ducharne, A. 2008, Importance of stream temperature to climate change impact on water quality. *Hydrology and Earth System Science*, 12, 797–810.

Dunn, S.M., Brown, I., Sample, J., Post, H.2012, Relationship between climate, water resources, land use and diffuse pollution and the significance of uncertainty in climate change. *Journal of Hydrology*, 434–435. [CrossRef]

Elliott, J.; Deryng, D.; Müller, C.; Frieler, K.; Konzmann, M.; Gerten, D.; Glotter, M.; Flörke, M.; Wada, Y.; Best, N. 2014, Constraints and potentials of future irrigation water availability on agricultural productionunder climate change. Proc. Natl. Acad. Sci. USA 111, 3239–3244. [CrossRef] [PubMed]

Field, C.B.; Barros, V.; Stocker, T.; Qin, D.; Dokken, D.; Ebi, K.; Mastrandrea, M.; Mach, K.; Plattner, G.; Allen, S. IPCC, 2012, Managing the Risks of Extreme Events and Disasters to Advance Climate Change Adaptation. A Special Report of Working Groups I and II of the Intergovernmental Panel on Climate Change; Cambridge University Press: Cambridge, UK; New York, NY, USA, 2012; Volume 30, pp. 7575–7613

Gassman, P.W., Reyes, M.R., Green, C.H., Arnold, J.G. 2005, SWAT peer-reviewed literature: A review. In Proceedings of the 3rd International SWAT Conference, Zurich, Switzerland, 13–15 July 2005.

Gombault, C.; Madramootoo, C.A.; Michaud, A.; Beaudin, I.; Sottile, M.-F.; Chikhaoui, M.; Ngwa, F. 2015, Impacts of climate change on nutrient losses from the Pike River watershed of southern Québec. Canada. *Journal of Soil Science*. [CrossRef]

Hargreaves, G. and Samani, Z.A. 1985, Reference crop evapotranspiration from temperature. *Applied Engineering in Agriculture*, 1, 96–99. [CrossRef]

Harvell, C.D.; Mitchell, C.E.; Ward, J.R.; Altizer, S.; Dobson, A.P.; Ostfeld, R.S.; Samuel, M.D. 2002, Climate warming and disease risks for terrestrial and marine biota. *Science*, 296, 58–62. [CrossRef] [PubMed]

Hoang, L.P.; Lauri, H.; Kummu, M.; Koponen, J.; van Vliet, M.; Supit, I.; Leemans, R.; Kabat,

P.; Ludwig, F. 2016, Mekong River flow and hydrological extremes under climate change. *Hydrology and Earth System Science*, 20, 3027–3041. [CrossRef]

IPCC. Summary for Policymakers. In Climate Change 2014: Mitigation of Climate Change. Contribution of Working Group III to the Fifth Assessment Report of the Intergovernmental Panel on Climate Change; Edenhofer, O.R., Pichs-Madruga, Y., Sokona, E., Farahani, S., Kadner, K., Seyboth, A., Adler, I., Baum, S., Brunner, P., Eickemeier, B., et al., 2014. Eds.; Cambridge University Press: Cambridge, UK; New York, NY, USA

Jacobs J.H. and Srinivasan R., 2005, Effects of curve number modification on runoff estimation using WSR-88D rainfall data in Texas watersheds, *Journal of Soil and Water Conservation*, 60 (5), pp 274-278.

Jain, M., Sharma, S.D. 2014, Hydrological modeling of Vamshadara River Basin, India using SWAT. International Conference on Emerging Trends in Computer and Image Processing (ICETCIP-2014), Pattaya, Thailand.

Journey, C.A. and Gill, A.C. 2001, Assessment of water-quality conditions in the J.B. Converse Lake Watershed, Mobile County, Alabama, 1990-98. U.S. Geological Survey Water-Resources Investigations Report 01-4225. [http://pubs.er.usgs.gov/publication/wri014225]. Last accessed 28 December 2020.

Kaste, O.; Wright, R.F.; Barkved, L.J.; Bjerkeng, B.; Engen-Skaugen, T.; Magnusson, J.; Saelthun, N.R. 2006, Linked models to assess the impacts of climate change on nitrogen in a Norwegian river basin and FJORD system. *Science of Total Environment*, 365, 1–3. [CrossRef]

Kharin, V.V.; Zwiers, F.; Zhang, X. Wehner, M. 2013, Changes in temperature and precipitation extremes in the CMIP5 ensemble. *Climate Change*, 119, 345–357. [CrossRef]

Khoi, D.N.; Suetsugi, T. 2014, The responses of hydrological processes and sediment yield to land-use and climate change in the Be River Catchment, Vietnam. *Hydrology Process*, 28, 640–652. [CrossRef]

Kittel, T. G.F., 2013, The Vulnerability of Biodiversity to Rapid Climate Change. Climate Vulnerability: Understanding and Addressing Threats to Essential Resources, 10.1016/B978-0-12-384703-4.00437-8.

Kløve, B., Ala-Aho, P., Bertrand, G., Gurdak, J.J., Kupfersberger, H., Kværner, J., Muotka, T.,

Mykrä, H., Preda, E., Rossi, P. 2014, Climate change impacts on groundwater and dependent ecosystems. *Journal of Hydrology*, 518, 250–266.

Krysanova, V.; Hattermann, F.F. 2017, Intercomparison of climate change impacts in 12 large river basins: Overview of methods and summary of results. *Climate Change*, 141, 363–379. [CrossRef]

Kuczera, G., Parent, E. 1998, Monte Carlo assessment of parameter uncertainty in conceptual catchment models: The Metropolis algorithm. *Journal of Hydrology*, 211(1/4), 69-85.

Kundzewicz, Z.W. 2008, Climate change impacts on the hydrological cycle. *Ecohydrology and Hydrobiology*., 8, 195–203. [CrossRef]

Kundzewicz, Z.W., Mata, L.J., Arnell, N.W., Döll, P., Kabat, P., Jiménez, B., Miller, K.A., Oki, T., Sen, Z., Shiklomanov, I.A.2007, Freshwater resources and their management. In Climate Change 2007: Impacts, Adaptation and Vulnerability. Contribution of Working Group II to the Fourth Assessment Report of the Intergovernmental Panel on Climate Change; Parry, M.L., Canziani, O.F., Palutikof, J.P., van der Linden, P.J., Hanson, C.E., Eds.; Cambridge University Press: Cambridge, UK, pp. 173–210.

Kundzewicz, Z.W.; Krysanova, V.; Dankers, R.; Hirabayashi, Y.; Kanae, S. 2017, Differences in flood hazard projections in Europe-their causes and consequences for decision making. *Hydrology Science*, 62, 1–14. [CrossRef]

Li, Z.; Liu,W.; Zhang, X.; Zheng, F. 2009, Impacts of land use change and climate variability on hydrology in an agricultural catchment on the Loess Plateau of China. *Journal of Hydrology*. 377, 35–42. [CrossRef]

Li, Z.; Huang, G.; Wang, X.; Han, J.; Fan, Y. 2016, Impacts of future climate change on river discharge based on hydrological inference: A case study of the Grand RiverWatershed in Ontario, Canada. *Science of the Total Environment*. 548–549, 198–210. [CrossRef]

Linderholm, H.W. 2006, Growing season changes in the last century. *Agriculture for Meteorology*, 137, 1–14. [CrossRef]

Lindner, M., Fitzgerald, J.B., Zimmermann, N.E., Reyer, C., Delzon, S., van der Maaten, E., Schelhaas, M.-J., Lasch, P., Eggers, J., van der Maaten-Theunissen, M. 2014, Climate change and European forests: What do we know, what are the uncertainties, and what are the implications for forest management? *Journal of Environmental Management*, 146, 69–83. [CrossRef] [PubMed]

Luo, Y.Z.; Ficklin, D.L.; Liu, X.M.; Zhang, M.H. 2013, Assessment of climate change impacts on hydrology and water quality with a watershed modeling approach. *Science of Total Environment*, 450, 72–82. [CrossRef]

Madsen, H.; Lawrence, D.; Lang, M.; Martinkova, M.; Kjeldsen, T.R. 2014, Review of trend analysis and climate change projections of extreme precipitation and floods in Europe. *Journal of Hydrology*, 519, 3634–3650. [CrossRef]

Marshall, L., Nott, D., Sharma, A.2004, A comparative study of Markov chain Monte Carlo methods for conceptual rainfall-runoff modeling. *Water Resources Research*, 40(2), 1-11. Mobile Area Water and Sewers Systems (MAWSS). 2011, Water System. [http://www.mawss.com/waterSystem.html]. Last accessed 31 December 2020.

McLeod, E., A. Green, E. Game, K. Anthony, J. Cinner,S. F. Heron, J. Kleypas, C. E. Lovelock, J. M. Pandolfi, R. L. Pressey, R. Salm, S. Schill, and C.Woodroffe. 2012, Integrating climate and ocean change vulnerability into conservation planning. *Coastal Management*, 40, 651–672.

Mehta, V.M.; Mendoza, K.; Daggupati, P.; Srinivasan, R.; Rosenberg, N.J.; Deb, D. High-Resolution Simulations of Decadal Climate Variability Impacts on Water Yield in the Missouri River Basin with the Soil and Water Assessment Tool (SWAT). *Journal of Hydrometeorology*, 2015, 17, 2455–2476. [CrossRef]

Miao, C.; Ashouri, H.; Hsu, K.-L.; Sorooshian, S.; Duan, Q. 2015, Evaluation of the PERSIANN-CDR Daily Rainfall Estimates in Capturing the Behavior of Extreme Precipitation Events over China. *Journal of Hydrometeorology*, 16, 1387–1396. [CrossRef]

Min, S.-K.; Zhang, X.; Zwiers, F.W.; Hegerl, G.C. 2011, Human contribution to more-intense precipitation extremes. *Nature*, 470, 378. [CrossRef] [PubMed]

Mimikou, M.A., Baltas, E., Varanou, E., Pantazis, K. 2000, Regional impacts of climate change on water resources quantity and quality indicators. *Journal of Hydrology*, 234, 95–109. [CrossRef]

Mirhosseini, G., Ph, D., Asce, S. M., Srivastava, P., & Ph, D. 2016a, Effect of irrigation and climate variability on water quality of coastal watersheds: case study in Alabama. *Journal of Irrigation and Drainage Engineering*, 142(2), 1–11.

Monteith, J. L. 1965, Evaporation and environment. Symposia of the Society for Experimental

Biology, 19, 205-234.

Moriasi, D. N., Gitau, M.W., Pai, N. and Daggupati, P. 2015, Hydrologic and water quality models: performance measures and evaluation criteria. Transaction of the Society of Agricultural and Biological Engineers (ASABE), 58 (6), 1763-1785. https://doi.org/ 10.13031/trans.58.10715

Moss, R.H., Edmonds, J. A., Hibbard, K. A., Manning, M. R., Rose, S. K., Vuuren, D. P. van, Carter, T. R., Emori, Kainuma, M., S. Kram, T., Meehl, G. A., Mitchell, J. F. B., Nakicenovic, N., Riahi, K., Smith, S. J., Stouffer, R. J., Thomson, A. M., Weyant, J. P. & Wilbanks, T. J. 2010, The next generation of scenarios for climate change research and assessment. *Nature*, Vol. 463, 747-756.

Neitsch, S.L., Arnold, J.G., Kiniry, J.R., Williams, J.R. 2002, Soil and Water Assessment Tool (SWAT) User's Manual; Version 2000; Grassland Soil and Water Research Laboratory: Temple, TX, USA; Texas Water Resources Institute: Collage Station, TX, USA,pp. 1–506.

Nyeko, M. 2014, Hydrologic modelling of data scarce basin with SWAT model: capabilities and limitations. *Water Resources Management*, 29, 81–94. [CrossRef]

Oki, T.; Kanae, S. 2006, Global hydrological cycles and world water resources. *Science*, 313, 1068–1072. [CrossRef] [PubMed]

Park, J.-Y.; Park, M.-J.; Joh, H.-K.; Shin, H.-J.; Kwon, H.-J.; Srinivasan, R.; Kim, S.-J. 2011, Assessment of MIROC3.2 HiRes Climate and CLUE-s Land Use Change Impacts on Watershed Hydrology Using SWAT. Transaction of the Society of Agricultural and Biological Engineers (ASABE), 54, 1713–1724. [CrossRef]

Priestley, C., Taylor, R.1972, On the assessment of surface heat flux and evaporation using large-scale parameters. *Monthly Weather Review*, 100, 81–92. [CrossRef]

Rathjens, H., Oppelt, N., Bosch, D.D., Arnold, J.G., Volk, M. 2015, Development of a grid-based version of the SWAT landscape model. *Hydrological Process*, 914, 900–914. [CrossRef]

Refsgaard, J. C. 1997, Parameterization, calibration, and validation of distributed hydrological models. *Journal of Hydrology*, 198, 69–97.

Santhi, C., Srinivasan, R., Arnold, J. G., & Williams, J. R. 2006, A modeling approach to

evaluate the impacts of water quality management plans implemented in a watershed in Texas. *Environmental Modelling & Software*, 21(8), 1141–1157.

Sajikumar, N.; Remya, R.S. 2015, Impact of land cover and land use change on runoff characteristics. *Journal of Environment Management*. 161, 460–468. [CrossRef] [PubMed]

Saxton, K.E. and Rawls, W.J. 2006, Soil water characteristic estimates by texture and organic matter for hydrologic solutions. *Soil Science Society of American Journal*, 1578, 1569 1578. [CrossRef]

Schewe, J.; Heinke, J.; Gerten, D.; Haddeland, I.; Arnell, N.W.; Clark, D.B.; Dankers, R.; Eisner, S.; Fekete, B.M.; Colón-González, F.J.2014, Multimodel assessment of water scarcity under climate change. Proc. Natl. Acad.S ci. USA, 111, 3245–3250. [CrossRef] [PubMed]

Shaver, B. R., Richardson, M. D., McCalla, J. H., Karcher, D. E., & Berger, P. J. 2006, Dormant seeding bermudagrass cultivars in a transition-zone environment. *Crop Science*, 46(4), 1787–1792. https://doi.org/10.2135/cropsci2006.02-0078

Sillmann, J.; Kharin, V.; Zwiers, F.; Zhang, X.; Bronaugh, D. 2013, Climate extremes indices in the CMIP5 multimodel ensemble: Part 2. Future climate projections. *Journal of Geophysical Research. Atmosphere*. 118, 2473–2493. [CrossRef]

Simić, Z. 2009, SWAT-based runoff modeling in complex catchment areas theoretical background and numerical. *Journal of the Serbian Society for Computational Mechanics*, 3, 38-63.

Sorribas, M.V.; Paiva, R.C.D.; Melack, J.M.; Bravo, J.M.; Jones, C.; Carvalho, L.; Beighley, E.; Forsberg, B.; Costa, M.H. 2016, Projections of climate change effects on discharge and I nundation in the Amazon basin. *Climate Change*, 136, 555–570. [CrossRef]

Srivastava, P., Gupta, A. K., & Kalin, L. 2010, An ecologically-sustainable surface water withdrawal framework for cropland irrigation: A case study in Alabama. *Environmental Management*, 46(2), 302–313.

Stisen, S.; Sandholt, I. 2010, Evaluation of remote-sensing-based rainfall products through predictive capability in hydrological runoff modelling. *Hydrological Process*, 24, 879–891. [CrossRef]

Stocker, T. Climate Change 2013: The Physical Science Basis: Working Group I Contribution to

the Fifth Assessment Report of the Intergovernmental Panel on Climate Change; Cambridge University Press: Cambridge, UK, 2014.

Su, F.; Hong, Y.; Lettenmaier, D.P. 2008, Evaluation of TRMM Multisatellite Precipitation Analysis (TMPA) and Its Utility in Hydrologic Prediction in the La Plata Basin. *Journal of Hydrometeorology*. 9, 622–640. [CrossRef]

Sun, X., Garneau, C., Volk, M., Arnold, J.G., Srinivasan, R., Sauvage, S., Sánchez-Pérez, J.M. 2015, Improved simulation of river water and groundwater exchange in an alluvial plain using the SWAT model. *Hydrological Process*, 30, 187–202. [CrossRef]

Tadesse,W.; Whitaker, S.; Crosson,W.;Wilson, C. 2015, Assessing the impact of land-use land-cover change on stream water and sediment yields at a watershed level using SWAT. *Open Journal of Mod Hydrology*, 5, 68. [CrossRef]

Taye, M.T.; Ntegeka, V.; Ogiramoi, N.; Willems, P. 2011, Assessment of climate change impact on hydrological extremes in two source regions of the Nile River Basin. *Hydrology and Earth System Science*, 15, 209–222. [CrossRef]

Taylor, K. E., Stouffer, R. J. & Meehl, G. A. 2009. A summary of the CMIP5 experimental design. http://cmip-pcmdi.llnl.gov/cmip5/experiment_design.html?submenuheader=1

Thakali, R.; Kalra, A.; Ahmad, S. 2016, Understanding the effects of climate change on urban stormwater infrastructures in the Las Vegas Valley. *Hydrology*, 3, 34. [CrossRef]

Tu, J. 2009, Combined impact of climate and land use changes on streamflow and water quality in eastern Massachusetts, USA. *Journal of Hydrology*, 379, 268–283. [CrossRef]

U.S. Department of Agriculture, 1994, State Soil Geographic (STATSGO) database for Alabama: U.S. Department of Agriculture, Natural Resources Conservation Service, Soil Survey Division, accessed July 31, 2020, at URL http://www.ftw.nrcs.usda.gov/ stat_data.html.

Van Griensven, A.; Meixner, T. 2006, Methods to quantify and identify the sources of uncertainty for river basin water quality models. *Water Science and Technology*, 53(1), 51-59.

Vrugt, J. A., Gupta H.V., Bouten, W. and Sorooshian, S. 2003, A shuffled complex evolution Metropolis algorithm for optimization and uncertainty assessment of hydrologic model parameters. *Water Resources Research*, 39(8), 1-14.

Walter, K.M.; Zimov, S.A.; Chanton, J.P.; Verbyla, D.; Chapin, F.S. 2006, Methane bubbling

from Siberian thaw lakes as a positive feedback to climate warming. *Nature*, 443, 71–75. [CrossRef] [PubMed]

Wang, X., Siegert, F., Zhou, A., Franke, J. 2013, Glacier and glacial lake changes and their relationship in the context of climate change, Central Tibetan Plateau 1972–2010. *Global Planetary Change*, 111, 246–257. [CrossRef]

Westra, S.; Alexander, L.V.; Zwiers, F.W. Global increasing trends in annual maximum daily precipitation. J. Clim. 2013, 26, 3904–3918. [CrossRef]

Whitehead, P.G., Wilby, R.L., Battarbee, R.W., Kernan, M., Wade, A.J.2009, A review of the potential impacts of climate change on surface water quality. *Hydrological Science Journal*, 54, 101–123. [CrossRef]

Willams, J. 1969, Flood routing with variable travel time or variable storage coefficients. Transaction of the Society of Agricultural and Biological Engineers (ASABE), 12, 100-103.

Williams, J.R., R.C. Izaurralde, and E.M. Steglich. 2008, Agricultural Policy/Environmental eXtender Model: Theoretical documentation version 0604 (Draft). BREC Report # 2008-17. Temple, TX: Texas AgriLIFE Research, Texas A&M University, Blackland Research and Extension Center.

Woznicki, S.A.; Nejadhashemi, A.P. 2013, Sensitivity analysis of best management practices under climate change scenarios. *Journal of Atmospheric Water Resource Association*, 48, 90–112. [CrossRef]

Wu, P.; Christidis, N.; Stott, P. Anthropogenic impact on Earth's hydrological cycle. *Nature Climate Change*, 3, 807. [CrossRef]

Yan, D., Werners, S.E.; Ludwig, F.; Huang, H.Q. 2015, Hydrological response to climate change:The Pearl River,China under different RCP scenarios. *Journal of Hydrology*, 4, 228–245. [CrossRef]

Young, R., Onstad, C., Bosch, D., Anderson, W. 1989, AGNPS: A nonpoint-source pollution model for evaluating agricultural watersheds. *Journal of Soil Water Conservation*, 44, 168–173.

Zhang, J., Li, Q., Guo, B. and Gong, H. 2015, The comparative study of multi-site uncertainty evaluation method based on swat model. *Hydrological Processes*, 29(13), 2994-3009.

Table 3.1: Management operations for cropland of the study area

Plant Type	Operation Date	Operation Type	Operation Attributes	Land use
Bermudagrass	01-March	Planting		Rangeland
	01-July	Harvesting		
Peanut	15-May	Planting		Agricultural land
	21-October	Harvesting		
Cotton	25-March	Tillage	Generic Conservation tillage	
	15-April	Planting		
	15-April	Fertilizer application	45 kg/ha Nitrogen	
	15-April	Fertilizer application	40 kg/ha Phosphorus	
	10-June	Fertilizer application	50 kg/ha Nitrogen	
	15-September	Harvesting		

Table 3.2: Model parameters and their descriptions in surface flow, total nitrogen and phosphorus calculations

Parameter	Parameter Description	Fitted value	Minimum value	Maximum value
ADJ_PKR	Peak rate adjustment factor for sediment routing in sub watershed	2	0.5	2
ALPHA_BF	Baseflow alpha factor (days)	0.1	0	1
BIOMIX	Biological mixing efficiency	0.2	0	1
CN	Curve number	Decrease 20%	35	98
EPCO	Plant evaporation compensation factor	0.95	0	1
ESCO	Soil evaporation compensation factor	1	0	1
GW_DELAY	Groundwater delay time (days)	20	0	500

GW_REVAP	Groundwater “revap” coefficient	0.02	0.02	0.2
OV_N	Manning's "n" value for overland flow "n" value for overland flow	1	0.01	30
PRF	Peak rate adjustment factor for sediment routing in the main channel	1	0	0
RCHRG_DP	Deep aquifer percolation factor	0.05	0	1
SOL_AWC	Available water capacity of soil layer	0.7	0	1
SOL_K	Saturated hydraulic conductivity	0.2	0	2000
SPEXP	Exponent parameter for calculating sediment retrained in channel sediment routing	1.5	1	1.5
USLE_P	USLE equation support practice factor	1	0	1
SOL_LABP	Initial soluble P concentration in sol layer	0.01	0	100
SOL_ORGP	Initial organic P concentration in sol layer	0.01	0	100
LAT_ORGN	Organic N in the baseflow	0.01	0	200
SOL_ORGN	Initial organic N concentration in the soil layer	0.01	0	10

Table 3.3: Sensitive parameters ranking based on t-Stat and p-Value

Parameter Name	t-Stat	P-Value
r__ESCO.bsn	-0.215278727	0.829640698
r__USLE_P.mgt	-0.226950855	0.820557782
r__BIOMIX.mgt	0.227096486	0.820444606
r__ALPHA_BF.gw	-0.278863619	0.780468599
r__SOL_K().sol	0.671455455	0.502250766
r__GW_REVAP.gw	-0.728852367	0.466444494
r__GW_DELAY.gw	0.846668373	0.39759842

r__SPEXP.bsn	-0.969346487	0.332856487
r__EPCO.bsn	1.115696614	0.265105646
r__CN2.mgt	-1.333777787	0.18290399
r__ADJ_PKR.bsn	-1.443612737	0.149494876
r__PRF_BSN.bsn	-1.948062549	0.051985146
r__RCHRG_DP.gw	-1.994993478	0.046603828
r__OV_N.hru	-2.862365089	0.004387183
r__SOL_AWC().sol	-38.3178933	0

Table 3.4: Statistical evaluation of the model for calibration and validation time periods

	R^2		**NSE**		**PBIAS**	
	Calibration	Validation	Calibration	Validation	Calibration	Validation
Stream Flow	0.81	0.81	0.77	0.73	-10.7	15.4
Nitrogen	0.75	0.77	0.62	0.65	9.34	-3.45
Phosphorus	0.5	0.54	0.34	0.24	-20.45	-21.76

Table 3.5: Average annual observed and simulated streamflow, total nitrogen and phosphorus

Variable	Average Annual Value
Average Observed Stream Flow	4.14 m^3/s
Average Simulated Stream Flow	4.16 m^3/s
Average Observed Nitrogen	5157.79 Kg/Ha
Average Simulated Nitrogen	6214.33 Kg/Ha
Average Observed Phosphorus	651.79 Kg/Ha
Average Simulated Phosphorus	1040.19 Kg/Ha

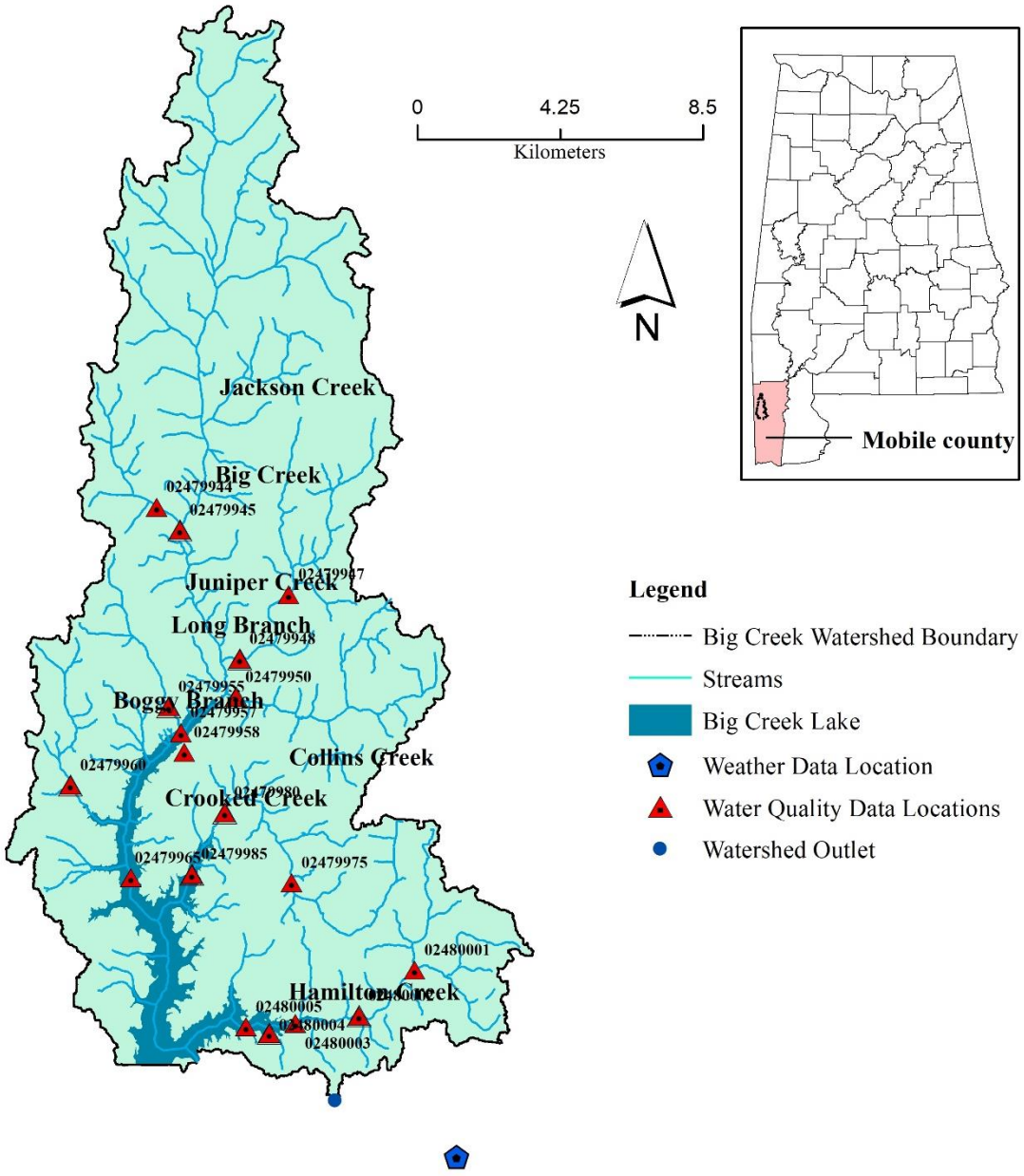

Figure 3.1: Location map of the study area

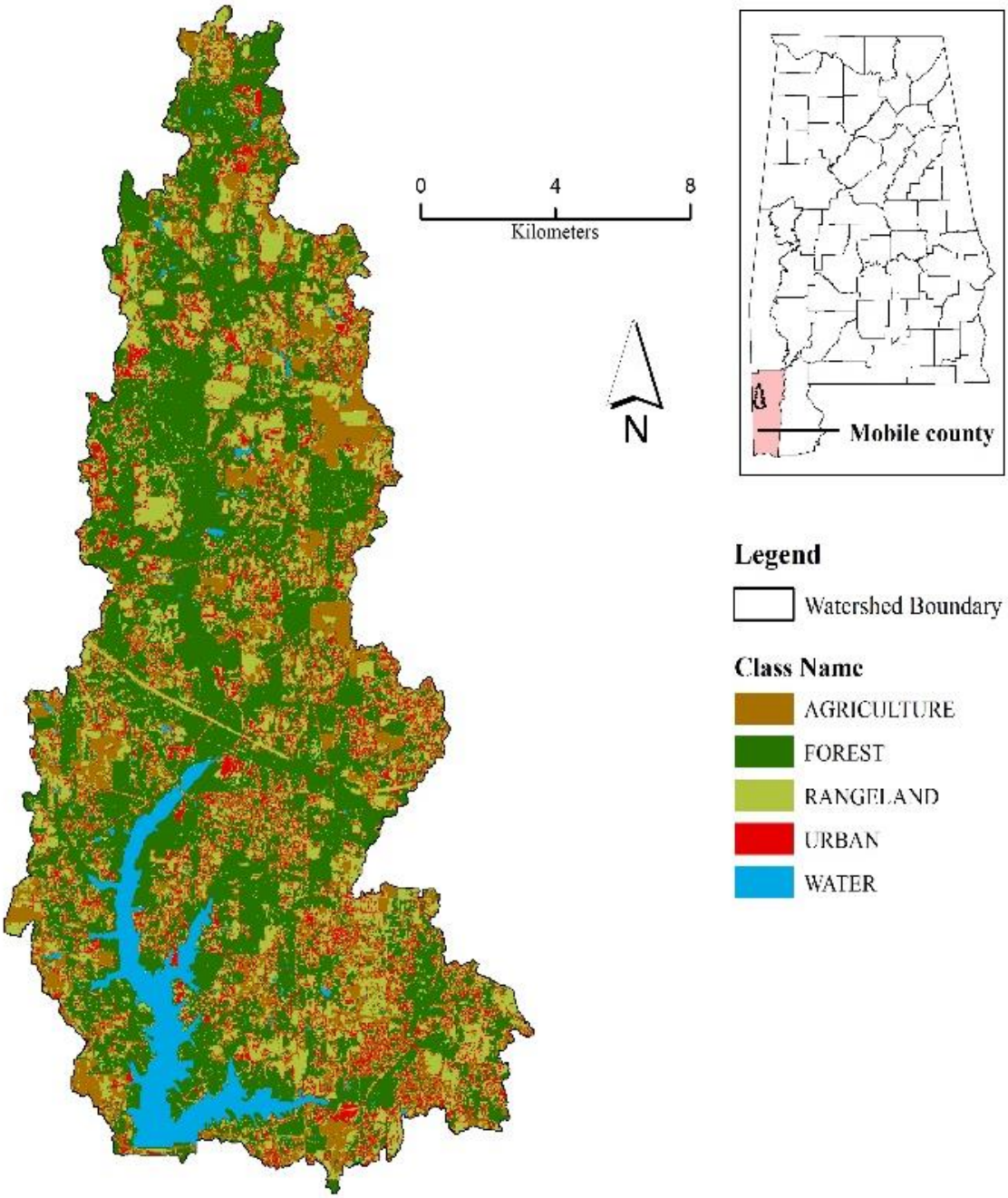

Figure 3.2: Land use map of the study area

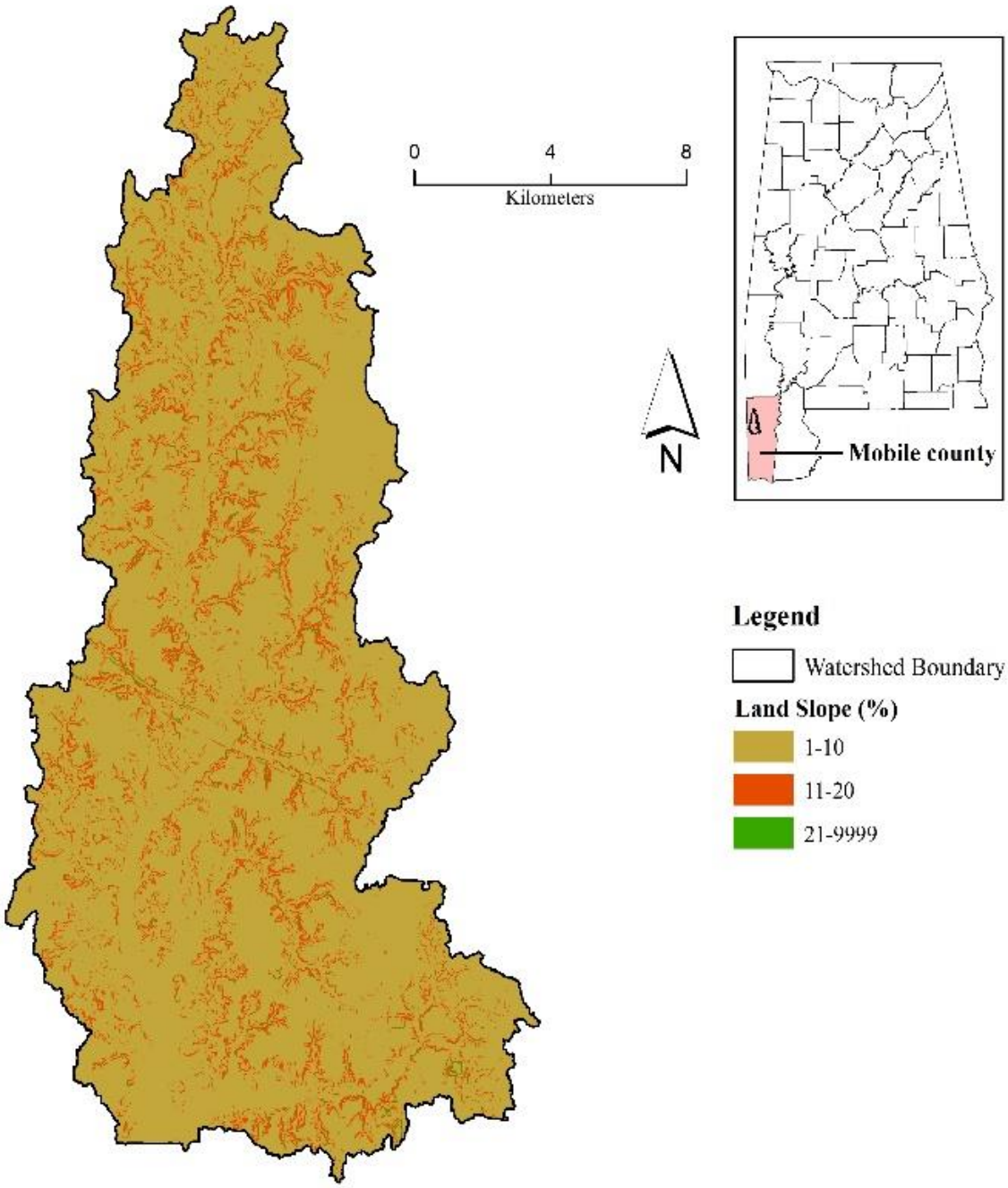

Figure 3.3: Slope class map of the study area

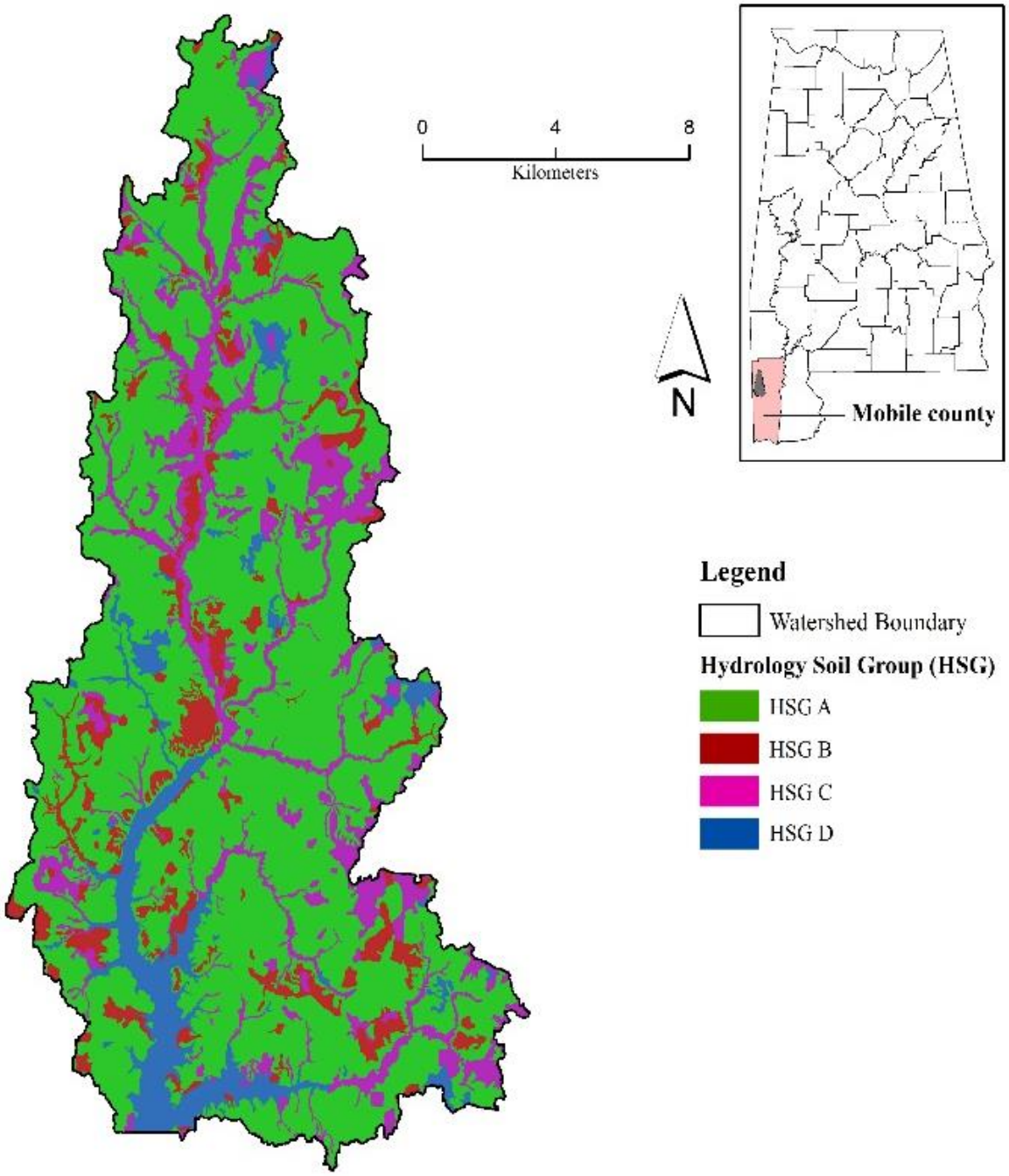

Figure 3.4: Soil class map of the study area

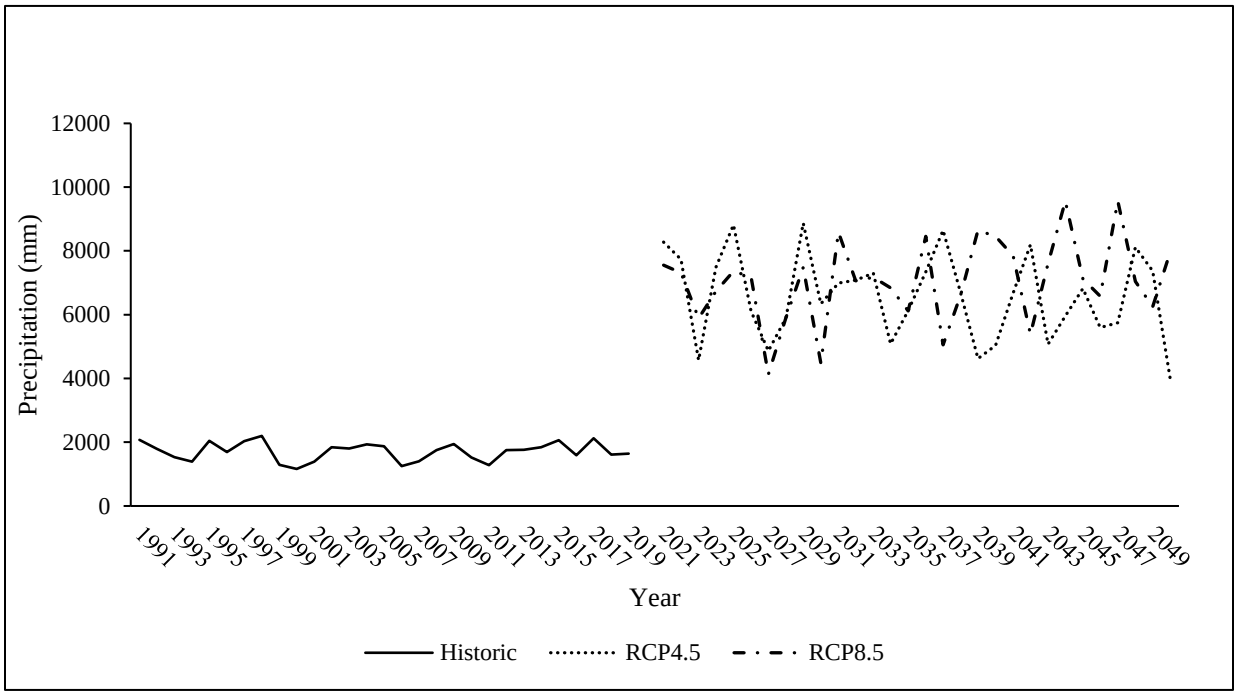

Fig 3.5: Annual Precipitation (mm) from 1991 to 2050

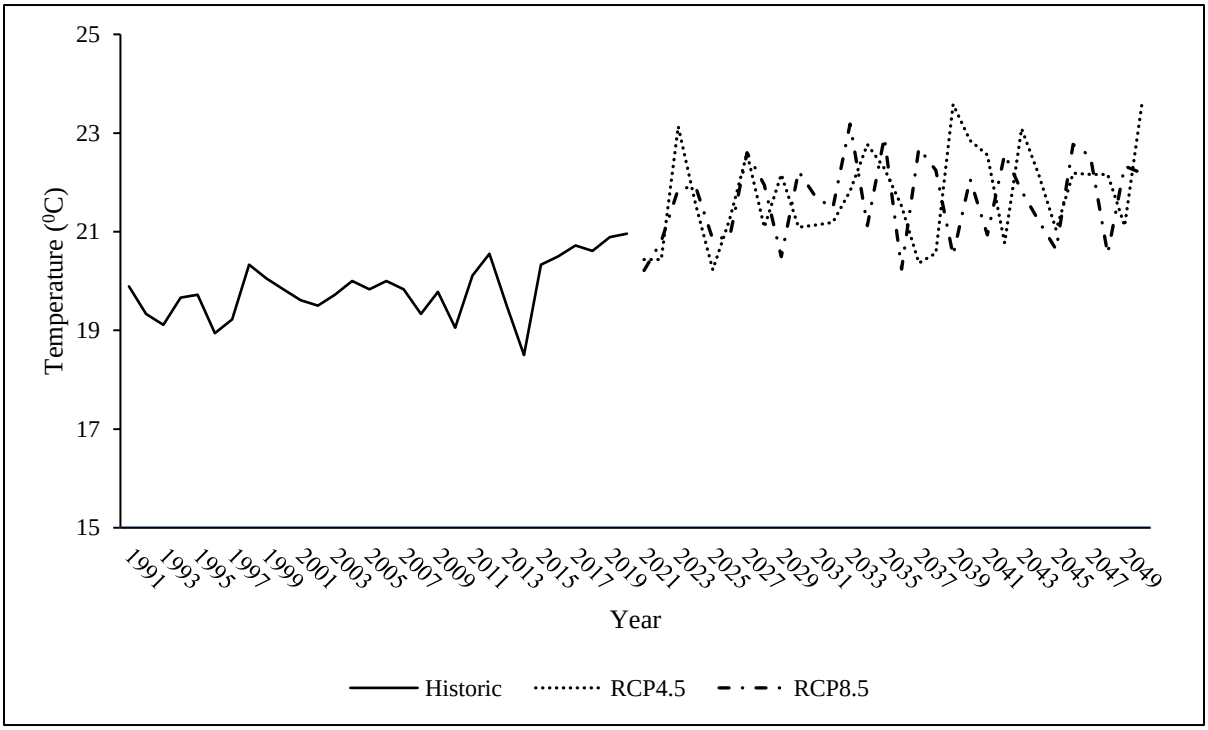

Fig 3.6: Annual Temperature (^{0}C) from 1991 to 2050

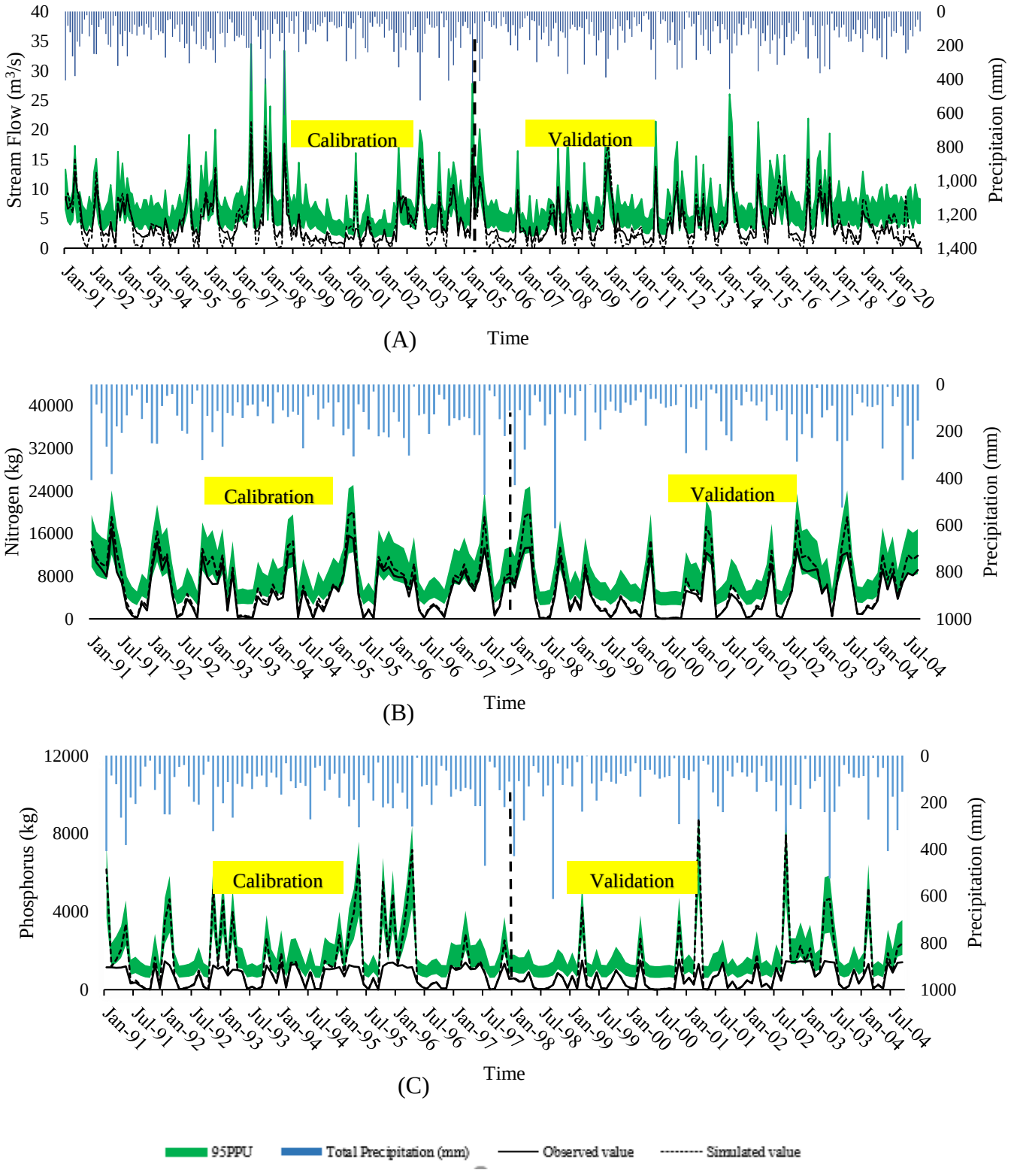

Figure 3.7: Observed vs. simulated stream flow (m^3/s) from 1991-2020 (A), total nitrogen (Kg/Ha) from 1991-2004 (B) and total phosphorus (Kg/Ha) (C) from 1991-2004

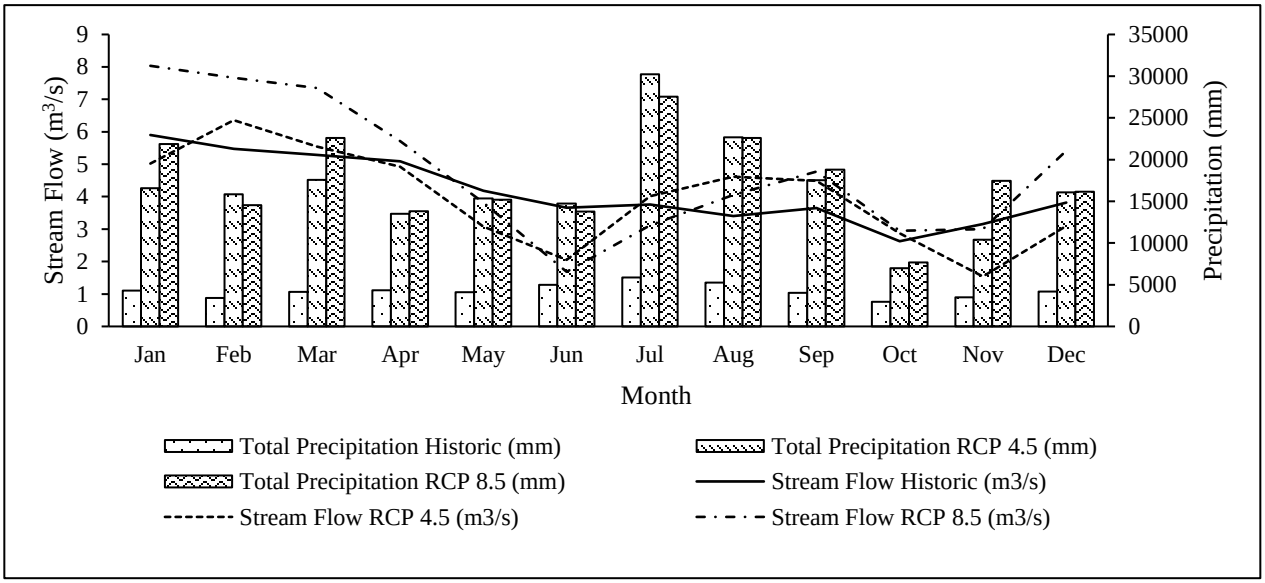

Fig 3.8: Precipitation vs. Stream Flow

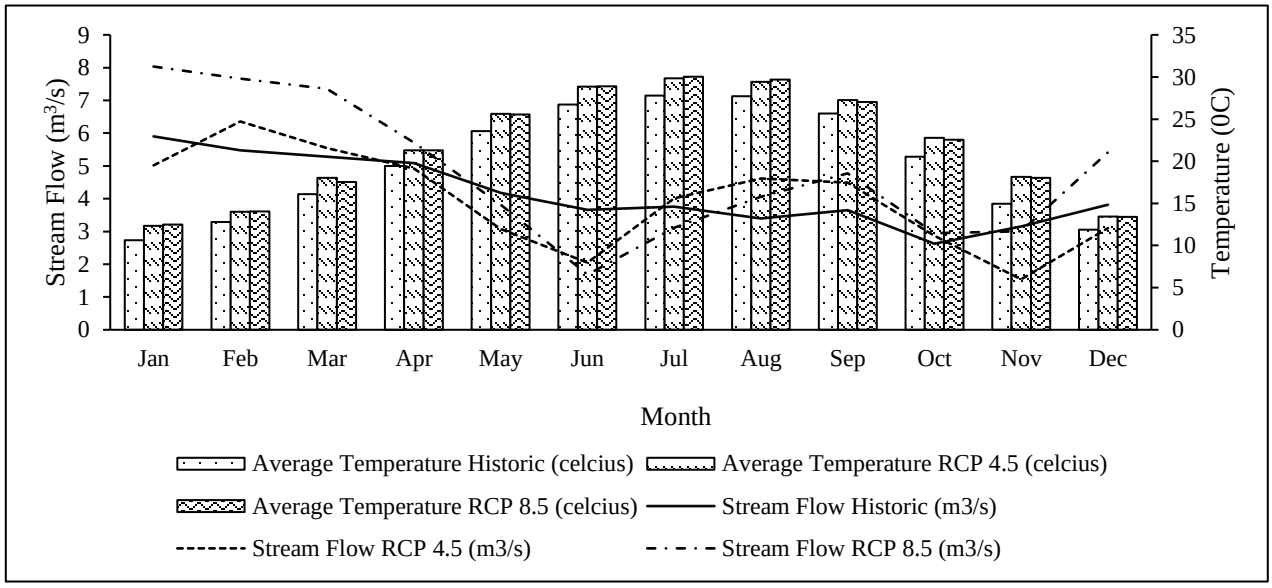

Fig 3.9: Temperature vs. Stream Flow

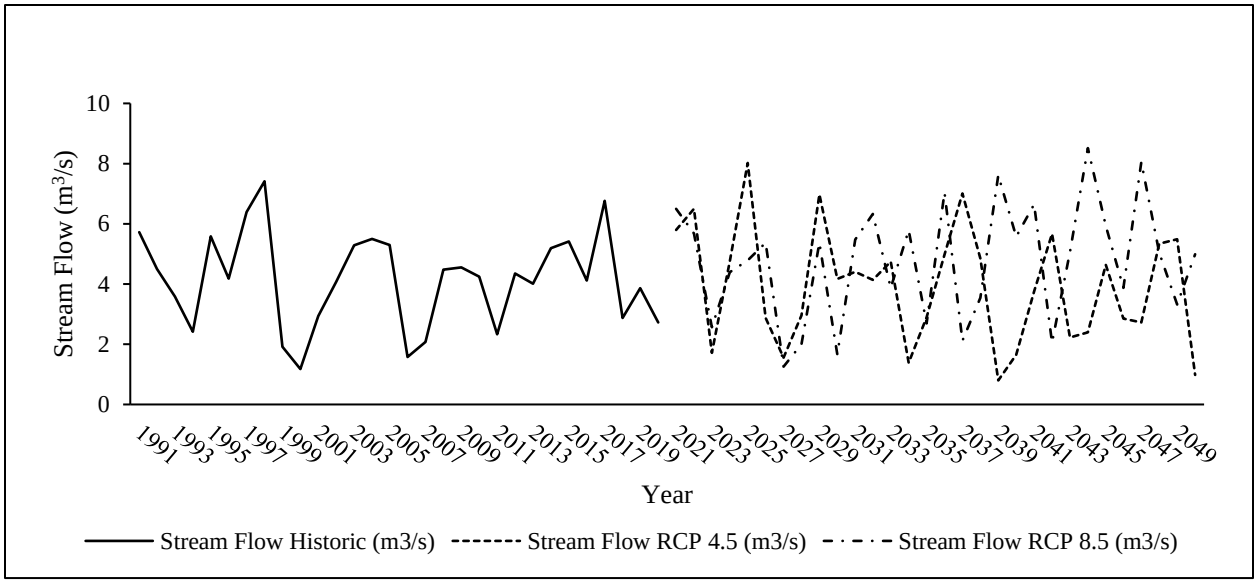

Fig 3.10: Stream Flow (m^3/s) Historic vs. RCP4.5 vs. RCP8.5 by Year

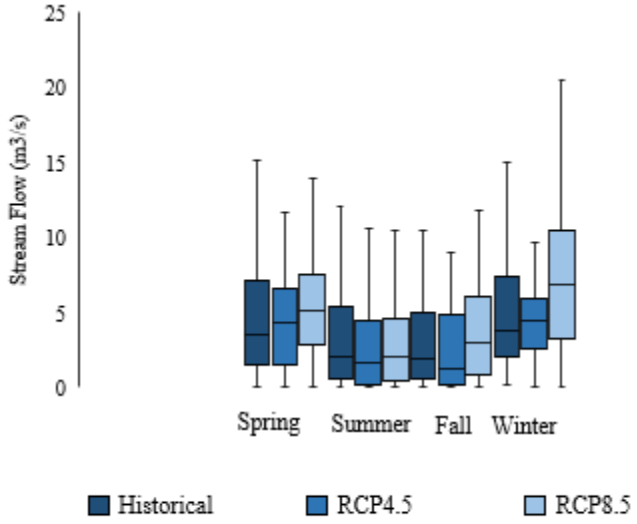

Fig 3.11: Stream Flow (m^3/s) Historic vs. RCP4.5 vs. RCP8.5 by Month

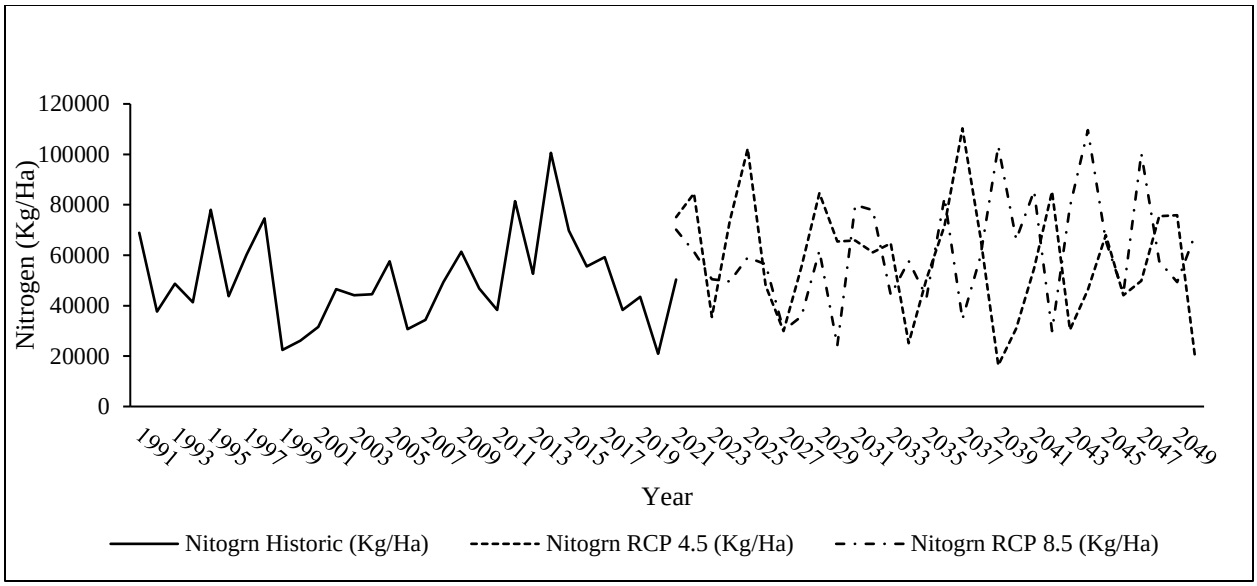

Fig 3.12: Nitrogen (Kg/Ha) Historic vs. RCP4.5 vs. RCP8.5 by Year

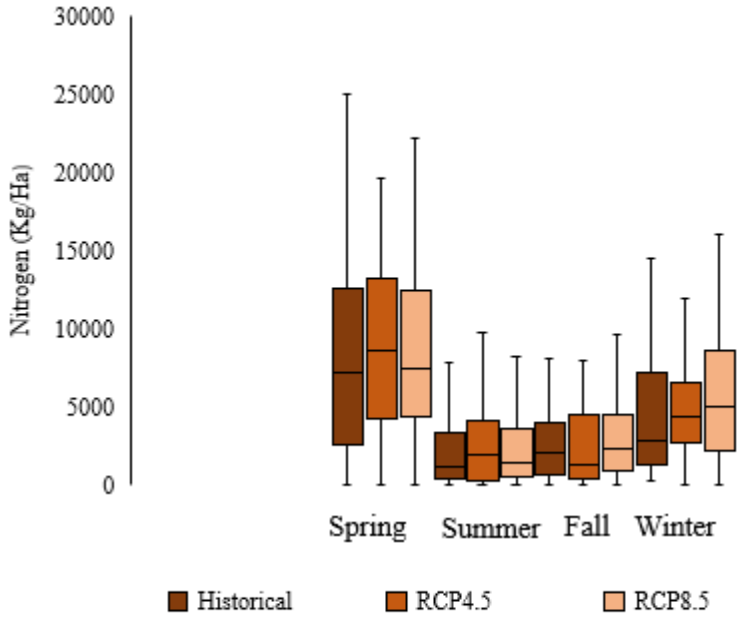

Fig 3.13: Nitrogen (Kg/Ha) Historic vs. RCP4.5 vs. RCP8.5 by Month

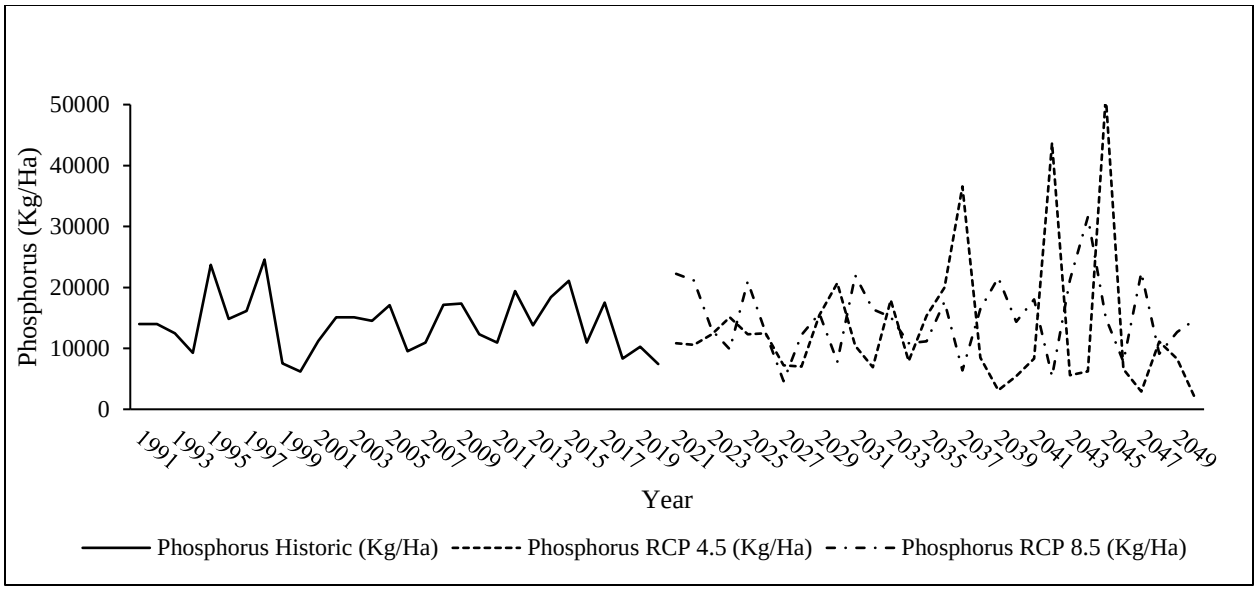

Fig 3.14: Phosphorus (Kg/Ha) Historic vs. RCP4.5 vs. RCP8.5 by Year

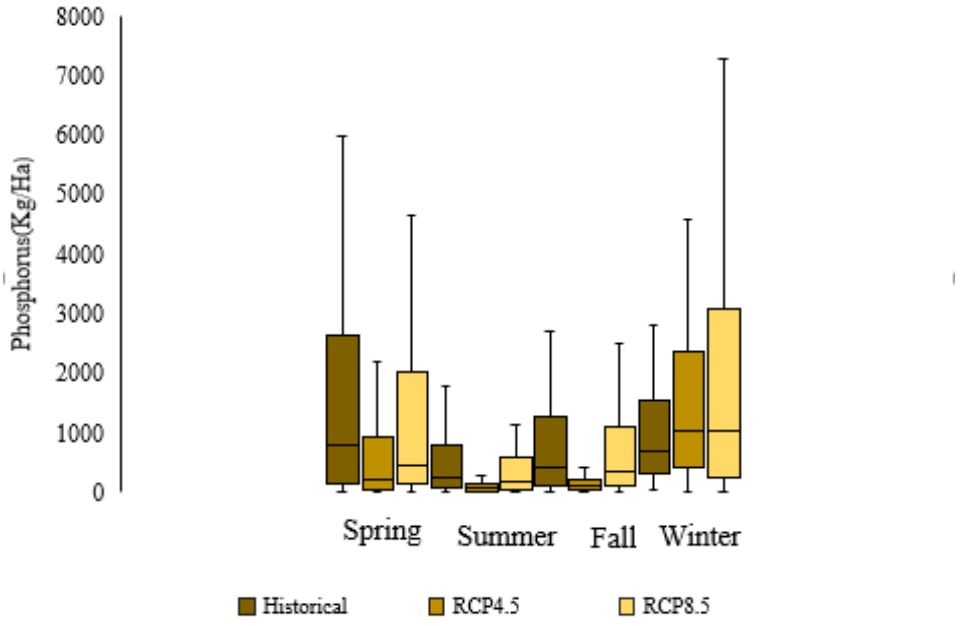

Fig 3.15: Phosphorus (Kg/Ha) Historic vs. RCP4.5 vs. RCP8.5 by Month

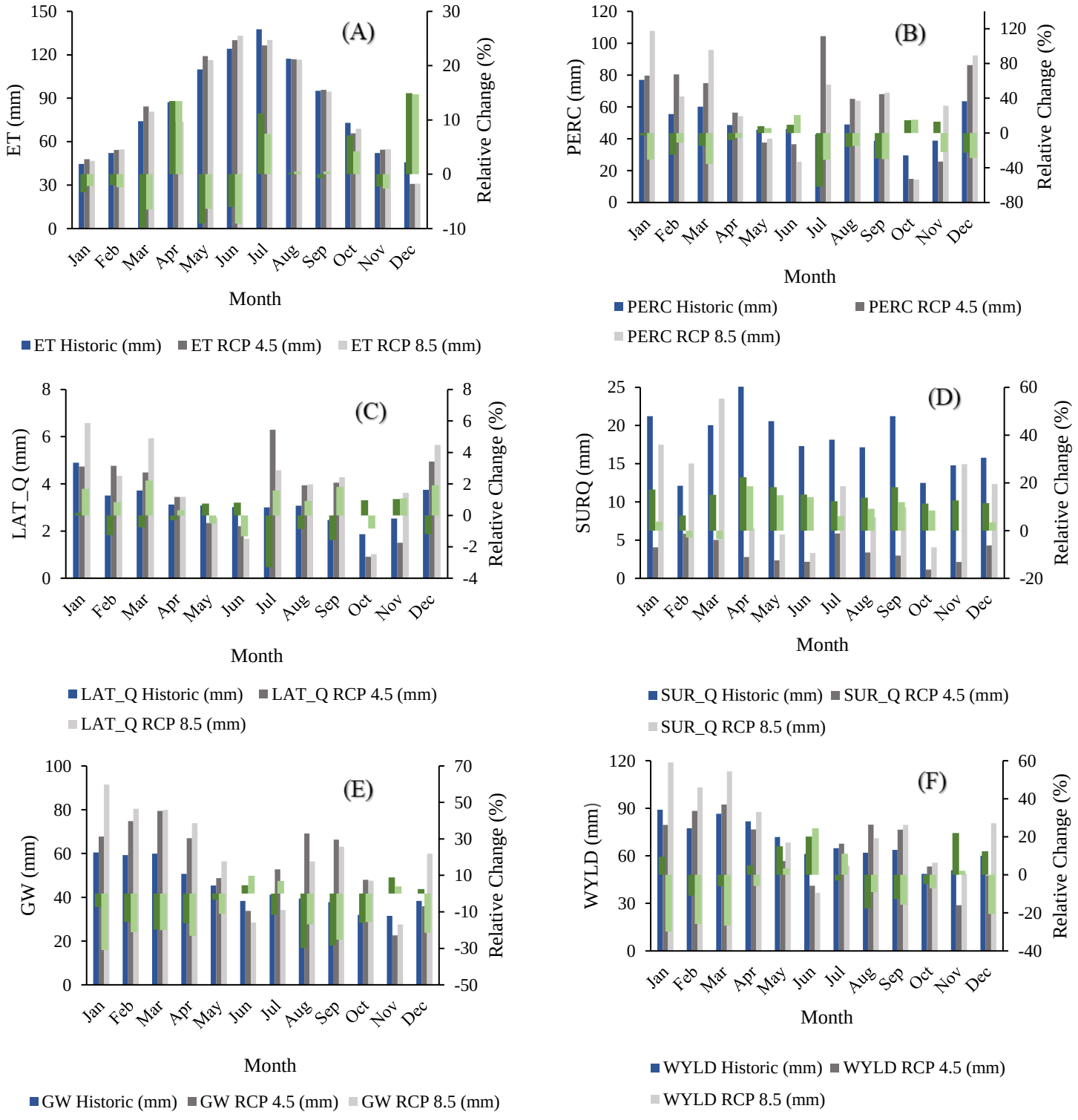

Figure 3:16: Monthly averages and relative changes of ET (A), PERC (B), SURQ (C), LAT_Q (D), GW_Q (E) and WYLD (F) for Historic, RCP 4.5 and RCP 8.5

CHAPTER 4
SUMMARY AND CONCLUSIONS

4.1 Conclusions

This study used the SWAT model to detect and predict the effects of changing LULC and climate on the stream flow and nitrogen and phosphorus. The major conclusions from this research were: (a) the stream flow has significant impact and on growing trend because of increasing agricultural and urban areas and decreasing forest land, (b) the amount of nitrogen and phosphorus have great effects and they are increasing because increasing agricultural area has likely increased the use of fertilizer and thus this increases the nitrogen and phosphorus in the stream flow, (c) though the stream flow will increase in both climate change scenarios, the rate of increasing is higher in RCP8.5 than RCP4.5 with the increase of the precipitation and decrease of the temperature, and (d) the nitrogen and phosphorus will also increase and again the increasing trend is higher in the RCP8.5 scenario than the RCP4.5 scenario because of increasing stream flow.

The agricultural land increased in a substantial amount as well as the urban area because of the increasing the population of the Mobile County. In addition, the reduction of the forest land is the result of the increasing stream flow and the increase in the agricultural land results in a growing amount of the nitrogen and phosphorus. The precipitation will increase in the future three decades comparing to the past three decades and this growing precipitation leads to increasing stream flow and nitrogen and phosphorus. The increasing precipitation has more impact on the increasing stream flow and deterioration of the water quality of the watershed than the increasing temperature.

4.2 Recommendations

The results of the study can be used for further studies. If the rate of stream flow and associated nitrogen and phosphorus has been increasing, then there will be environmental consequences. Water resource managers and policy makers should take some measures to reduce the stream flow and control the pollution of the water. Some management practices could be included such as crop rotation, reduction of fertilizers, irrigation water management, nutrient management and grass streamside buffers.